

UNIVERSIDADE FEDERAL DO RIO GRANDE DO SUL
FACULDADE DE AGRONOMIA
PROGRAMA DE PÓS-GRADUAÇÃO EM FITOTECNIA

RESPOSTAS FISIOLÓGICAS E MOLECULARES À ALTA TEMPERATURA NA
ANTESE EM ARROZ IRRIGADO

Silmara da Luz Correia
Mestre em Agronomia/UFRGS

Tese apresentada como um dos requisitos
à obtenção do Grau de Doutora em Fitotecnia
Ênfase Fisiologia e Manejo Vegetal

Porto Alegre (RS), Brasil
Fevereiro de 2018

CIP - Catalogação na Publicação

Correia, Silmara da Luz
RESPOSTAS FISIOLÓGICAS E MOLECULARES À ALTA
TEMPERATURA NA ANTESE EM ARROZ IRRIGADO / Silmara da
Luz Correia. -- 2018.

115 f.

Orientador: Paulo Regis Ferreira da Silva.

Coorientadora: Carla Andrea Delatorre.

Tese (Doutorado) -- Universidade Federal do Rio
Grande do Sul, Faculdade de Agronomia, Programa de
Pós-Graduação em Fitotecnia, Porto Alegre, BR-RS, 2018.

1. Estresse térmico. 2. RNA-seq. 3. fertilidade
de espiguetas. I. Silva, Paulo Regis Ferreira da,
orient. II. Delatorre, Carla Andrea, coorient. III.
Título.

SILMARA DA LUZ CORREIA
Engenheira Agrônoma - UFRGS
Mestre em Fitotecnia - UFRGS

TESE

Submetida como parte dos requisitos
para obtenção do Grau de

DOUTOR EM FITOTECNIA

Programa de Pós-Graduação em Fitotecnia
Faculdade de Agronomia
Universidade Federal do Rio Grande do Sul
Porto Alegre (RS), Brasil

Aprovado em: 21.02.2018
Pela Banca Examinadora

Homologado em: 19.03.2018
Por

PAULO REGIS FERREIRA DA SILVA
Orientador - PPG Fitotecnia
UFRGS

CHRISTIAN BREDEMEIER
Coordenador do Programa de
Pós-Graduação em Fitotecnia

CARLA ANDREA DELATORRE
Coorientadora - PPG Fitotecnia
UFRGS

CHRISTIAN BREDEMEIER
PPG Fitotecnia-UFRGS

MÁRCIA MARIA AUXILIADORA
NASCHENVENG PINHEIRO MARGIS
PPG Genética e Biologia Molecular
UFRGS

SAMUEL CORDEIRO VITOR MARTINS
PPG Fisiologia Vegetal - UFV/MG

CARLOS ALBERTO BISSANI
Diretor da Faculdade
de Agronomia

DEDICATÓRIA

Aos meus pais e ao Ricardo,
pelo incentivo para o cumprimento
de mais essa etapa.

“Sempre em frente, porque este é o lugar dos fortes”

Paulo Regis Ferreira da Silva

AGRADECIMENTOS

À Universidade Federal do Rio Grande do Sul (UFRGS), em especial ao Programa de Pós-Graduação (PPG) em Fitotecnia, pela oportunidade e estrutura oferecidas.

Ao professor Paulo Regis pela orientação, dedicação, amizade e exemplo de profissionalismo.

Aos professores do PPG em Fitotecnia, em especial aos professores Christian Bredemeier e Carla A. Delatorre pelos ensinamentos, motivação e discussões engrandecedoras. Aos professores de outros PPGs da UFRGS onde cursei disciplinas e realizei parte das análises laboratoriais, pelo acolhimento e disponibilidade.

Ao Conselho Nacional de Desenvolvimento Científico e Tecnológico (CNPq) e à Coordenação de Aperfeiçoamento de Pessoal de Nível Superior (CAPES), pelas bolsas de estudo e apoio financeiro concedidos, durante o período de Doutorado e Doutorado Sanduíche no Exterior, respectivamente.

Aos servidores e técnicos administrativos do Departamento de Plantas de Lavoura e do PPG em Fitotecnia, pela prestatividade, ajuda e amizade.

Aos colegas do PPG em Fitotecnia pela amizade, incentivo e conhecimentos compartilhados.

À Dra Colleen Doherty pela co-orientação, motivação e amizade durante o período de Doutorado Sanduíche no Exterior na North Carolina State University, Raleigh/EUA. E aos Colegas da mesma instituição, pela troca de experiências, ensinamentos e amizade.

Aos meus pais Vorly Correia e Julia Correia, pelas palavras de incentivo e pelo apoio.

Ao meu marido Ricardo Manke pelo apoio, compreensão e carinho.

À sociedade brasileira, que através do CNPq e da CAPES financiaram esta pesquisa.

RESPOSTAS FISIOLÓGICAS E MOLECULARES À ALTA TEMPERATURA NA ANTESE EM ARROZ IRRIGADO¹

Autor: Silmara da Luz Correia

Orientador: Paulo Regis Ferreira da Silva

Co-orientadora: Carla Andrea Delatorre

RESUMO

Em um cenário futuro de mudanças climáticas, espera-se que os episódios de alta temperatura ocorram mais frequentemente. Isso pode coincidir com fases de desenvolvimento em que as estruturas vegetais estejam mais susceptíveis, como o período reprodutivo do arroz, causando redução no rendimento de grãos. O principal objetivo desse trabalho foi comparar características fisiológicas e moleculares de cultivares de arroz irrigado submetidas à alta temperatura (AT) na fase de antese e discutir os possíveis processos fisiológicos e/ou moleculares envolvidos. Três cultivares de arroz (IRGA 409, IRGA 428 e DULAR) foram submetidas à AT na antese (38°C) e à condição controle (29°C) durante sete horas, em períodos consecutivos de três, cinco ou sete dias. Foram avaliados a fertilidade de espiguetas e parâmetros relacionados à fotossíntese na folha bandeira. Na panícula de duas cultivares (IRGA 409 e IRGA 428) foi realizada análise de sequenciamento de mRNA (RNA-seq), com coleta de espiguetas nas condições de três dias de estresse e no controle. A AT reduziu a fertilidade de espiguetas com o aumento da duração do estresse em todas as cultivares comparado à condição controle, com redução significativa no número de grãos formados no estresse com sete dias de duração. No entanto, com três dias de duração do estresse IRGA 409 foi a mais tolerante à AT, uma vez que apresentou maior percentagem de espiguetas fertilizadas. A análise de RNA-seq mostrou que genes comumente expressos em resposta à AT, como os *OsHsf*, *OsHSP* e *OsFKBP62b*, apresentaram expressão similar nas panículas de ambas as cultivares, apesar dessas plantas não serem especificamente selecionadas para tolerância a esse estresse. A expressão de genes envolvidos na fotossíntese na panícula em resposta à AT foi uma grande diferença entre as duas cultivares. Este estudo indicou que a manutenção da expressão de genes relacionados à fotossíntese da panícula e à capacidade de manter a fotossíntese ativa na folha bandeira durante o período de ocorrência da AT estiveram associados à maior fertilidade de espiguetas nessa condição. Esses resultados evidenciaram potenciais marcadores a serem usados na identificação de genótipos tolerantes à alta temperatura. No entanto, os processos moleculares envolvidos no efeito desse estresse no transporte de elétrons através da atividade dos fotossistemas I e II e a conexão entre atividade fotossintética das folhas e panícula de arroz necessitam ser elucidados.

¹Tese de Doutorado em Fitotecnia, Faculdade de Agronomia, Universidade Federal do Rio Grande do Sul, Porto Alegre, RS, Brasil (116f.) Fevereiro, 2018.

PHYSIOLOGICAL AND MOLECULAR RESPONSES TO HIGH TEMPERATURE STRESS AT ANTHESIS IN FLOODED RICE ¹

Author: Silmara da Luz Correia
Adviser: Paulo Regis Ferreira da Silva
Co-adviser: Carla Andrea Delatorre

ABSTRACT

High temperature episodes are expected to occur more frequently in future climates, which may coincide with vulnerable reproductive processes leading to significant reduction in rice yield. The present study aims to compare the physiological and molecular characteristics of flooded rice cultivars at anthesis stage under high temperature and to discuss the possible process involved in heat tolerance. Three rice cultivars (IRGA 409, IRGA 428 and DULAR) were submitted to daytime high temperature treatment (38 °C) and to control condition (29 °C) for seven hours during a period of three, five or seven days at anthesis stage. This study investigated the spikelet fertility and physiological parameters in the flag leaf during anthesis. At three days of stress duration, an RNA-sequencing (RNA-seq) approach of heat and control treated spikelets was carried out using the cultivars IRGA 409 and IRGA 428. Compared with the control, heat treatment with seven days duration significantly reduced spikelet fertility with the increase of the stress duration in all cultivars, leading to a significant reduction in the number of grain filled. However, at three days of stress duration, cultivar IRGA 409 was more tolerant to heat treatment, maintaining the highest spikelet fertility among the cultivars. Comparative transcriptome analysis between the two cultivars shows that in response to heat stress, more genes are differentially expressed in the more tolerant cultivar (IRGA 409) than in the more sensitive (IRGA 428). In panicle tissue, most canonical heat responsive genes, such as transcription factor family (*Hsf*), heat shock proteins family (*sHSP*) and gene *OsFKBP62b*, showed a similar expression response in both Brazilian cultivars, despite the fact that these cultivars have not been specifically selected for heat tolerance. Photosynthetic genes expression in response to heat stress was a major difference between the two cultivars. This study indicated that the basal expression of photosynthetic genes in the panicle and the ability to maintain photosynthetic capacity in the flag leaf during heat stress provided improved spikelet fertility during this stress. This may provide potential markers that can be used to identify heat tolerant genotypes among the Brazilian cultivars. However, the detailed molecular processes involved on heat effects on electron transport through photosystems I and II and the connection between photosynthesis activity in the leaves and in the rice panicle remain to be further elucidated.

¹Doctoral thesis in Plant Science, Faculdade de Agronomia, Universidade Federal do Rio Grande do Sul, Porto Alegre, RS, Brazil (116p.) February, 2018.

SUMMARY

	Page
1 INTRODUCTION	1
2 LITERATURE REVIEW.....	6
2.1 Climate change and Rice.....	6
2.1.1 Rice – an important cereal crop.....	6
2.1.2 Climate change.....	8
2.2 Effect of high temperature on rice growth and development.....	9
2.2.1 Vegetative phase	11
2.2.2 Reproductive phase.....	12
2.3 How can high temperature stress cause plant injury?	13
2.3.1 Photosynthesis	13
2.3.2 Carbohydrate accumulation and partitioning	15
2.3.3 Heat shock proteins.....	16
2.3.4 Membrane injury.....	18
2.3.5 Pollen germination and spikelet sterility.....	19
2.4 Screening for high temperature stress tolerance	20
2.4.1 Morpho-physiological markers.....	21
2.4.2 Molecular markers and genomic approaches	22
2.5 Mitigation and adaptation to high temperature stress	23
2.6 Conclusion and future perspectives.....	24
3 MATERIAL AND METHODS.....	26
3.1 Plant material.....	26
3.2 Plant growth.....	28
3.3 Filled spikelets/panicle and spikelet fertility (%).....	28
3.4 Percentage of fertility reduction in spikelet	29
3.5 Photosynthetic parameters	29
3.6 Chlorophyll fluorescence	29

	Page
3.7 Hydrogen peroxide content.....	30
3.8 Statistical analysis	31
3.9 High-throughput mRNA sequencing (RNA-seq)	31
3.9.1 RNA extraction and RNA-seq library preparation	31
3.9.2 RNAseq data alignment and quantification.....	32
3.9.3 Differential expression	33
3.9.4 Functional annotation	34
4 RESULTS	35
4.1 Fertilized spikelets	35
4.2 Photosynthesis parameters	37
4.3 Fluorescence parameters	39
4.4 Hydrogen peroxide content.....	41
4.5 High-throughput mRNA sequencing (RNA-seq)	42
4.5.1 Transcriptome sequencing and mapping of the reads	42
4.5.2 Global analysis of gene expression	43
4.5.3 Pathway enrichment for DEGs	49
4.5.3.1 High temperature effects - MapMan ontology.....	49
4.5.4 Cellular response in rice panicle to heat treatment.....	53
4.5.5 Light-reaction response by high temperature in IRGA 428.....	54
4.5.6 Interaction between cultivar and heat stress.....	56
5 DISCUSSION.....	64
5.1 Physiological response to heat stress	64
5.2 Common heat responsive genes in rice panicle	67
5.3 Induction of light reaction genes in response to heat stress.....	70
6 CONCLUSIONS.....	74
7 REFERENCES	75
8 APPENDIX.....	81
9 VITA	101

LIST OF TABLES

	Page
1. Origin, subspecies and high temperature tolerance of the cultivars used in the previous study of tolerance to high temperature at anthesis stage. UFRGS, Porto Alegre, RS, Brazil. 2018.....	27
2. Scheme of application of thermal treatments (three, five and seven days) in a period of 24 hours. UFRGS, Porto Alegre, RS, Brazil. 2018.	28

LIST OF FIGURES

	Page
1. Effect of duration of high temperature on percentage (%) of spikelet fertility (A) and on reduction of fertilized spikelets (B) in three flooded rice cultivars. Each value represents means of five replications \pm SD. Means followed by the same capital letter do not differ significantly among cultivars in each treatment condition and lowercase letter do not differ significantly among treatment conditions in each cultivar by Tukey's test (p-value <0.05). UFRGS, Porto Alegre, RS, Brazil. 2018.....	36
2. Effect of duration of high temperature on photosynthetic rate (A) and on stomatal conductance (B) in three flooded rice cultivars. Each value represents means of five replications \pm SD. Means followed by the same capital letter do not differ significantly among cultivars in each treatment condition and lowercase letter do not differ significantly among treatment conditions in each cultivar by Tukey's test (p-value <0.05). UFRGS, Porto Alegre, RS, Brazil. 2018.....	38
3. Effect of duration of high temperature stress on quantum yield of PSII (A) and electron transport rate (ETR) (B) in three flooded rice cultivars. Each value represents means of five replications \pm SD. Means followed by the same capital letter do not differ significantly among cultivars in each treatment condition and lowercase letter do not differ significantly among treatment conditions in each cultivar by Tukey's test (p-value <0.05). UFRGS, Porto Alegre, RS, Brazil. 2018.....	40
4. Effect of duration of high temperature on hydrogen peroxide content relative to control in three flooded rice cultivars. The dashed line represents untreated plants. Each value represents means of five replications \pm SD. Means followed by the same capital letter do not differ significantly among cultivars in each period of duration stress and lowercase letter do not differ significantly among period of duration stress in each cultivar by Tukey's test (p-value <0.01). UFRGS, Porto Alegre, RS, Brazil. 2018.....	41

5. RNA-seq reads from rice flowers mapped to the reference genome of *japonica* (Nipponbare) and *indica* (MH63). Percentage of mapped reads in each reference genome, in black bars the total covered by mapped reads, in light-grey bars the percentage of mapped reads that have no mismatches or InDels and, in dark-grey bars the percentage of mapped reads to multiple locations such as repeat sequences. UFRGS, Porto Alegre, RS, Brazil. 2018.....43
6. Differential expression of genes in response to high temperature compared to control condition in two flooded rice cultivars. Numbers of DEGs identified when mapped in *indica* and *japonica* reference genome are represented in black and gray bars, respectively. The differences in gene expression were obtained based on the LogFC ≥ 0.5 and adjusted p -value < 0.001 . UFRGS, Porto Alegre, RS, Brazil. 2018.....45
7. Venn diagram, overlap of expressed genes in response to high temperature stress in two flooded rice cultivars, for up and down-regulated genes. UFRGS, Porto Alegre, RS, Brazil. 2018.....46
8. Overview of pathways overrepresented in conserved genes up-regulated (A) and down-regulated (B), according to enrichment analysis using MapMan ontology visualized by Cytoscape plug-in BiNGO. The color scale indicates significance of enrichment analysis and the size of nodes indicates the numbers of genes were mapped. The arrows represent the relationship between parent-child terms. UFRGS, Porto Alegre, RS, Brazil. 2018.....47
9. Overview of pathways overrepresented in the cultivars IRGA 409 (A) and IRGA 428 (B), according to enrichment analysis using MapMan ontology visualized by Cytoscape plug-in BiNGO. The color scale indicates significance of enrichment analysis and the size of nodes indicates the numbers of genes which were mapped. The arrows represent the relationship between parent-child terms. UFRGS, Porto Alegre, RS, Brazil. 2018.....51
10. Expression profile of the genes in cellular response. MapMan was used to visualize heat response genes in the cultivars IRGA 409 (A) and IRGA 428 (B). Each square represent one transcript that colored with red for down-regulation or with blue for up-regulation. The scale is shown in the figure. UFRGS, Porto Alegre, RS, Brazil. 2018.....54
11. Expression profiles of the genes involved in light reaction process of the photosynthesis system. MapMan was used to visualize heat responsive DEGs in the cultivar IRGA 428. Each square represent one transcript that colored with red for down-regulation or with blue for up-regulation. The scale is shown in the figure. UFRGS, Porto Alegre, RS, Brazil. 2018.....55

12. Differentially expressed genes involved in photosynthesis pathway in response to high temperature, relative expression value computed from the counts per million (CPM). Bar graph shows each gene and transcript expression value annotated with error bars (\pm SD) that capture both cross-replicate variability and measured uncertainty as estimated by EdgeR statistical model of RNA-seq (adjusted p -value <0.001). UFRGS, Porto Alegre, RS, Brazil. 2018.....56
13. Overview of pathways overrepresented in the multi-factor contrast analysis, according to enrichment analysis using MapMan ontology visualized by Cytoscape plug-in BiNGO. The color scale indicates significance of enrichment analysis and the size of nodes indicates the numbers of genes which were mapped. The arrows represent the relationship between parent-child terms. UFRGS, Porto Alegre, RS, Brazil. 2018.....57
14. Differentially expressed genes involved in abiotic stress (A, B, C and D) and light reaction (E & F) pathways in response to high temperature in the contrast analysis, relative expression value computed from the counts per million (CPM). Bar graph shows each gene and transcript expression value annotated with error bars (\pm SD) that capture both cross-replicate variability and measured uncertainty as estimated by EdgeR statistical model of RNA-seq (adjusted p -value <0.001). UFRGS, Porto Alegre, RS, Brazil. 2018.....59
15. Differentially expressed genes involved in miscelanea pathway (A-F) in response to high temperature in the contrast analysis, relative expression value computed from the counts per million (CPM). Bar graph shows each gene and transcript expression value annotated with error bars (\pm SD) that capture both cross-replicate variability and measured uncertainty as estimated by EdgeR statistical model of RNA-seq (adjusted p -value <0.001). UFRGS, Porto Alegre, RS, Brazil. 2018.....60
16. Differentially expressed genes involved in minor CHO metabolism (A) and hormone metabolism (B & C) pathways in response to high temperature in the contrast analysis, relative expression value computed from the counts per million (CPM). Bar graph shows each gene and transcript expression value annotated with error bars (\pm SD) that capture both cross-replicate variability and measured uncertainty as estimated by EdgeR statistical model of RNA-seq (adjusted p -value <0.001). UFRGS, Porto Alegre, RS, Brazil. 2018.....61

17. Differentially expressed genes involved in mitochondrial electron transport (A & B) and secondary metabolism (C & D) pathways in response to high temperature in the contrast analysis, relative expression value computed from the counts per million (CPM). Bar graph shows each gene and transcript expression value annotated with error bars (\pm SD) that capture both cross-replicate variability and measured uncertainty as estimated by EdgeR statistical model of RNA-seq (adjusted p -value <0.001). UFRGS, Porto Alegre, RS, Brazil. 2018.62
18. Differentially expressed genes involved in metal transport (A & B) and transport major intrinsic protein (C) pathways in response to high temperature in the contrast analysis, relative expression value computed from the counts per million (CPM). Bar graph shows each gene and transcript expression value annotated with error bars (\pm SD) that capture both cross-replicate variability and measured uncertainty as estimated by EdgeR statistical model of RNA-seq (adjusted p -value <0.001). UFRGS, Porto Alegre, RS, Brazil. 2018.63
19. Venn diagram showing heat responsive genes identified in one independent rice heat stress data set. List of heat responsive genes from González-Schain et al., (2015) was compared with the list obtained by RNA-seq analysis in the present study. UFRGS, Porto Alegre, RS, Brazil. 2018.70

1 INTRODUCTION

Rice (*Oryza sativa* L.) is one of the world's most important sources of food for human nutrition, serving as a staple food for more than three billion people. The population of rice consuming countries continues to grow and it is estimated that the production must increase 40% to meet the demand in 2030 (SOSBAI 2016). Achieving high yields in irrigated rice is already faces many challenges, such as overuse of fertilizers and pesticides and water availability in rice-growing areas. In the future, the new challenges will include climate change and its consequences such as the rise in the global average surface air temperature (Krishnan *et al.*, 2011). At the end of the twenty-first century, climate projections predict an increase in surface air temperature around 1.4–5.8 °C, in several places, including Brazil (IPCC, 2013).

In Brazil, the largest rice producing country outside Asia, rice is grown practically in all states and consumed by all social classes. The state of Rio Grande do Sul (RS) located at the Southern part of the country is the top national rice producer (SOSBAI 2016). Currently, the average rice yield in RS is approximately 7.9 t ha⁻¹, being higher than the Brazilian and worldwide average 5.0 and 4.4 t ha⁻¹, respectively; (IRGA 2018; USDA 2017). In RS state, the average yield has increased in the last decade due to the adoption of cultivars with high yield potential and new management, however, oscillations in productivity

have been observed between crop growing seasons. This variation between seasons occurs, among other factors, due to the interference effects of climatic conditions (solar radiation and temperature) in the growing regions (Menezes *et al.*, 2012).

Most of the rice is currently cultivated in regions where temperatures are above the optimal for growth (28/22 °C) (Prasad *et al.*, 2006). Any further increase in mean temperature or episodes of high temperatures during sensitive stages may drastically reduce rice yields. In tropical environments, high temperature is already one of the major environmental stresses limiting rice productivity, with relatively higher temperatures causing reductions in grain weight and quality. Studies in rice have reported about 10% direct yield losses for each 1 °C increase in minimum temperature during the growing season (Baker *et al.*, 1992).

In rice, flowering is considered to be the most sensitive stage to variation in temperature. At flowering period two important yield components are defined: number of grains per panicle and grain weight. High temperatures at microsporogenesis and anthesis reduce anther dehiscence, pollen viability and germination, all these factors limiting grain yield (Matsui *et al.*, 1997). Therefore, grain yield depends mainly on the success of the spikelet fertilization.

The extent of reduction in rice yield due to heat stress also depends on several other factors, such as the duration and intensity of heat and the growth stage at which the heat episode occurs. High temperature stress induces many biochemical, physiological and molecular changes, as well as responses that influence various cellular processes of the plant (Rizhsky *et al.*, 2004). The importance to understand the molecular basis of rice heat tolerance is driven by the interest in basic knowledge and the prospect that such knowledge might

provide new strategies for improving heat tolerance in rice. Addressing the physiological and molecular mechanisms conferring heat tolerance during anthesis will help to develop rice germplasm capable of adapting to changing climates.

In plants, high temperature tolerance has been shown to be a complex phenomenon, where different genotypes have evolved different ways to cope with it (Sailaja *et al.*, 2015). Understanding the complex genetic control of heat tolerance can be reached using whole transcriptome sequencing (RNA-seq) that is currently the most powerful tool to identify genes differentially regulated (Wang *et al.*, 2009). Heat responses differ greatly between sensitive and tolerant genotypes, mainly in terms of the amount of genes and pathways involved in the response and differences in the expression level of constitutive genes in many pathways (Fracasso *et al.*, 2016). However, in rice little is known about functional elements in the genome (gene expression) involved in high temperature tolerance in reproductive structures.

With the accelerated process of global warming, heat stress damage has become a major concern in rice production throughout the world. A large number of studies have investigated the effects and mechanisms of high temperature stress on rice growth, development, grain yield and quality (Jagadish *et al.*, 2007; Sailaja *et al.*, 2015; Shi *et al.*, 2017). While in Asia and other regions, rice research has focused on heat tolerance and varieties with enhanced tolerance to heat stress have been developed, in Brazil there has been less focus on tolerance to heat stress. The focus on the last ten years in Brazil has been primarily on the development of rice cultivars with enhanced cold tolerance at seedling establishment (Menezes *et al.*, 2012). It is possible that this selection has left Brazilian varieties particularly sensitive to episodes of extreme heat.

The predicted changes include increasing frequency of extreme events, such as heat waves (Teixeira *et al.*, 2013). In 2014, a heat wave with temperatures around 40 °C, at rice flowering stage, contributed to a reduced rice production average in the RS state (IRGA 2014). Based on that, the main hypothesis of this study is that there is genetic variability between the ability of Brazilian flooded rice cultivars to tolerate heat stress at anthesis stage and in the physiological response to heat stress. Little is known about the genetic variability in heat tolerance in Brazilian cultivars and the results presented here are a first step towards understanding the potential for developing cultivars with enhanced heat tolerance and the functional dynamics of the transcripts in response to heat stress in the rice panicle.

Main objectives:

The present study aims to compare the physiological and molecular characteristics of Brazilian flooded rice cultivars with variable sensitivity to heat stress at anthesis stage and to discuss the possible processes involved in heat tolerance.

Specific objectives:

- To verify the effect of different durations of high temperature stress at anthesis stage on the spikelet fertility in different flooded rice cultivars.
- To identify differences in physiological processes that may be involved in the spikelet fertility in different flooded rice cultivars.
- To verify the effect of high temperature stress at anthesis stage on the rice panicle transcriptome.

- To identify molecular responses and metabolic pathways involved with high temperature tolerance at anthesis stage in two different flooded rice cultivars.

2 LITERATURE REVIEW

2.1 Climate change and Rice

2.1.1 Rice – an important cereal crop

Rice (*Oryza sativa* L.) is an important global crop and provides food security for many countries. Traditionally, it has been grown as a fully flooded crop and has been the major source of calories for more than half of the world's population (Normile, 2008). Rice is probably one of the most diverse crops in the world, growing in areas stretching from latitude 50 °N to 40 °S, and from sea level to an altitude of 3,000 m. In this extensive geographical area used for rice cultivation, temperatures not favorable to plant development can occur in one or more growth stages (Krishnan *et al.*, 2011). Since rice has been cultivated as a summer crop, high temperatures could occur during the seed production period, resulting in spikelet sterility and yield reduction (Prasad *et al.*, 2006). Current high temperatures have led to reduction in rice yield in many growing areas (Wassmann *et al.*, 2009). In future climatic conditions, rice yields may be reduced, depending on growing season environmental conditions.

Rice is grown on about 158 million hectares annually or on about 11% of the world's cultivated land. The ten largest rice producing countries are in decreasing order: China, India, Indonesia, Bangladesh, Vietnam, Thailand, Burma, Philippines, Japan and Brazil. Of the ten top rice producing countries, Brazil is the

only one outside Asia (USDA, 2017). Rice cultivated area in Brazil is around two million hectares and over half of it is from only one State, in the Southernmost part of the country. The State of Rio Grande do Sul (RS) is the largest national producer, and is responsible for almost 70% of the total rice produced in Brazil (SOSBAI, 2016). In RS, rice is cultivated in the Southern half of the state, where the environment is most appropriate for its cultivation.

Analyzing the history of flooded rice yield in RS, it can be noticed that the average productivity has increased in the last decade, from 5.3 Mg ha⁻¹ in 2002 to 7.9 Mg ha⁻¹ in 2017, due to the adoption of “Project 10” technologies (IRGA, 2018; Menezes *et al.*, 2012). Basically, that increase was because the adoption of cultivars with high yield potential, grain quality and with tolerance to abiotic stress, mainly cold-tolerance in the vegetative phase. Also, better field management practices, such as sowing in the recommended period was important. The recommended sowing season (September to early November) allows overlapping the plant reproductive stage with the months of the year with higher amount of solar radiation (Menezes *et al.*, 2012). When sowing occurs in the beginning of the recommended period the occurrence of low temperature at the early vegetative stage can be a limiting factor. To minimize this effect, the State breeding program focuses on low temperature tolerance at this stage (SOSBAI, 2016).

With the sowing date in the recommended period it is possible to enjoy the benefits of more favorable conditions of solar radiation in the months of December and January. However, in these months the occurrence of high temperatures during reproductive phase is more frequent, which may be harmful to flooded rice plants and limit grain yield (Sailaja *et al.*, 2015). Therefore, oscillations in productivity have been observed among crop growing seasons mainly due to the

interference effects of climatic conditions such as solar radiation and temperature during the growing season (SOSBAI, 2016; Menezes *et al.*, 2012).

2.1.2 Climate change

Intensive research on climate change in recent times shows that rising temperature may intensify storms, flooding and other severe weather events worldwide, and eventually affect food production. Climate models predict that global surface air temperatures may increase by 4-5.8 °C in the next few decades (IPCC, 2013). A gradual increase in temperature, as reflected in fewer cold days and more frequent hot days, is already discernible in most regions and will intensify in the future. In turn, the higher temperatures will further increase the intensity and frequency of stressful temperatures during crop-growing season. This future scenario has serious implications for agricultural production and human survival.

Most of the rice is currently cultivated in regions where temperature is already above the optimal growth temperatures (28/22 °C). Therefore, any further increase in mean temperature or episodes of high temperature during sensitive stages of the crop may adversely affect the growth and yield of rice. According to Baker *et al.* (1992), yield decrease was about 7-8% in rice for each 1°C increase in daytime maximum/nighttime minimum in temperature from 28/21 to 34/27. Considering the global harvested area, climate models predict that, by 2030, 16% of the rice-growing area would be exposed to at least 5 d of temperatures above the critical threshold during the reproductive period, with a non-linear increase to 27% by 2050 (Gourdji *et al.*, 2013). According to Teixeira *et al.* (2013), in the South East of Brazil, a study indicates an increase in the area of heat risk for the

cultivation of flooded rice. Similarly, a global heat-risk map for 2071–2100, with 1971–2000 as a reference, involving short episodes of heat stress coinciding with the reproductive period, resulted in more than 120 million hectares of suitable wetland rice area to be under threat (Teixeira *et al.*, 2013).

Heat waves are likely to become more frequent with global warming. A heat wave with temperatures of 38 °C, lasting for 10–20 d, contributed to an estimated total paddy yield loss of 5.18 million tons in China (Shi *et al.*, 2017). In 2014, occurrence of temperatures between 35 to 40 °C, during at least 20 days at rice flowering stage, directly affected the yield causing reduction of 8% in the RS state average (IRGA, 2014). Heat stress damage is particularly severe when high temperatures occur concomitantly with critical crop development stages, particularly the reproductive period (Jagadish *et al.*, 2009). In this sense, peaks of high temperature, even when occurring for just a few hours, can drastically reduce the production of important food crops.

Due to the significant impact of climate change on plants, the scientific community has been dedicated to study its possible impacts on crop growth, development and productivity. The largest concentration of rice production and consumption in the world is in Asia, and for that reason it is also in Asia that most of the research on rice is conducted (USDA 2017; Wassmann *et al.*, 2009). The potential negative effects of climate change on rice cultivation are a constant concern of researchers as a result of global food security.

2.2 Effect of high temperature on rice growth and development

Temperature is one of the key physical parameters affecting life on Earth. Plants are sessile organisms, so they must adapt their development in function of

the prevailing environmental conditions. Temperature is largely responsible for controlling the rate of plant development. In most cases, temperature integrated with photoperiod cues and internal plant signals, determines the duration from sowing to flowering (Rezaei *et al.*, 2015). This developmental response to temperature has provided the growing degree-day concept and does well to describe rice development. The generalized relationship between temperature and length of time required to complete development is curvilinear, indicating that time required for plant development is lengthened below and above optimum temperatures (Krishnan *et al.*, 2011).

High temperature stress affects both vegetative and reproductive development (Rezaei *et al.*, 2015). Heat stress is a complex function of intensity (temperature in degrees), duration and rate of increase in temperature (Wahid *et al.*, 2007). Rice plants are differentially sensitive to temperature stress at different times during the life cycle. Critical temperatures differ according to cultivars, duration of critical temperature and physiological status of the plant.

There are two sequential growth stages: vegetative phase from germination to panicle initiation and reproductive phase from panicle initiation to maturity (Counce *et al.*, 2000). Temperature strongly influences the rates at which these phases proceed and is probably one of the reasons for the different crop cycle length in temperate and tropical environments (Hasanuzzaman *et al.*, 2013). The entire growth process from germination to maturity includes many physiological and biochemical processes. Some processes may be temperature insensitive, others may be linearly dependent on temperature, and still others may be logarithmically dependent on temperature.

2.2.1 Vegetative phase

Morpho-physiological characteristics such as phenology, partitioning, plant-water relations, and shoot growth and extension are seriously hampered by heat stress. Increasing the temperature accelerates biochemical reactions and consequently development rate, declining the growth season length (Rezaei *et al.*, 2015). A moderate increase in temperature speeds up leaf emergence, and temperature is a principal environmental determinant of leaf appearance in rice (Counce *et al.*, 2000).

Tillers are branches that develop from the leaf axils at each unelongated node of the main shoot, the tillering rate is increased by high temperature. Tiller number per plant determines panicle number per area which is a key component of grain yield. However, rice plants with more tillers can show a greater inconsistency in mobilizing assimilates and nutrients among tillers, resulting in variations in grain development and yield among tillers (Krishnan *et al.*, 2011). Therefore, high temperature can affect the synchronism between tillers and main stem, causing mobilization of assimilates and nutrients among tillers and reducing the number of grains in the panicle of the main stem.

As high temperature accelerates crop development, the duration of crop growth phases decreases, producing negative effects on grain weight and yield in crops (Kim *et al.*, 2011). High temperature causes decline in shoot dry biomass due to reduction of vegetative phase. A major impact of high temperatures on shoot growth is the severe reduction in the internode length and leaf size, therefore, it reduces carbohydrate reserves (Wahid *et al.*, 2007). For that reason, under high temperatures, tissues and organs have less time to acquire

photoassimilates, which can result in fewer and/or smaller organs leading to less biomass accumulation.

2.2.2 Reproductive phase

Although all plant tissues are susceptible to heat stress at almost all the growth and developmental stages, the reproductive tissue is the most sensitive, and a few degrees elevation in temperature during flowering time can result in the loss of entire grain crop cycle (Hasanuzzaman *et al.*, 2013). Male reproductive organ development and its viability are determining factors for maintaining spikelet fertility under heat (Jagadish *et al.* 2010, 2014). Additionally, the formation of the rice panicle, as well as the number of spikelets per panicle during floral meristem differentiation can be affected by heat stress. The fixation of grain numbers is, therefore, a dynamic process that is determined continuously by the environment throughout reproductive development (Krishnan *et al.*, 2011).

Heat treatment (>33 °C) at rice anthesis stage significantly reduces anther dehiscence and pollen fertility rate, leading to reduction in number of pollens on the stigma which are the cause of reduced fertilization and subsequent spikelet fertility and sterile seed (Prasad *et al.*, 2006; Jagadish *et al.*, 2007). Although temperature during grain filling affects the weight per grain, the 1000-grain weight of a particular cultivar is considered to be almost constant under different environments and cultural practices (Krishnan *et al.*, 2011). The severe decline in grain yield with high temperature is related to changes in source activity, but also to sink limitation resulting from the sensitivity of flowering and pollen sterility to high temperatures (Wahid *et al.*, 2007).

2.3 How can high temperature stress cause plant injury?

Stresses can cause variable effects at all functional levels of plants. When plants are stressed, there are decreases in activity and energy for growth and development. High-temperature stress affects various biochemical and physiological processes (Krishnan *et al.*, 2011). Understanding adaptive mechanisms in plants is critical for identifying and developing high temperature tolerant cultivars.

2.3.1 Photosynthesis

Photosynthesis is one of the most heat sensitive physiological processes in plants and maintenance of high photosynthetic capacity is critical for tolerance (Hasanuzzaman *et al.*, 2013). In chloroplast, carbon metabolism of the stroma and photochemical reactions in thylakoid lamellae are considered as the primary sites of injury from heat stress. The thylakoid membrane is highly susceptible to heat stress. Major alterations occur in chloroplasts like altered structural organization of thylakoids, loss of grana stacking and swelling of grana under heat stress. Additionally, the photosystem II (PSII) activity is greatly reduced or even stops under heat stress. Also, heat stress reduces the amount of photosynthetic pigments as a result of lipid peroxidation of chloroplast and thylakoid membranes (Nouri *et al.*, 2015).

The ability of plant to sustain leaf gas exchange and CO₂ assimilation rates under heat stress is directly correlated with heat tolerance. Heat markedly affects the leaf water status, leaf stomatal conductance (g_s) and intercellular CO₂ concentration. Closure of stomata under heat stress is another reason for impaired photosynthesis that affects the intercellular CO₂ concentration (Krishnan *et al.*,

2011). Furthermore, chlorophyll fluorescence, the maximum quantum yield of PSII photochemistry (F_v/F_m), and the base fluorescence (F_0) correlate with heat tolerance (Yamada *et al.*, 1996). The F_v/F_m ratio is an important parameter for the PSII activity and any decrease in its value indicates the loss of PSII activity (Wahid *et al.*, 2007). At higher temperatures, there is an inverse relationship between maximal efficiency of PSII and the accumulated ROS.

Heat inactivation of PSII is mainly due to dissociation of oxygen-evolving complex (OEC) (Allakhverdiev *et al.*, 2008). In molecular studies, the protein abundance and transcripts of light-harvesting chlorophyll, photosystems subunits and ATP synthase complex were all decreased under heat stress, which is thought to be the main reason of photosynthesis inhibition. Around 100 proteins are controlling the reactions in thylakoid membranes. The proteins are mainly involved in the conversion of light energy to chemical energy, but several other proteins have a function in assembly, maintenance, and regulation of the multiprotein complexes (Nouri *et al.*, 2015). To cope with heat stress, plants have developed a sophisticated mechanism to repair damage to the photosynthetic apparatus. PSII reaction center D1 protein turnover plays a key role in the PSII repair cycle. This protein under heat stress conditions is phosphorylated and degraded afterwards. The plant's ability to cope with adverse heat stress is related to an efficient mechanism to avoid photosynthesis apparatus damage and, also, the activity of repair mechanisms (Wang *et al.*, 2017).

The ROS production rate in leaves increases with long durations of heat stress. The reaction centers of PSII and PSI in chloroplasts are the major site of ROS generation. Heat stress can induce oxidative stress through peroxidation of membrane lipids and disruption of cell membrane stability by protein denaturation

(Hasanuzzaman *et al.*, 2013). Therefore, a decrease in photosynthetic light reaction induces oxidative stress through ROS production caused by increased electron leakage from thylakoid membrane.

Overall, heat stress affects photosynthesis in physiological, biochemical and molecular aspects, such as destacking of thylakoid membrane, PSII damage, inhibition of cytochrome b6/f complex and ribulose-1,5-bisphosphate carboxylase/oxygenase (RuBisCO), as well as ROS production. Plants have developed several heat avoidant or tolerant strategies, such as stomatal closure, accumulation of osmoprotectants, modulation of fatty acids composition and saturation, increase of heat shock proteins, activation of ROS-scavenging enzymes activity, as well as synthesis of secondary metabolites (Wang *et al.*, 2017).

2.3.2 Carbohydrate accumulation and partitioning

Under heat stress, a reduction in source (flag leaf blade) and sink (panicle) activities may occur leading to severe reductions in grain yield. Remobilization of carbohydrate from leaves and stem of rice to grains has an important contribution to yield. However, there is considerable genotypic variation among rice genotypes for assimilate partitioning (Krishnan *et al.*, 2011). Also, the balance between carbon partitioning into storage or into export in leaf blades changes with increasing temperature. Thus, the leaf sheath plays a significant role in the temporary storage of starch.

The shorter duration of grain filling at higher temperature is determined by the earlier loss of sink activity rather than the earlier loss of source activity. Early loss of sink activity at high temperature may result from a reduction of

translocation ability and/or a loss of activity of starch synthesis-related enzymes in the grain (Wahid *et al.*, 2007). Therefore, decrease in rice grain weight is attributed to shortening of the grain filling duration due to accelerated senescence of the panicle, rather than leaf senescence (Kim *et al.*, 2011).

The sucrose synthase activity of rice grain has been observed to be positively correlated with grain sink strength and starch accumulation. At high temperatures, leaf sucrose concentration increased total nonstructural carbohydrate concentration in leaf blades, leaf sheaths, and stem (Jagadish *et al.*, 2015).

2.3.3 Heat shock proteins

Heat shock proteins (HSPs) are important for protecting cells against high temperature and other stress. HSPs can function as molecular chaperones to prevent but not reverse protein denaturation and aggregation, and as membrane stabilizers (Allakhverdiev *et al.*, 2008). Heat shock factors (HSFs) are the transcriptional activators of HSPs and other heat responsive transcripts. Induction of HSPs seems to be a universal response to temperature stress, being observed in all organisms ranging from bacteria to human. Certain HSPs are also expressed in some cells under cyclic or developmental control, such as embryogenesis, germination, pollen development and fruit maturation (Wahid *et al.*, 2007).

In plants, well-characterized HSPs can be grouped into five different families: HSP100 (or ClpB), HSP90, HSP70 (or DnaK), HSP60 (or GroE) and HSP20 (or small HSP, sHSP). The HSP70 and HSP60 proteins are among the most highly conserved proteins in nature, consistent with a fundamental role in response to heat stress. In most of the plant species, HSFs are constitutively

expressed and in normal conditions, these proteins (HSFs) are present as a monomer bound to an HSP70 in the cytoplasm. Once the plant has sensed a heat stress (increase in temperature), HSP70 dissociates from cytoplasmic monomeric HSFs and then the HSF enters into the nucleus and form a trimer that can bind with the conserved heat shock elements in the promoter region of heat responsive genes. HSF binding recruits other transcriptional components, resulting in gene expression within minutes of increased temperature (Baniwal *et al.*, 2004). Depending on whether the temperature increase is rapid or gradual, differences are observed in the production of HSPs. Under heat stress condition, HSP70 and HSP90 mRNAs can increase ten-fold, while low molecular weight HSPs can increase as much as 200-fold (Kim *et al.*, 2011).

Fast accumulation of HSPs in sensitive organs/tissues can play an important role in protection of metabolic apparatus of the cell, thereby acting as a key factor for plant adaptation to, and survival under, stress. Purified chloroplast-localized HSPs conferred heat tolerance to the photosynthetic electron transport chain in isolated chloroplast. In vivo, experiments demonstrated that small HSPs could associate with thylakoid and protect O₂ evolution and OEC proteins of PSII against heat stress. Evidence for their role in improving tolerance in plant was obtained in tomato species (Allakhverdiev *et al.*, 2008; Heckathorn *et al.*, 2002). Neta-Shair *et al.* (2005) demonstrated that chloroplasts small HSP (HSP21) induced by heat treatment in tomato leaves protected PSII from temperature-dependent oxidative stress. It is thought that chloroplast HSPs do not participate in the repair of stress-related damage, but rather they function to prevent damage (Heckathorn *et al.*, 2002).

2.3.4 Membrane injury

The cellular membranes, which regulate the flow of materials between cells and the environment as well as their internal compartments, are critical sites of high-temperature stress (Mittler *et al.*, 2012). Membranes are the first structures involved in the perception and transmission of external stress signals. Adverse effects of temperature stress on the membranes include the disruption of cellular activity or death (Saidi *et al.*, 2010). Injury to membranes from a sudden heat stress event may result either from denaturation of the membrane proteins or from melting of membrane lipids, which leads to membrane rupture and loss of cellular content, and is measured by ion leakage (Krishnan *et al.*, 2011).

High temperature increases the membrane fluidity by melting the lipid bilayer, increasing membrane permeability, and increasing leakage of ions and other cellular compounds from the cell. It was determined that an increase in saturated fatty acids in mature leaves elevated melting temperature of plasma membranes thus reducing the heat tolerance of the plant (Wahid *et al.*, 2007). Modifications in membrane structure and composition play a key role in plant adaptation to high temperature stress. In fact, maintaining proper membrane fluidity is essential for temperature stress tolerance (Sailaja *et al.*, 2015).

Increased cell damage as a result of high-temperature stress can decrease membrane thermostability, thereby disrupting water, ion, and organic solute movement across plant membranes, affecting all other metabolic activities (Saidi *et al.*, 2010). Membrane thermal stability, measured as the conductivity of electrolytes leaking from leaf disks at high temperature, is a simple technique to evaluate the performance of plants under high temperatures. According to Sailaja *et al.* (2015) rice genotypes which showed better membrane integrity also

presented the least reduction in spikelet fertility at high temperature, suggesting that plants with less electrolyte leakage/relative injury in membrane are more thermotolerant. Therefore, membrane fluidity is proposed to be the initial stress signal triggering downstream signaling processes and transcription controls, which activate stress-responsive mechanisms to reestablish homeostasis and protect and repair damaged proteins and membranes.

2.3.5 Pollen germination and spikelet sterility

Reduced fertility is a common problem associated with heat, and has been found to be caused by high temperatures during anthesis in rice. The male reproductive organs and, in particular, pollen development are the most heat sensitive. Exposure rice plants to high temperature stress during flowering result in a reduction of pollen viability and germination (Prasad *et al.*, 2006; Jagadish *et al.*, 2010). Spikelet opening triggers rapid pollen swelling, leading to anther dehiscence and pollen shedding from the anthers' apical and basal pores (Matsui *et al.*, 2001). Maternal tissues of the pistil and the female gametophyte have traditionally been considered to be more thermotolerant (Yoshida *et al.*, 1981).

High temperature was found to cause anther dehiscence outside the spikelets in susceptible cultivars resulting in poor pollination. Shedding of a high number of pollen grains on stigma, even at high temperatures, was found to be a characteristic of tolerant cultivars such as cultivar N22. The percentage fertility was found to be positively correlated with the amount of pollen on stigma at 38 °C, more than 20 germinated pollen grains are required for normal fertilization of rice spikelet (Jagadish *et al.*, 2009).

According to Buu *et al.* (2013) spikelet sterility is the characteristic with the highest correlation with high temperature tolerance in the anthesis phase. Temperatures at which spikelet sterility occurs vary among cultivars, according to Matsui 1997, temperature above 35 °C during anthesis can result in 90% of spikelet sterility in several rice cultivars. Spikelet fertility increases linearly with the number of germinated pollen grains per stigma (Matsui *et al.*, 2001; Jagadish *et al.*, 2009)

2.4 Screening for high temperature stress tolerance

There is great variation among rice genotypes regarding the high temperature tolerance during anthesis, which can be defined by different temperature thresholds. Plants from *indica* subspecies are considered more tolerant to high temperature stress than *japonica* subspecies, although tolerant genotypes have been found in both subspecies (Jagadish *et al.*, 2009). The phenotypic characteristics and genetic information to identify useful germplasm, which is crossed to create populations that are then grown and scored for important traits, need prioritization. Unfortunately, many factors affect the ability to screen for high temperature tolerance. The rate of temperature increase, the duration of high temperature, the timing of the heat stress in the context of the day, all these affect different aspects of the heat response. In field conditions, a heat stress can expose plants to combinations of these factors. Therefore identifying both physiological and molecular traits for characterization across experiments is an important demand. The knowledge of the biochemical components and their physiological effects needs to be improved to facilitate identification or selection of

material that responds well to elevated temperature while maintaining productivity in current temperature condition (Krishnan *et al.*, 2011).

Nevertheless, several screening methods and selection criteria have been developed/proposed by different researchers. Some morpho-physiological and molecular markers have been associated with heat tolerance in rice and can be used in future rice breeding programs to develop cultivars with high yield under heat stress (Zafar *et al.*, 2017).

2.4.1 Morpho-physiological markers

In rice, a strong positive correlation has been observed between high pollen fertility and yield under high temperature. Thus, evaluation of germplasm to identify sources of heat tolerance has regularly been accomplished by screening for spikelet fertility under high temperature (Jagadish *et al.*, 2009; Prasad *et al.*, 2006).

Among the physiological processes, photosynthetic rate is very heat sensitive. High photosynthetic rate at rice anthesis is positively correlated with heat tolerance (Wang *et al.*, 2017). Nagina22 (N22), the most heat tolerant cultivated *O. sativa*, maintains high photosynthetic rate and high levels of protective proteins such as HSP at anthesis stage under heat stress (Sailaja *et al.*, 2015).

The thermal stability of cell membrane can also be used as selection marker for high temperature tolerance. Heat stress effects are notable at various levels, including plasma membrane and biochemical pathways operative in the cytosol or cytoplasmic organelles. Membranes show more fluidity of lipid bilayer under heat stress (Zafar *et al.*, 2017). Rice genotypes which showed less

membrane injury also presented higher spikelet fertility under high temperature stress, being a useful marker in screening for heat tolerance (Sailaja *et al.*, 2015).

2.4.2 Molecular markers and genomic approaches

Heat tolerance is a complex trait - controlled by multiple genes at different growth plant stages. At flowering stage, it behaves like polygenic traits in rice, hence making difficult to explore its genetics and utilize in breeding program (Krishnan *et al.*, 2011). Plants usually overcome such stresses by the coordinated expression of several genes in different pathways (González-Schain *et al.*, 2015; Zhang *et al.*, 2012). A number of analyses approaches can be undertaken to study the expression of various genes. For example, rice transcriptomic and proteomic profiles under heat stress at multiple growth stages can be studied to observe differential response of genes. Thus, the accessions-genotypes-cultivars expressing the genes conferring tolerance to high temperature can be selected for future breeding purposes (Zafar *et al.*, 2017).

The identified germplasm can be explored for studying the molecular mechanisms and can also be used for identifying DNA markers which can be used in marker-assisted breeding. The use of DNA markers as diagnostic tools speeds up the breeding process (unlike traditional breeding practices). Thus, the integration of modern genomic tools in breeding would lead to meet the future global food demand. The advent of next generation sequencing approaches made the implementation of these assays accessible in exploring the rice genome (Zafar *et al.*, 2017; Krishnan *et al.*, 2011).

2.5 Mitigation and adaptation to high temperature stress

The tolerance to heat stress is addressed by making adjustments in various morphological, physiological, biochemical and molecular traits in rice plants. Plants have evolved multiple mechanisms including escape, avoidance or survival under high temperatures (Zafar *et al.*, 2017). The plasticity under heat stress in rice plant can be enhanced by facilitating basal tolerance, improving protection of components (ie photosynthesis), increasing the rapidity of the response and promoting heat escape methods.

The use of wild rice species in breeding programs can be a promising source of genes that control high temperature stress tolerance. Heat escape mechanisms can be used by wild rice species to avoid high temperature stress by moving heat-sensitive processes, such as pollen development to cooler times of the day (Jagadish *et al.*, 2015; Ohama *et al.*, 2017). Recently, the exploration of the time of day of flowering in rice, wherein the early morning flowering trait has been systematically phenotyped and isolated from wild rice *Oryza officinalis*, proved to be a useful criterion for selecting heat tolerant rice plants/genotypes. Advances in the molecular technologies have allowed for targeted incorporation of this trait into popular Asian rice cultivars, advancing their flowering time of the day to less stressful cooler hours of the morning, as an avoidance strategy (Bheemanahalli *et al.*, 2017; Prasad *et al.*, 2017).

The advent of transcriptome sequencing (RNA-seq) methods made possible to investigate gene variations and identifying large numbers of sequences more efficiently (Zhang *et al.*, 2012). Transcriptomic knowledge is essential to unveil functional elements in the genome and interpret phenotypic variation associated with gene expression. RNA-seq technology quantifies transcripts with

reduced bias compared to previous methods. RNA-Seq provides a digital count of transcript abundance which provides a more accurate reflection of the transcriptome at a given snapshot in time than previous techniques. The advantages of this improved quantification enable a more accurate picture of the biological functions and molecular networks that are responsive to a stress such as high temperature (Wang *et al.*, 2009). This allows a greater understanding of the complexity of heat tolerance in rice, which has been associated to a multigenic network.

2.6 Conclusion and future perspectives

The ability of the plant to cope with or adjust to heat stress varies across and within species, as well as at different developmental stages. The emergence of heat tolerant cultivars such as N22, which can tolerate high temperature stress in different development stages and wild rice varieties that employ heat-escape strategies by flowering in cooler times of the day, provide excellent opportunities to breed for improved resilience to heat stress. Novel genetic donors can also be identified that can tolerate heat stress across sensitive developmental stages and different environmental conditions. The search for and identification of multiple strategies to improve heat resilience needs to be intensified to provide sufficient options to mitigate the impacts of heat stress in rice. There is an urgent need to understand the rice growth and development under high temperature stress, for the purpose of identifying, selecting and breeding suitable cultivars, which are the most important tools to mitigate the adverse effects of high temperature.

The response of plants to heat stress have been studied intensively in recent years, however, a complete understanding of thermotolerance mechanisms

remains an important priority. To overcome damage at the flowering stage, phenotyping protocols have been standardized for quantifying pollen viability, but a more reliable and high-throughput technique or markers that can potentially allow assessment of large genetic panels have yet to be identified. Increased scientific knowledge on the effects of heat stress (which is predicted to increase with climate change) on rice and its cultivation will help to maintain and potentially improve yields even in the face of weather uncertainties.

3 MATERIAL AND METHODS

3.1 Plant material

In this study were used three flooded rice cultivars which were selected from previous study of heat tolerance at reproductive stage (Table 1). The cultivars are from the Germplasm Bank of IRGA Breeding Program (IRGA – Instituto Riograndense do Arroz) at Cachoeirinha/RS/Brazil. Also, the cultivars were selected to study heat response shown the following characteristics: BR-IRGA 409, one of the first modern Brazilian cultivars (released 1981) and it is known for high yield and grain quality; IRGA 428 contains the gene that confers herbicide resistance to the chemical group of imidazolinones; and DULAR has shown heat tolerance during vegetative phase (SOSBAI, 2016; Buu *et al.*, 2013). Based on results available in the literature, the temperature of 38 °C at anthesis stage (R₄ of the Counce *et al.* (2000) scale) was chosen to differentiate cultivars' sensibility. The experiment was conducted at the College of Agronomy at Federal University of Rio Grande do Sul, in Porto Alegre/RS/Brazil.

TABLE 1. Origin, subspecies and high temperature tolerance of the cultivars used in the previous study of tolerance to high temperature at anthesis stage. UFRGS, Porto Alegre, RS, Brazil. 2018.

Cultivars	Origin	Subspecie	High temperature ¹
BR-IRGA 409²	Brazil	<i>Indica</i>	Susceptible³
IRGA 417	Brazil	<i>Indica</i>	Susceptible
IRGA 428²	Brazil	<i>Indica</i>	Tolerant
IRGA 429	Brazil	<i>Indica</i>	Moderately tolerant
IRGA 430	Brazil	<i>Indica</i>	Susceptible
BLUEBELLE	USA	<i>Japonica</i>	Susceptible
CALORO	USA	<i>Japonica</i>	Susceptible
DIAMANTE	Chile	<i>Japonica</i>	Moderately tolerant
DULAR²	India	<i>Indica</i>	Susceptible

¹Five days of heat stress (38 °C for 7h/day) and light intensity of 300 $\mu\text{mol m}^{-2} \text{s}^{-1}$ at anthesis stage.

²Cultivars used in the present study. ³Heat tolerance classification by spikelet fertility (Jagadish *et al.*, 2009).

The experiment was conducted in a randomized experimental design, with the treatments arranged in a 3 x 3 two-factor scheme. Factor A consisted of cultivars and factor B, the duration of thermal stress. The number of biological replicates was ten plants per heat treatment and genotype. The treatments consisted of three flooded rice cultivars (Table 1), submitted to high temperature (38 °C) for seven hours during a period of three, five and seven days at anthesis stage (R₄) and the same three cultivars maintained in control conditions for three, five, and seven days.

Plants were grown in plastic pots with a capacity of 400 mL containing a commercial potting soil mix (Humossolo™), and maintained under flooded conditions for the whole growth period. Tillers from all the plants were removed, leaving only the main stem. This step was performed to produce uniform main culms for spikelet fertility test. No major pests and diseases were noticed during the experiment. Flag leaf was used for physiological and biochemical assays and spikelets from the middle third of the panicle were used for RNA extraction. To study the molecular response, RNA-seq was analyzed in two cultivars, IRGA 428

and IRGA 409, these were selected based on the fertilized spikelet analysis at three days of stress duration and also because they have similar flowering time and maturity duration.

3.2 Plant growth

Plants were maintained until panicle exposure at greenhouse with climate control, when they were moved to controlled-environment chambers (Conviron BDW40), and subject to different temperature treatments. After, plants were returned to the greenhouse until the harvest. The photoperiod was 14/10 hours (day / night) and the photosynthetic photon flux density was maintained at 600 $\mu\text{mol m}^{-2}\text{s}^{-1}$. The CO_2 concentration was not measured. Treated and untreated plants were maintained at growth chambers for three, five and seven days. Table 2 shows the scheme of thermal treatments during a period of 24 hours. Plants were submitted to high temperature (38 °C) from 9:00 am to 4:00 pm.

TABLE 2. Scheme of application of thermal treatments (three, five and seven days) in a period of 24 hours. UFRGS, Porto Alegre, RS, Brazil. 2018.

Treatment	8 pm to 6 am	6 am to 9 am	9 am to 4 pm	4 pm to 8 pm
Untreated	25 °C	29 °C	29 °C	29 °C
Treated	25 °C	29 °C	38 °C	29 °C

3.3 Filled spikelets/panicle and spikelet fertility (%)

At harvest, the filled and unfilled spikelets were separated from the panicle and counted. Whether the spikelet was filled or not was determined by pressing each floret between the forefinger and the thumb. Spikelets were considered filled for both completely and partially filled grains. Spikelet fertility was determined

using the ratio of the number of filled spikelets to the total number of spikelets (florets), in the average of four replicates. It was calculated using the formula:

$$\text{Number of filled spikelets} / \text{Total number of spikelets} \times 100$$

3.4 Percentage of fertility reduction in spikelet

Sensitivity to high temperature was expressed as the percentage of reduction in spikelet fertility obtained by the formula:

$$\% \text{ fertility reduction} = [(\% \text{ fertility at high temperature treatment} \times 100) / \% \text{ fertility at control treatment}] - 100$$

3.5 Photosynthetic parameters

To evaluate the effect of heat stress duration on photosynthesis, photosynthetic characteristics were measured in all cultivars at anthesis stage. Net photosynthetic rate (P_N) and stomatal conductance (g_s) were measured on the flag leaf using LI6400XT portable photosynthesis measuring system (LI-COR Environmental, USA). Measurements were made at PAR (photosynthetically active radiation) of $1,000 \mu\text{mol m}^{-2} \text{s}^{-1}$ with CO_2 concentration maintained at $400 \mu\text{mol mol}^{-1}$ and 60 of relative humid. The parameters were sampled always in the same time of the day (11:00 am) and in five replicates.

3.6 Chlorophyll fluorescence

Chlorophyll fluorescence was measured on flag leaf of plants submitted to thermal treatments on the third, fifth and seventh day of stress duration with a portable fluorometer (OS1-FL Chlorophyll Fluorometer - Opti-Sciences). The photosystem II (PSII) quantum yield and the electron transport rate (ETR) were

measured. The parameters were sampled always in the same time of the day (11:00 am) and in five replicates.

3.7 Hydrogen peroxide content

Flag leaf of the three cultivars was collected at anthesis stage (on the third, fifth and seventh day). Hydrogen peroxide (H_2O_2) content was measured in plants under heat stress and control condition. H_2O_2 content was normalized to the control condition, the values presented are relative to the control in each evaluation day for each cultivar. One gram of leaf tissue was first ground in liquid nitrogen with pre chilled mortar and pestle. The ground tissue was homogenized in 0.1 mM phosphate buffer (pH 7.0) containing 0.5 M EDTA. The homogenized tissue was centrifuged at 3000 rcf for 15 min at 4 °C and collected the supernatant. The amount of H_2O_2 released by leaf was determined by the Amplifu® Red (Sigma-Aldrich) oxidation method, as described previously (Smith *et al.*, 2004). After preparation of all solutions, an aliquot of stock solution of Bradford-Sigma-Aldrich reagent was diluted 5x. Individual wells of an Elisa microplate, 195 μL of that reagent, 1 μL of Amplex® Red reagent/HRP, 1 μL of extraction buffer and 1 μL of peroxidase p8375-Sigma-Aldrich per well at a concentration of 2 μM were pipetted. Then, 5 μL of sample and BSA were added at increasing and known concentrations to make the standard curve. Samples were incubated for 10 minutes at room temperature and analyzed on Spectro Max M4 spectrophotometer for excitation and emission at the wavelengths of 563 nm (slit 5 nm) and 587 nm (slit 5 nm), respectively.

3.8 Statistical analysis

The data were analyzed by Analysis of Variance (ANOVA), using the statistical computer program Assistat Ver. 7.7. The differences among cultivars and duration of heat treatments were compared using the Tukey test (p-value <0.05).

3.9 High-throughput mRNA sequencing (RNA-seq)

3.9.1 RNA extraction and RNA-seq library preparation

Tissue samples were stored at -80°C until needed. Panicle samples were first ground in liquid nitrogen with pre chilled mortar and pestle. Total RNA was extracted from spikelet from the middle third of the panicle with Concert™ Plant RNA Reagent (Invitrogen), according to the manufacturer's protocol. The RNA concentration was measured with NANODrop 2000 (Thermo Fisher Scientific). It was used for sequence analysis the RNA from cultivars IRGA 428 and IRGA 409, at three days of duration stress.

RNA samples were shipped on RNastable tubes (Biomatrica, San Diego/USA) to NCSU (North Carolina State University) for RNA-seq. Two micrograms of RNA was used with NEBNext Poly(A) Magnetic mRNA isolation kit (New England Biolabs, Ipswich/USA). Oligo(dT) attached to magnetic beads isolated mRNA by attaching to poly(A) modified mRNA. Before library preparation, mRNA was heated to 95 °C for the recommended 15 minutes to achieve 150-200bp fragment sizes. NEBNext Ultra Directional RNA Library Prep Kit for Illumina (New England Biolabs, Ipswich/USA) was then used to prepare mRNA for sequencing. The handbook recommendations were followed in all steps. Second synthesis was done with a dUTP mix for a directional RNA library. AMPure beads

were then used to clean the cDNA before and after end repair and adaptor ligation steps. After, end repair and adaptor ligation size selection with AMPure beads followed the recommended volumes to isolate 150-200bp fragments and to remove any leftover adaptors. PCR library enrichments were then done with inclusion of USER step for strand specificity following protocol recommendations. Fifteen cycles (the maximum recommended number of cycles) were used for amplification. It was not observed over amplification peaks.

Libraries were run on 2100 Agilent Bioanalyzer (Raleigh/USA) high sensitivity DNA chip after a 1:4 (or 1:10 if necessary dilution) for quantification. Finally, libraries were diluted to 10 nmol/μl concentrations before being sent to sequencing. Sequencing was done at NCSU's Genomics Science Laboratory (Raleigh/USA). Samples were run on Illumina Hiseq 2500 150bp single end reads. The raw reads were stored in a fastq format.

3.9.2 RNAseq data alignment and quantification

Initial quality control was performed using FastQC version 0.11.5 (Merchant *et al.*, 2016) (Appendix 8). After FastQC, fastq files were trimmed by Trimmomatic version 0.33 (Bolger *et al.*, 2014; Merchant *et al.*, 2016). Short reads were filtered by removing adaptor contaminations and low-quality reads. It was used the quality filtering functionality of this tool with sliding window, which scans through reads from the 5' end, and removes following bases from the 3' end once the average quality score within the window drops below a user-specified value (HEADCROP:9; ILLUMINACLIP:Adapters.fa:2:30:10; SLIDINGWINDOW:4:15 MINLEN:36) (Appendix 9).

Trimmed files were aligned using Hisat v2.05 (Merchant *et al.*, 2016). Reads were mapped to the *indica* variety MH63 and *japonica* rice Nipponbare (MSU v7). The *indica* reference genome and annotation files were obtained from <http://rice.hzau.edu.cn/rice> (Zhang *et al.*, 2016). The *japonica* reference genome and annotation files were obtained from the rice IRGSP-1.0 genome (Kawahara *et al.*, 2013). Library type was set to firststrand and the rest of the parameters remained as the default. The resulting bam files were then piped to HTseq count version 0.6.1 (Merchant *et al.*, 2016). Using the options -f bam, -s reverse, and -m intersection-nonempty, counts per gene were generated for the annotated genes in MH63 (*indica* subspecies) and MSUv7 (*japonica* subspecies) genomes. Each sample had 80 % or more reads mapped against the MH63 genome annotation and 90 % or greater reads mapped against the japonica annotation.

3.9.3 Differential expression

Raw counts matrix was used for differential expression analysis with EdgeR version 3.10.5 in R version 3.2.1. First, genes were filtered by counts; genes with less than five counts in less than three samples were discarded. Normalization was performed according to the EdgeR pipeline. To test for differential expression, EdgeR's generalized linear models were used and a likelihood ratio test determined differential expression of transcripts. Using filtered and aligned reads, transcript levels were used to find differentially expressed genes (DEGs) at different thermal condition and cultivars. DEGs were identified using EdgeR, if the difference in expression was greater than a Log₂ Fold Change of 0.5 (LogFC ≥0.5) and the Benjamini-Hochberg adjusted *p*-value was <0.01. Stricter cutoffs were

used for some comparisons as described in the main text. The base R plot function was used to create the plot figures related to transcript level of the DEGs.

3.9.4 Functional annotation

After DEGs, the genes mapped to *indica* genome were converted to genes orthologous to *japonica* genome (MSU - Michigan State University Rice Genome Annotation Project) (Ouyang *et al.*, 2007). Orthologous genes were obtained by submitting MH63 gene IDs in the platform Rice information GateWay (RIGW, <http://rice.hzau.edu.cn/>), then returned MSU gene IDs. This allowed to obtain Gene Ontology (GO) annotation to perform functional classification. GO is a standardized gene functional classification system. GO enrichment analysis allows to compare the biological functions of DEGs. The DEGs in response to heat stress were further analyzed for GO functional annotation, using MapMan ontology (Thimm *et al.*, 2004) visualized by Cytoscape plug-in BiNGO (Maere *et al.*, 2005), and calculating gene numbers for every term.

The significance of the overlap between the DEGs identified in this study and previous studies was determined by hypergeometric enrichment test. Since the total number of genes tested in the previous studies was not information that was provided, we used 16,240 as the total detected number for this data set. This number is representative for the number of detected genes in this and in other RNA-Seq studies in rice cultivars.

4 RESULTS

4.1 Fertilized spikelets

Significant effect of cultivars and duration of heat stress was recorded for number of filled spikelet per stem (Figure 1 A and B). For all cultivars, spikelet fertility was decreased with increasing duration of the heat stress. At seven days in high temperature stress, the maximum reduction of fertilized spikelet was observed for all cultivars (above 95 %) compared with control plants. At three days of duration stress, IRGA 409 maintained the highest spikelet fertility (55 %) compared to the other two cultivars (IRGA 428 – 39 %; DULAR – 22 %). Across all cultivars, high temperature stress showed a significant negative impact on spikelet fertility.

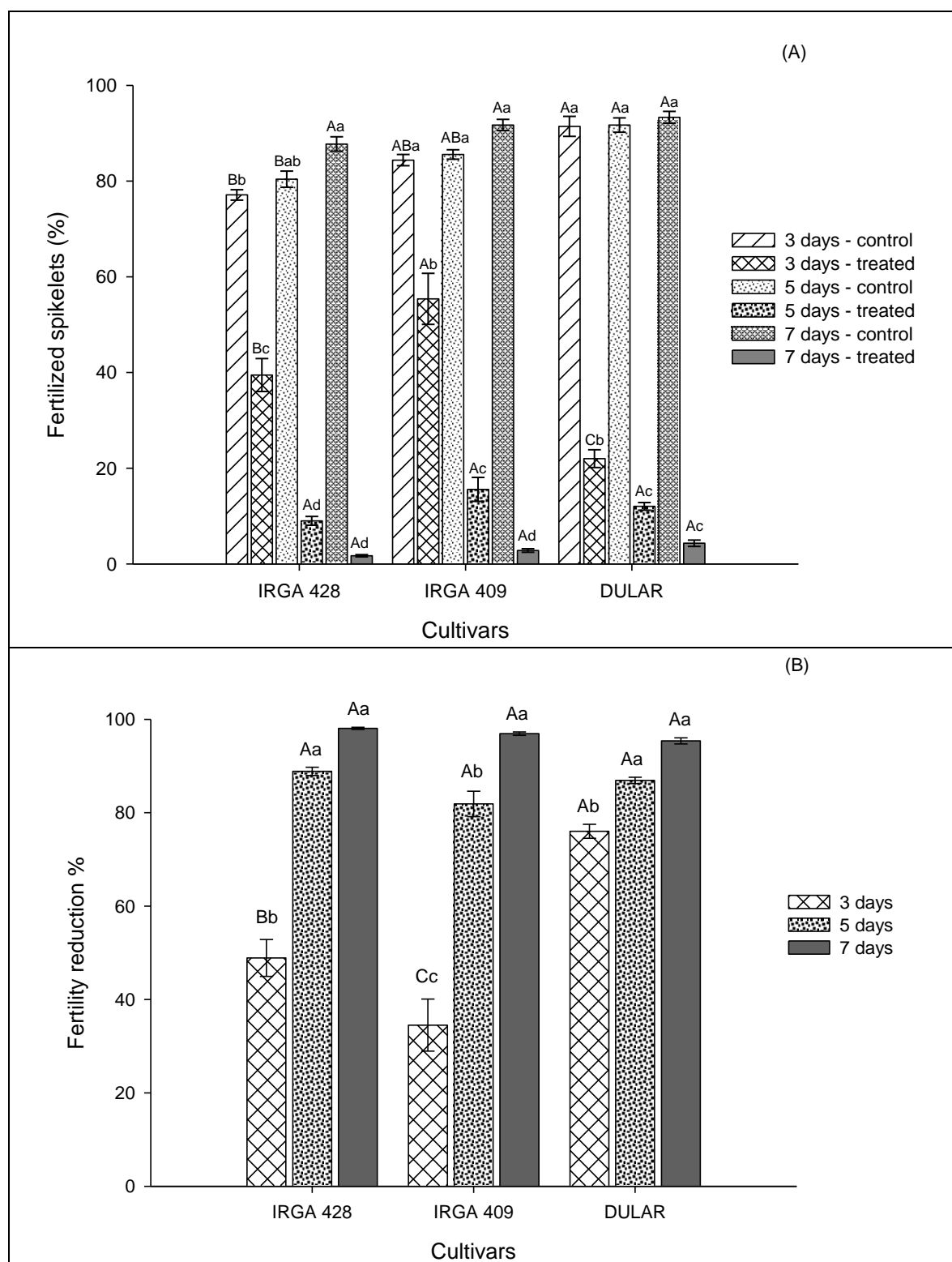


FIGURE 1. Effect of duration of high temperature on percentage (%) of spikelet fertility (A) and on reduction of fertilized spikelets (B) in three flooded rice cultivars. Each value represents means of five replications \pm SD. Means followed by the same capital letter do not differ significantly among cultivars in each treatment condition and lowercase letter do not differ significantly among treatment conditions in each cultivar by Tukey's test (p -value < 0.05). UFRGS, Porto Alegre, RS, Brazil. 2018.

4.2 Photosynthesis parameters

Reduction in net photosynthetic rate (P_N) was observed in IRGA 428 and IRGA 409 cultivars across all durations of heat stress when compared with control condition (Figure 2A). On the contrary, in DULAR, an increase in P_N was observed at three and five days of stress duration. At seven days of high temperature stress, IRGA 428 showed the maximum reduction of P_N (66 %), whereas minimum reduction of P_N was observed in IRGA 409 (14 %) at the same time. Similar results were observed for stomatal conductance (g_s), IRGA 428 and IRGA 409 cultivars showed reductions in g_s at three and five days of stress duration (Figure 2B). However, at seven days there was a large difference in g_s between IRGA 409 which increased g_s (+12 %) and IRGA 428 which showed a continued reduction reaching 79 % of the control. In contrast, cultivar DULAR increased g_s in three and five days of heat stress duration, but showed no significant difference between heat stress and control at seven days.

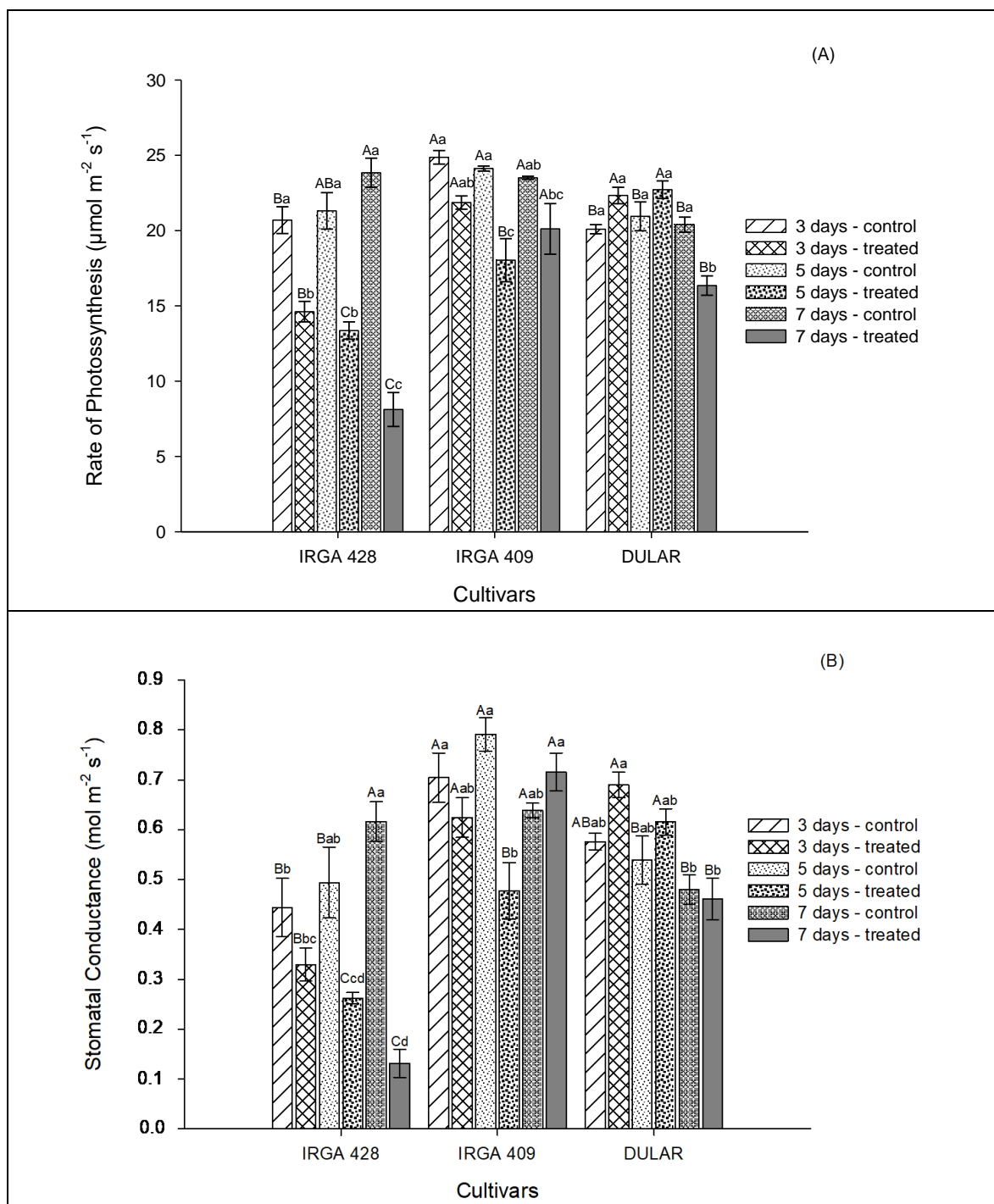


FIGURE 2. Effect of duration of high temperature on photosynthetic rate (A) and on stomatal conductance (B) in three flooded rice cultivars. Each value represents means of five replications \pm SD. Means followed by the same capital letter do not differ significantly among cultivars in each treatment condition and lowercase letter do not differ significantly among treatment conditions in each cultivar by Tukey's test (p -value < 0.05). UFRGS, Porto Alegre, RS, Brazil. 2018.

4.3 Fluorescence parameters

There was significant effect of stress duration and cultivar on the fluorescence parameters such as quantum yield of photosystem II (PSII) and electron transport rate (ETR) (Figure 3 A & B). Both DULAR and IRGA 428 cultivars showed a marginal reduction in quantum yield and ETR, with the most significant reduction at seven days of heat stress. Cultivar IRGA 409 showed a slight increase in quantum yield of PSII across all stress duration.

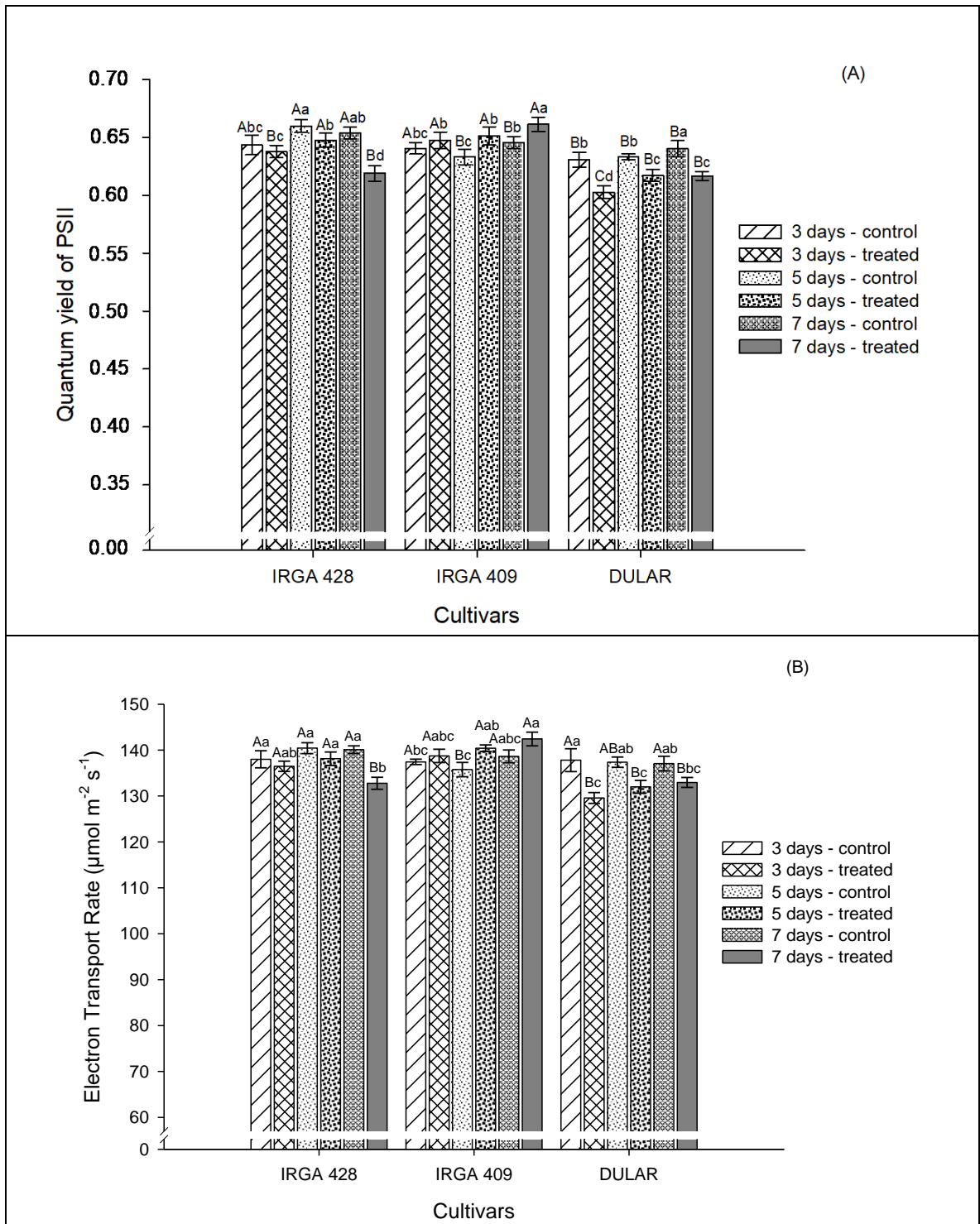


FIGURE 3. Effect of duration of high temperature stress on quantum yield of PSII (A) and electron transport rate (ETR) (B) in three flooded rice cultivars. Each value represents means of five replications \pm SD. Means followed by the same capital letter do not differ significantly among cultivars in each treatment condition and lowercase letter do not differ significantly among treatment conditions in each cultivar by Tukey's test (p -value < 0.05). UFRGS, Porto Alegre, RS, Brazil. 2018

4.4 Hydrogen peroxide content

Significant differences in H_2O_2 content was observed among cultivars and periods of stress duration (Figure 4). IRGA 409 and IRGA 428 cultivars showed increases in the H_2O_2 content among periods of stress duration. On the other hand, DULAR showed a reduction in H_2O_2 content after five days of heat stress when compared with control. Maximum increase was observed in the cultivar DULAR at three days of stress duration. IRGA 409 increased H_2O_2 content with increasing stress duration. In contrast, the H_2O_2 content in IRGA 428 decreased with longer exposure to heat stress, peaking at three days of stress.

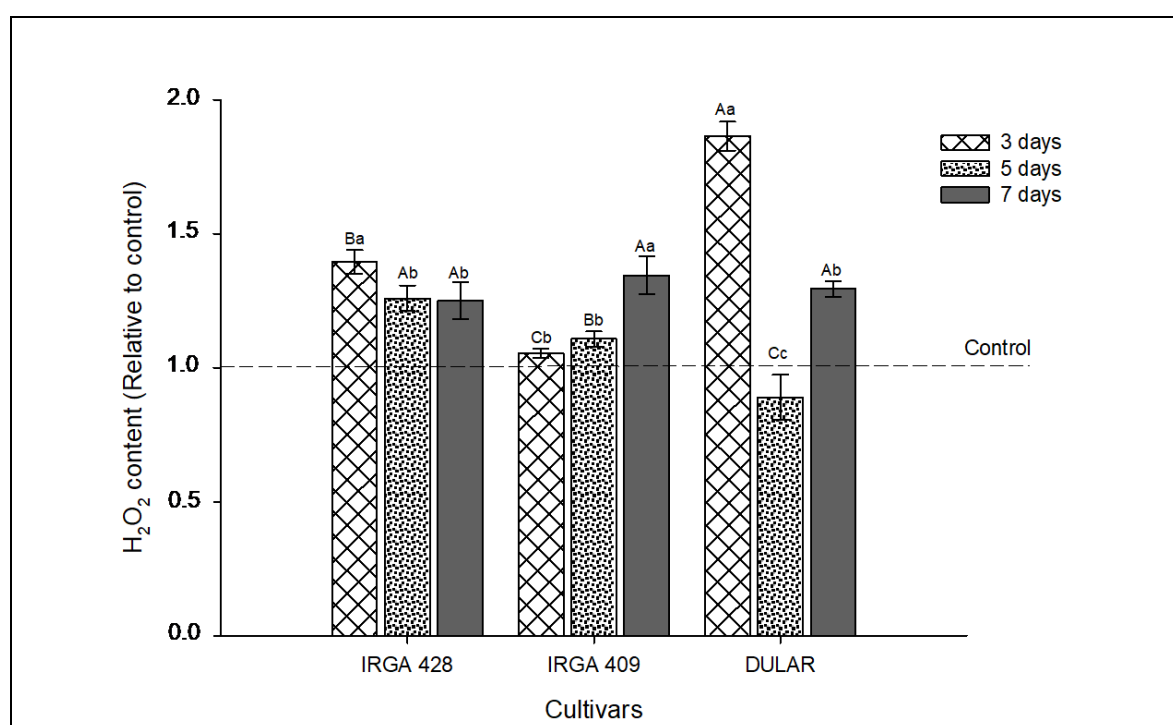


FIGURE 4. Effect of duration of high temperature on hydrogen peroxide content relative to control in three flooded rice cultivars. The dashed line represents untreated plants. Each value represents means of five replications \pm SD. Means followed by the same capital letter do not differ significantly among cultivars in each period of duration stress and lowercase letter do not differ significantly among period of duration stress in each cultivar by Tukey's test (p -value < 0.01). UFRGS, Porto Alegre, RS, Brazil. 2018.

4.5 High-throughput mRNA sequencing (RNA-seq)

4.5.1 Transcriptome sequencing and mapping of the reads

To understand the gene expression change of rice spikelet in response to heat stress, it was performed RNA-Seq analysis on the IRGA 409 and IRGA 428 cultivars after three days of thermal treatment. At this time point, the cultivars showed the highest difference in spikelet fertility after heat treatment, 55 % for IRGA 409 and 39 % for IRGA 428. There are reference genomes available for *japonica* (Kawahara *et al.*, 2013) and *indica* (Zhang *et al.*, 2016) rice subspecies. However, since IRGA 409 and IRGA 428 are a mix of the *japonica* and *indica* backgrounds, reads were mapped to both the *japonica* (*Nipponbare*) and the *indica* (*MH63*) reference genomes and compared the ability to identify differentially expressed genes depending on the mapping background. When both cultivars were mapped to the *japonica* genome there were 2.9 % more totally mapped reads than when mapped to the *indica* genome (Figure 5). Uniquely mapped reads, which refer to the number of reads that have no mismatches or insertions/deletions (InDels) were similar between reference genomes, 73.6 % for *japonica* and 74.2 % for *indica* genome. However, mapping to the *japonica* genome resulted in more multiple mapped reads (3.9 %) than when mapped to the *indica* genome. Because these results suggest that the choice of reference genome may have a substantial effect on the downstream analysis, it was continued to examine the results of both mappings for differential expression analysis.

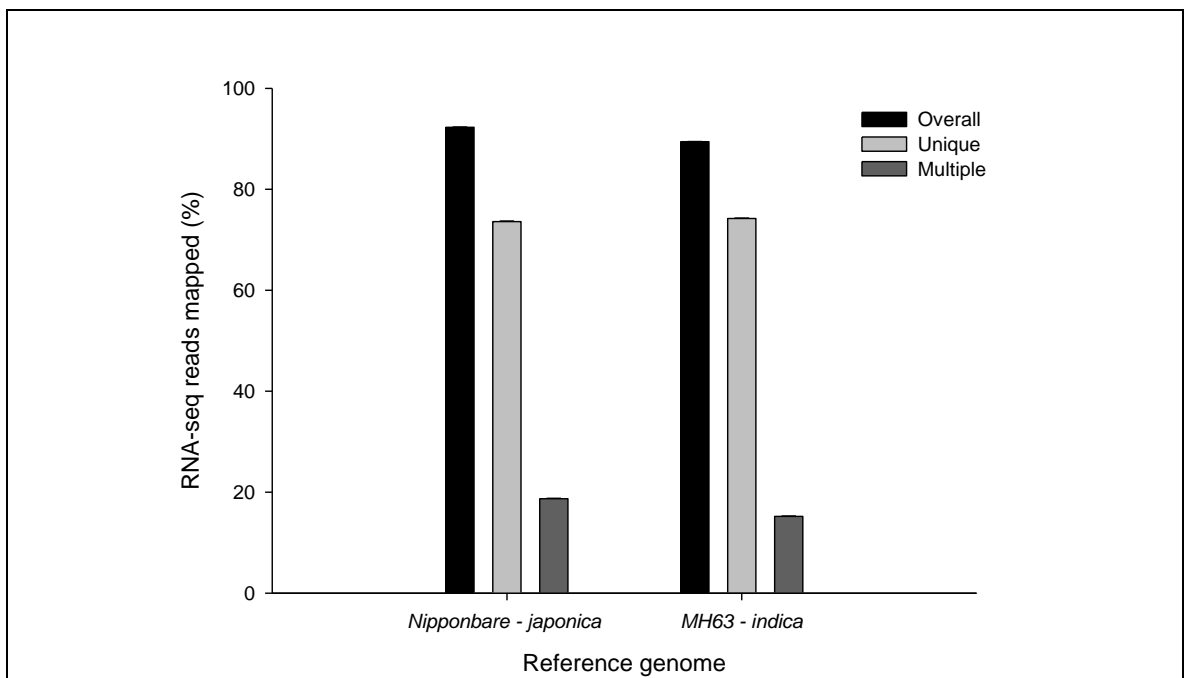


FIGURE 5. RNA-seq reads from rice flowers mapped to the reference genome of *japonica* (Nipponbare) and *indica* (MH63). Percentage of mapped reads in each reference genome, in black bars the total covered by mapped reads, in light-grey bars the percentage of mapped reads that have no mismatches or InDels and, in dark-grey bars the percentage of mapped reads to multiple locations such as repeat sequences. UFRGS, Porto Alegre, RS, Brazil. 2018.

4.5.2 Global analysis of gene expression

It was analyzed differentially expressed genes (DEGs) between different treatments to identify genes with a significant change in expression in response to heat stress for each cultivar (Figure 6). The choice of mapping genome has a significant effect on the identified DEGs. Identifying DEGs in response to heat for each cultivar (multi-factor analysis - cultivars vs control and high temperature) when mapped to the *indica* genome resulted in 2,064 genes for IRGA 409 and in 1,078 genes for IRGA 428 that showed a response to heat stress (adjusted p -value <0.001). In contrast, the same analysis using reads mapped to the *japonica* genome resulted in 1,735 and 524 genes (adjusted p -value <0.001), for IRGA 409 and IRGA 428, respectively. When it was examined the multi-factor responsive

genes, that is genes with an interaction between cultivar and heat stress, it was identified 65 and 14 DEGs in the *indica*- and *japonica*-mapped reads (adjusted p -value <0.001), respectively.

To better understand heat response in each mapped genome, it was presented the DEGs in up and down-regulated genes (Figure 6). For the DEGs mapped to the *indica* genome it was identified 758 significantly down-regulated genes in IRGA 409 and 507 genes in IRGA 428 (adjusted p -value <0.001). The up-regulated genes for the same condition and mapped genome revealed 1,306 significantly genes in IRGA 409 and 571 genes in IRGA 428 (adjusted p -value <0.001) (Figure 6). For the same analysis the DEGs mapped to the *japonica* genome, it was identified 590 significantly down-regulated genes in IRGA 409 and 230 genes in IRGA 428 (adjusted p -value <0.001). Thus, the up-regulated genes mapped to the same genome revealed 1,145 significantly genes in IRGA 409 and 294 genes in IRGA 428 (adjusted p -value <0.001). This result shows that, for the time point analyzed, the effect of high temperature stress in both cultivars and mapped genomes resulted in more induction than repression of gene expression. On the other hand, DEGs in multi-factor contrast analysis, comparing cultivar and heat response interactions, showed more down-regulated than up-regulated genes in both mapped genome (adjusted p -value <0.001).

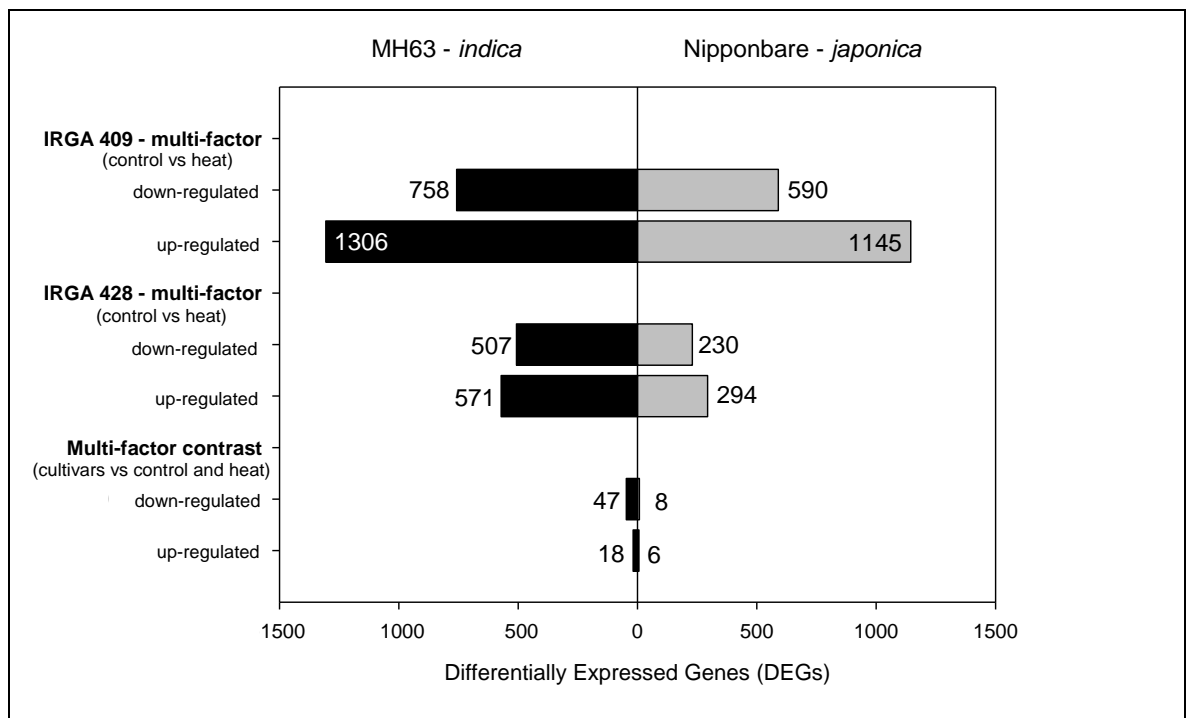


FIGURE 6. Differential expression of genes in response to high temperature compared to control condition in two flooded rice cultivars. Numbers of DEGs identified when mapped in *indica* and *japonica* reference genome are represented in black and gray bars, respectively. The differences in gene expression were obtained based on the LogFC ≥ 0.5 and adjusted p -value < 0.001 . UFRGS, Porto Alegre, RS, Brazil. 2018.

Differences in gene expression were explored in DEGs mapped to *indica* reference genome, which showed less multiple mapping and more number of DEGs compared to the *japonica* genome. To visualize the unique and conserved responses to high temperature in IRGA 409 and IRGA 428, it was examined the overlap in up and down-regulated DEGs (Figure 7). The Venn diagram indicates the overlap of DEGs in response to heat stress between cultivars. Of the 1,877 genes identified as induced in response to this stress at three days in either cultivar, 11.1 % (187 genes) were shared between both cultivars.

The functional categorization of the genes that were up-regulated in response to heat in both cultivars using enrichment analysis by MapMan ontology (Thimm *et al.*, 2004), visualized in Cytoscape plug-in BiNGO (Maere *et al.*, 2005),

was also examined. These conserved responses were enriched for heat stress response (p -value $<1 \times 10^{-9}$) and RNA processing (p -value <0.13) (Figure 8A). The genes that were down-regulated in response to heat showed a conserved set between cultivars that was 29 % (284 genes) of the total 1,877 down-regulated genes observed in either cultivar. These conserved down-regulated genes showed enrichment for transcription regulation (p -value $<1 \times 10^{-6}$), DNA synthesis (p -value $<1 \times 10^{-15}$), cell cycle, and organization (p -value <0.01) (Figure 8B). The unique response in each cultivar was examined next. At the same stringency level, IRGA 409 had almost three times as many transcripts that were up-regulated and more than twice as many down-regulated DEGs in response to heat stress compared to cultivar IRGA 428 (Figure 7).

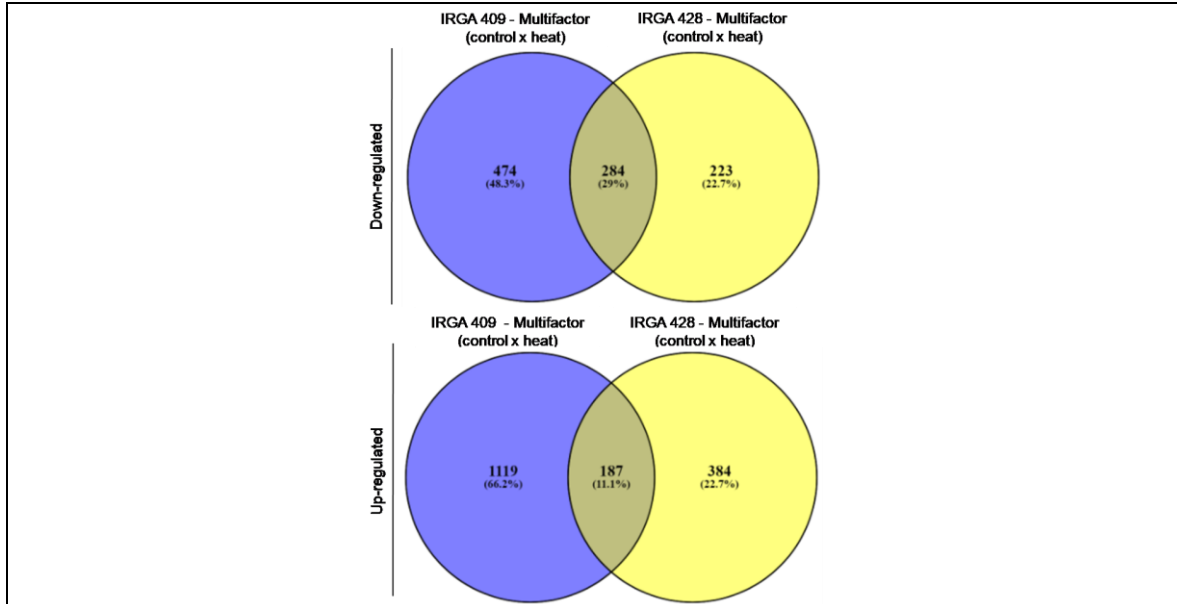


FIGURE 7. Venn diagram, overlap of expressed genes in response to high temperature stress in two flooded rice cultivars, for up and down-regulated genes. UFRGS, Porto Alegre, RS, Brazil. 2018.

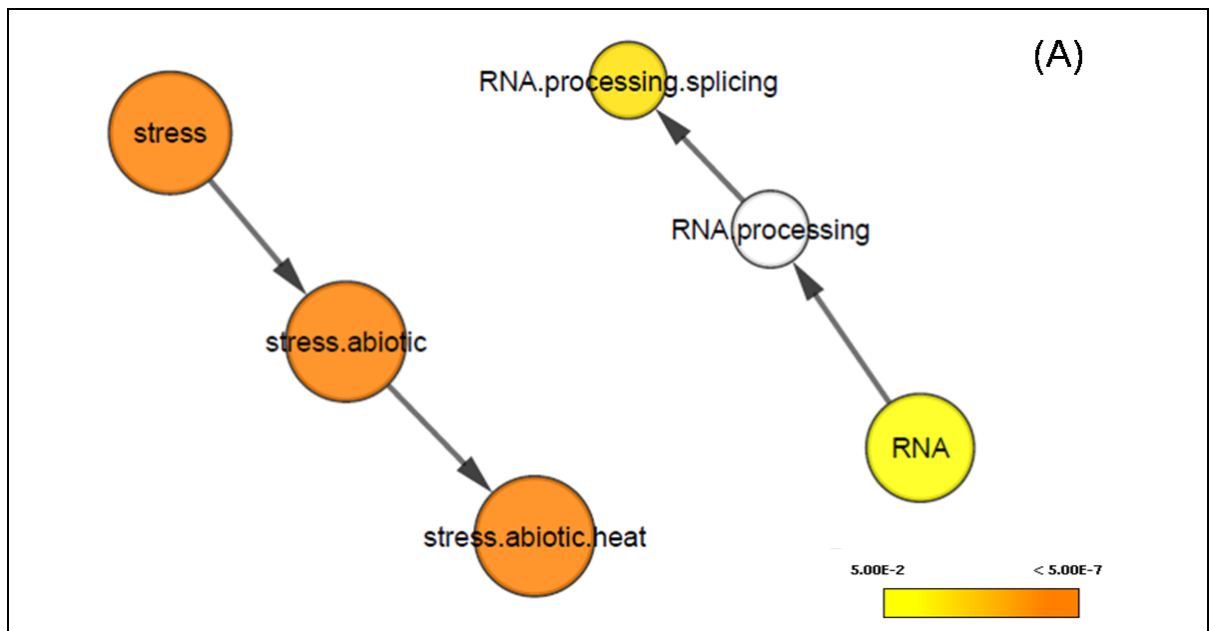
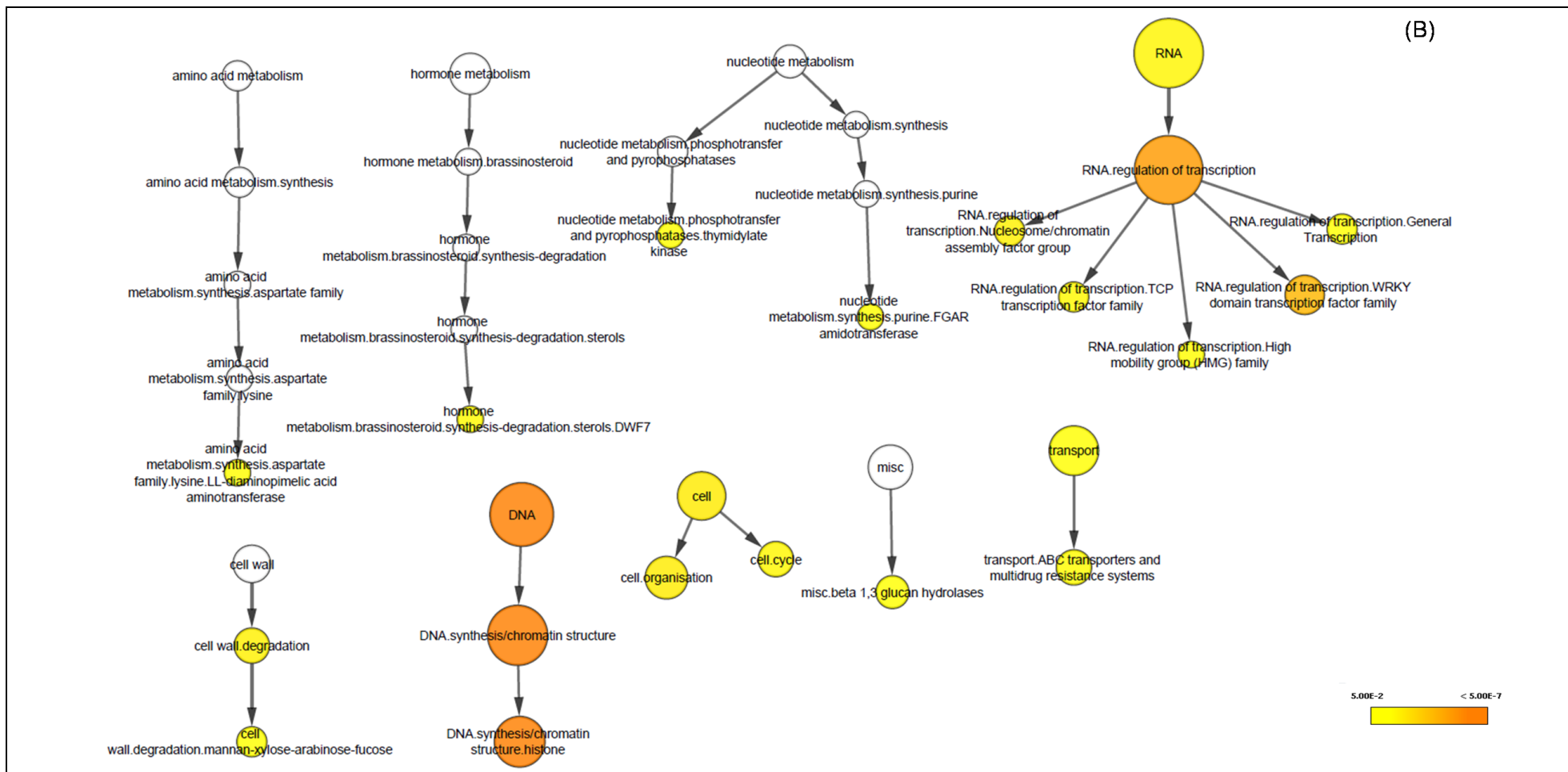


FIGURE 8. Overview of pathways overrepresented in conserved genes up-regulated (A) and down-regulated (B), according to enrichment analysis using MapMan ontology visualized by Cytoscape plug-in BiNGO. The color scale indicates significance of enrichment analysis and the size of nodes indicates the numbers of mapped genes. The arrows represent the relationship between parent-child terms. UFRGS, Porto Alegre, RS, Brazil. 2018.



Continuation FIGURE 8. Overview of pathways overrepresented in conserved genes up-regulated (A) and down-regulated (B), according to enrichment analysis using MapMan ontology visualized by Cytoscape plug-in BiNGO. The color scale indicates significance of enrichment analysis and the size of nodes indicates the numbers of genes were mapped. The arrows represent the relationship between parent-child terms. UFRGS, Porto Alegre, RS, Brazil. 2018.

4.5.3 Pathway enrichment for DEGs

Enrichment analysis was performed to verify the pathways and biological processes that are altered at the mRNA level in response to three days of heat stress in IRGA 409 and IRGA 428, using the MapMan and GO ontologies. GO enrichment analysis was performed to reveal the biological processes overrepresented under heat stress in each cultivar and also focused on the unique response in IRGA 428 cultivar. Additionally, GO enrichment was accomplished in the genes of contrast analysis (interaction between cultivars and heat stress).

4.5.3.1 High temperature effects - MapMan ontology

In Figure 6 are shown 2,064 DEGs from cultivar IRGA 409 (1402 genes orthologous to *japonica* to which the ontologies are mapped). The enrichment analysis identified 17 MapMan enriched categories (p -value <0.05) (Figures 9A). Each functional category is size and color-coded, so that larger nodes have more genes and darker nodes are more significantly enriched. The enrichment of the functional categories observed included hormone metabolism (p -value $<7 \times 10^{-5}$), major carbohydrate metabolism (p -value $<6 \times 10^{-4}$), transcriptional regulation (p -value $<4 \times 10^{-4}$), cell wall degradation (p -value $<3 \times 10^{-4}$), protein degradation (p -value <0.005), protein modification (p -value <0.01), transport (p -value $<4 \times 10^{-19}$), heat stress responses (p -value $<8 \times 10^{-9}$), and DNA synthesis/chromatin structure (p -value $<1 \times 10^{-6}$). While most of these categories were also observed to be enriched in the DEGs responsive to heat in IRGA 428, a few differences stand out.

Of the 1,078 DEGs (777 genes orthologous to *japonica*) in IRGA 428, the enrichment analysis identified 11 MapMan categories significantly enriched (Figure 9B). Unlike IRGA 409, in the DEGs in IRGA 428, enrichment was observed for

genes associated with tetrapyrrole synthesis, and many categories in a single pathway associated with photosynthesis activity. In contrast, the pathway of major carbohydrate metabolism, including sucrose invertases, was identified as enriched in the DEGs from IRGA 409, but not for IRGA 428. In IRGA 409, the category for hormone metabolism and the subcategories associated with gibberellin and ethylene were enriched, while in IRGA 428, auxin signal transduction was enriched.

While many of the larger categories were similar, the enrichment of subcategories suggests a unique response in each cultivar. For example, although the category for cell wall was identified as enriched in both cultivars, in IRGA 409 the subcategories associated with cell wall degradation were enriched (p -value $<3 \times 10^{-4}$). In contrast, in IRGA 428 the cell wall subcategories of cell wall proteins leucine rich receptor kinases (p -value <0.01) and arabinogalactan proteins (p -value $<3 \times 10^{-4}$) were enriched. Other categories unique to IRGA 428 include cell-cycle (p -value <0.01), transport-associated major intrinsic proteins (p -value $<5 \times 10^{-5}$), TCP (TEOSINTE BRANCHED 1/CYCLOIDEA/PROLIFERATING CELL FACTOR 1) transcription factors (p -value <0.02). Categories unique to IRGA 409 include calcium-signaling (p -value <0.01), transport-associated potassium transport (p -value <0.004), p - and v -type ATPases (p -value <0.004), MADS box (MCM1/AGAMOUS/DEFICIENS/SRF) transcription factors (p -value <0.01), mitochondrial membrane associated metabolite transport (p -value <0.005), and amino acid transport (p -value <0.01).

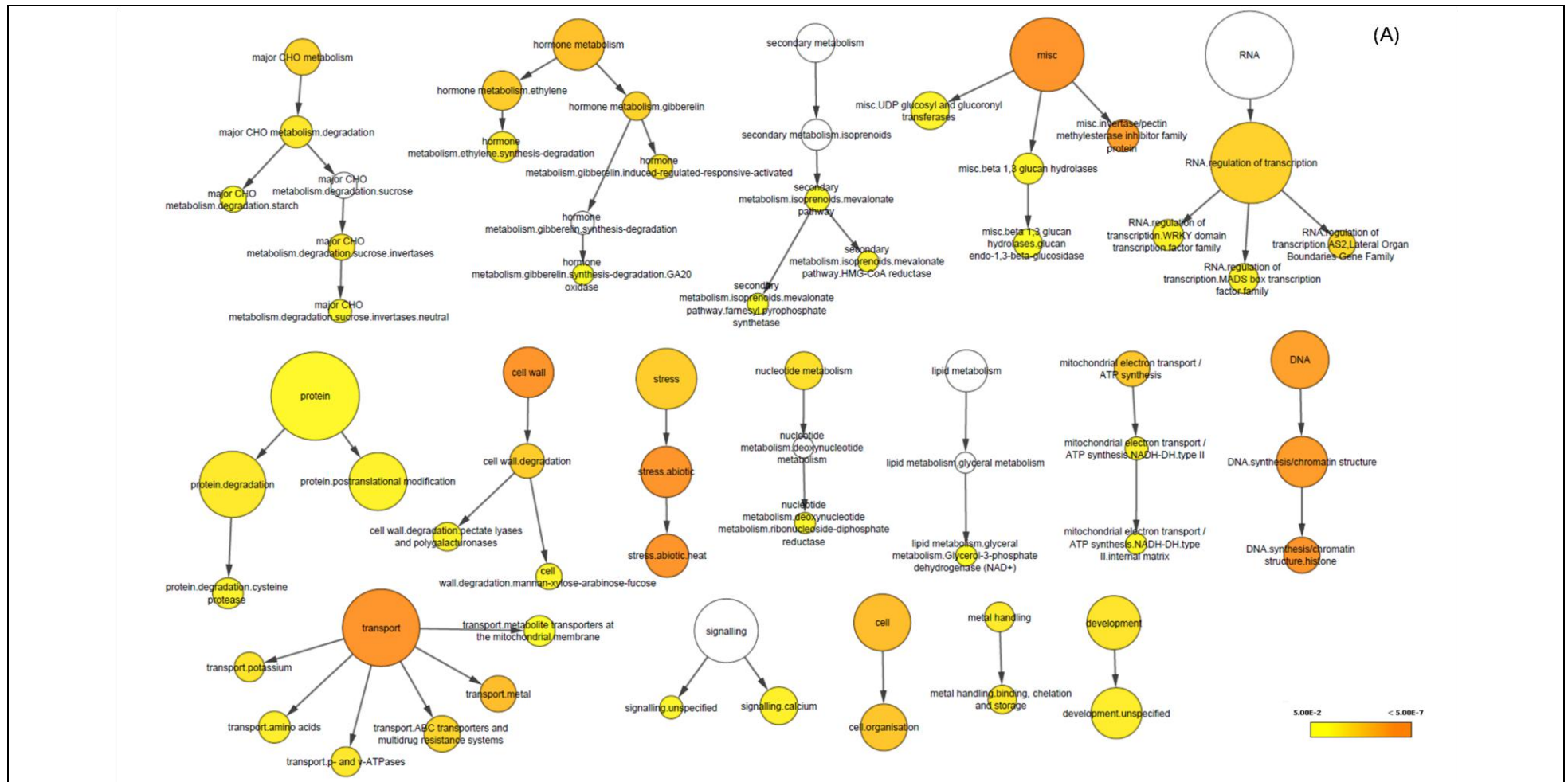
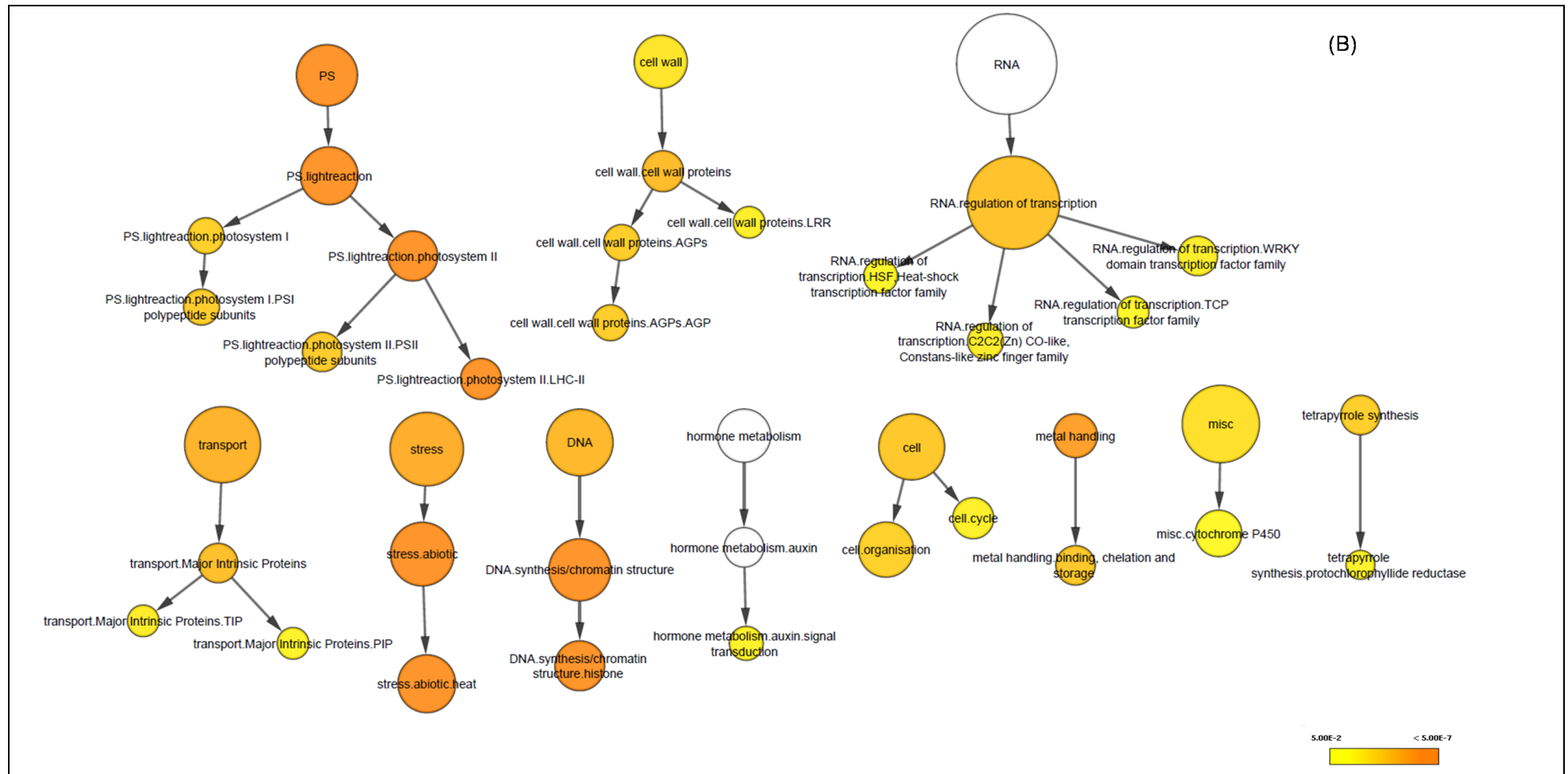


FIGURE 9. Overview of pathways overrepresented in the cultivars IRGA 409 (A) and IRGA 428 (B), according to enrichment analysis using MapMan ontology visualized by Cytoscape plug-in BiNGO. The color scale indicates significance of enrichment analysis and the size of nodes indicates the numbers of genes which were mapped. The arrows represent the relationship between parent-child terms. UFRGS, Porto Alegre, RS, Brazil. 2018.



Continuation FIGURE 9. Overview of pathways overrepresented in the cultivars IRGA 409 (A) and IRGA 428 (B), according to enrichment analysis using MapMan ontology visualized by Cytoscape plug-in BiNGO. The color scale indicates significance of enrichment analysis and the size of nodes indicates the numbers of genes which were mapped. The arrows represent the relationship between parent-child terms. UFRGS, Porto Alegre, RS, Brazil. 2018.

4.5.4 Cellular response in rice panicle to heat treatment

To understand how these functional categories were responding in each cultivar, specific MapMan categories were examined and visualized if the DEGs in that category were up or down regulated. IRGA 409 and IRGA 428 cultivars were enriched for stress response-related genes that are in the cellular response category (Figure 10). These genes were primarily up-regulated in both cultivars. Most of those genes are related to *small heat shock proteins* (*sHSP* and *DnaJ*) and heat shock factor (*HSF*), family members. Also, genes related to redox pathway were observed, most of them related to thioredoxin, ascorbate peroxidase and glutathione.

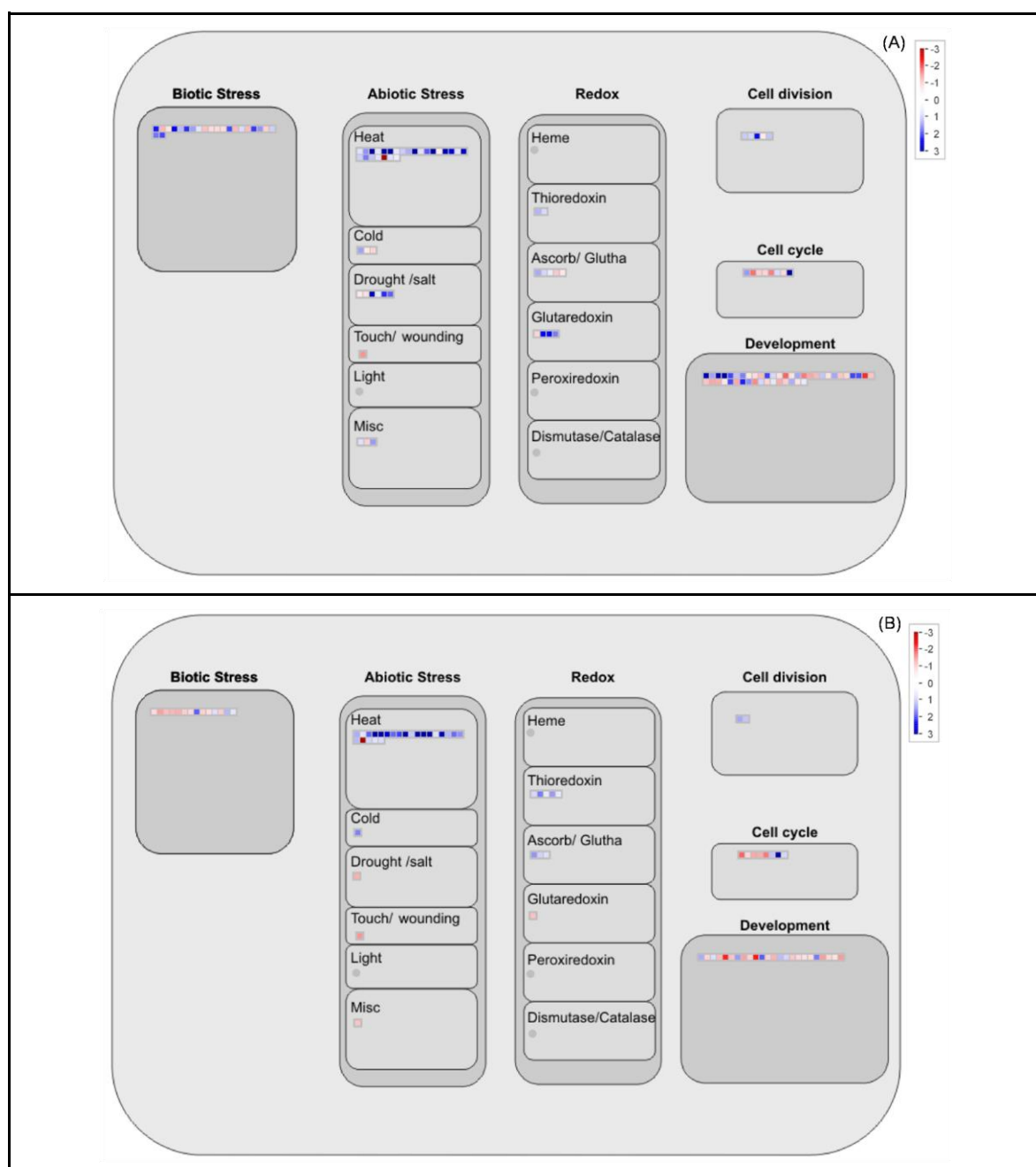


FIGURE 10. Expression profile of the genes in cellular response. MapMan was used to visualize heat response genes in the cultivars IRGA 409 (A) and IRGA 428 (B). Each square represent one transcript that colored with red for down-regulation or with blue for up-regulation. The scale is shown in the figure. UFRGS, Porto Alegre, RS, Brazil. 2018.

4.5.5 Light-reaction response by high temperature in IRGA 428

The present study showed that light reaction activities were enriched only in the cultivar IRGA 428 (Figure 9B). The response to heat stress triggered the up-regulation of almost all genes related to this pathway in this cultivar (Figure 11).

Photosynthesis pathway was enriched mainly due to the induction of light reaction involving genes in Photosystems I and II under heat shock in rice panicle. IRGA 428 had 24 DEGs associated with light reaction pathway (p -value $<1 \times 10^{-12}$). These same genes did not show differential response to heat stress in IRGA 409 at the same time point of sampling. For many of these genes (17 genes, 71 %) their level in control conditions in IRGA 409 was already as high as the heat-induced level in IRGA 428 (Figure 12 A & B). This suggests that they may not need to be induced in response to heat in IRGA 409, because they are already highly expressed. However, not all genes in this pathway are already highly expressed in IRGA 409 controls (e.g., Figure 12C).

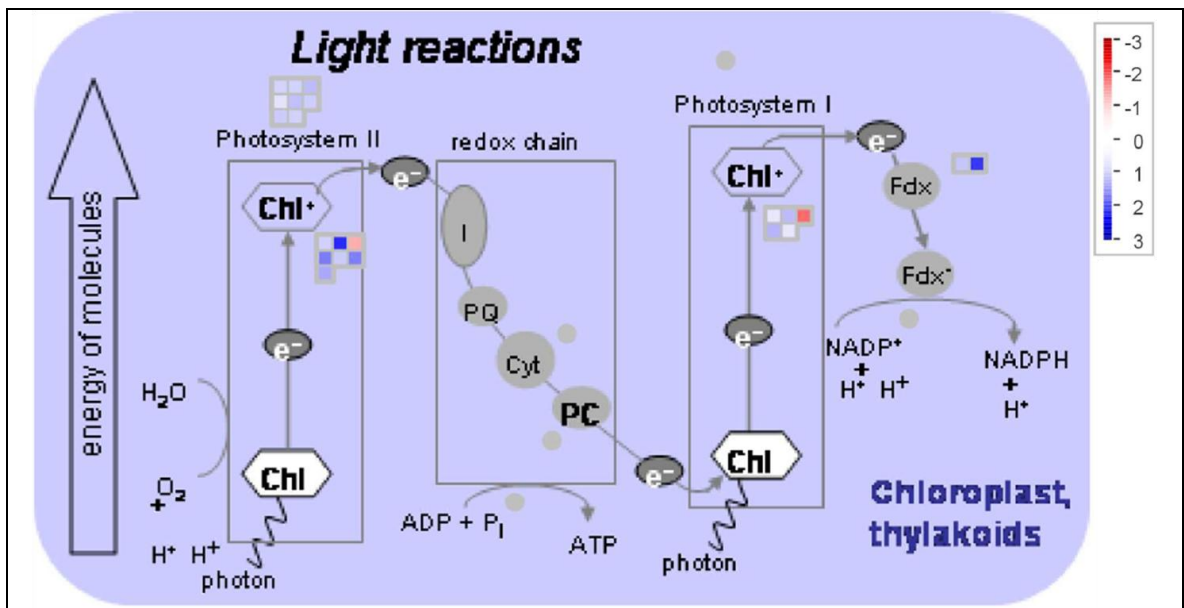


FIGURE 11. Expression profiles of the genes involved in light reaction process of the photosynthesis system. MapMan was used to visualize heat responsive DEGs in the cultivar IRGA 428. Each square represent one transcript that colored with red for down-regulation or with blue for up-regulation. The scale is shown in the figure. UFRGS, Porto Alegre, RS, Brazil. 2018.

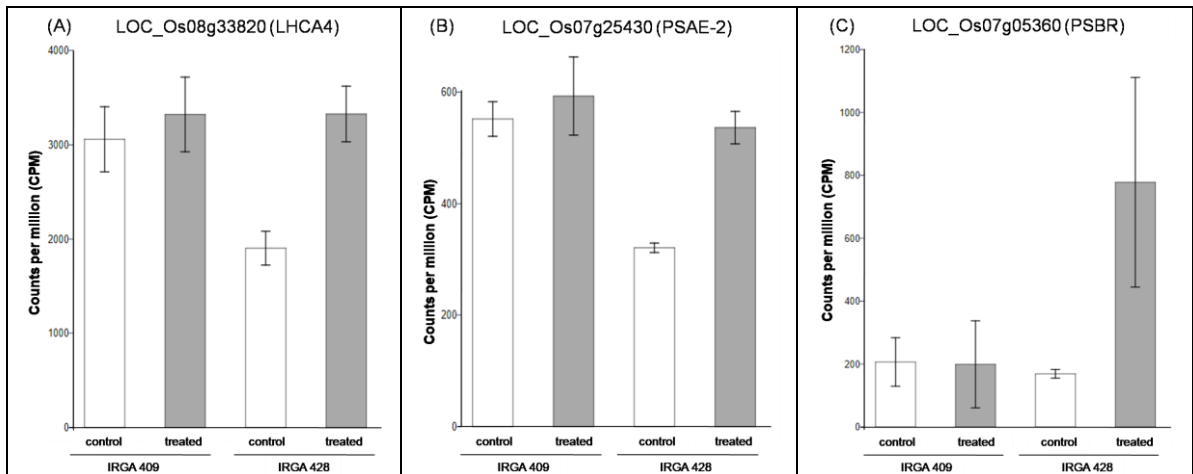


FIGURE 12. Differentially expressed genes involved in photosynthesis pathway in response to high temperature, relative expression value computed from the counts per million (CPM). Bar graph shows each gene and transcript expression value annotated with error bars (\pm SD) that capture both cross-replicate variability and measured uncertainty as estimated by EdgeR statistical model of RNA-seq (adjusted p -value <0.001). UFRGS, Porto Alegre, RS, Brazil. 2018.

4.5.6 Interaction between cultivar and heat stress

To further explore the transcriptional differences between cultivars in response to heat, focus was given on the 65 DEGs (57 orthologous genes to *japonica*) we identified multi-factor contrast analysis, comparing genotype and environmental interactions. These transcripts show a significant cultivar effect in response to heat stress and may be candidates to explain the observed physiological differences in the cultivars heat responses. Functional analysis of these genes showed that nine pathways are overrepresented, according to enrichment analysis by MapMan Software (Figure 13). It was identified twenty-four genes associated with those pathways.

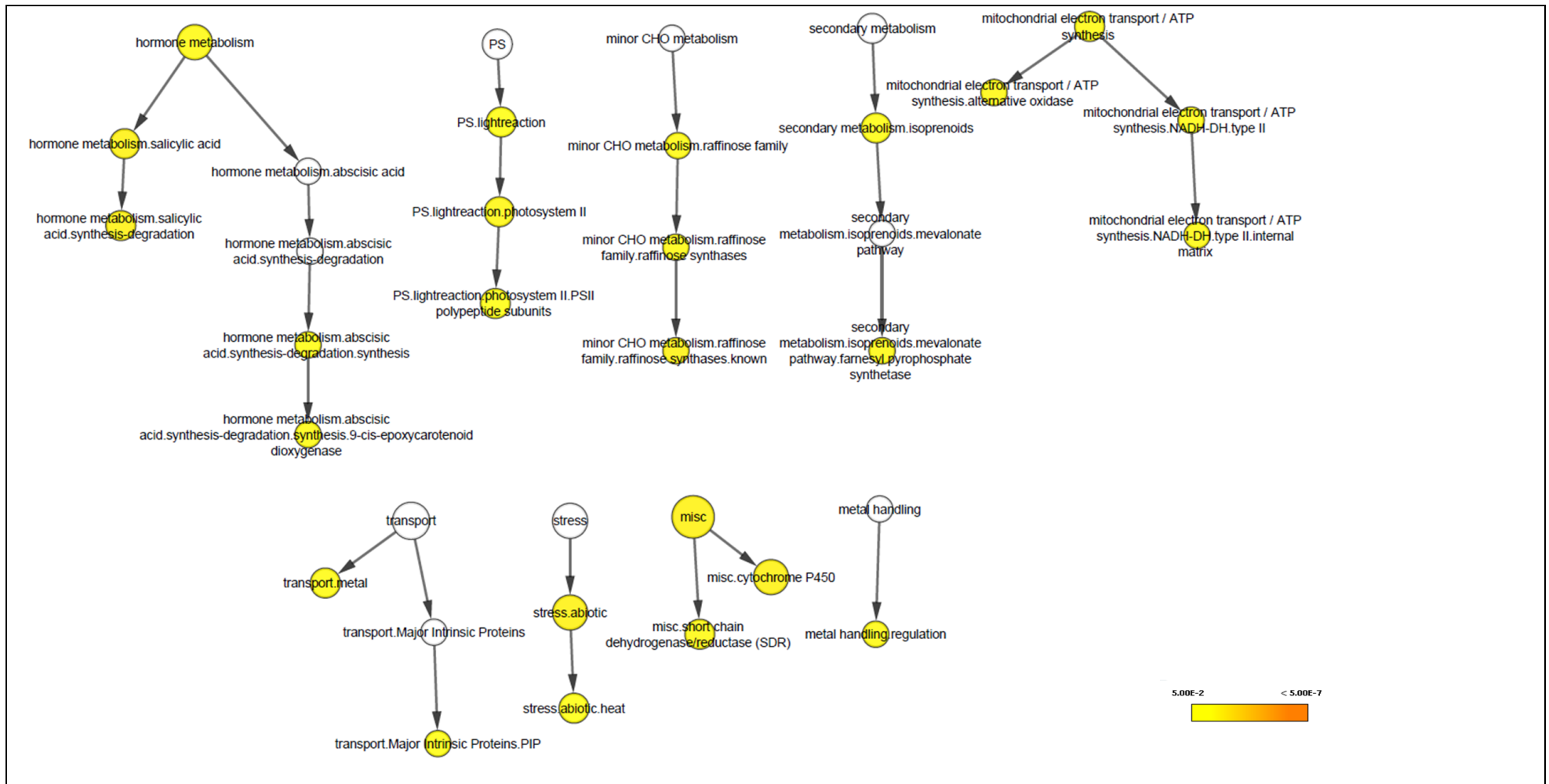


FIGURE 13. Overview of pathways overrepresented in the multi-factor contrast analysis, according to enrichment analysis using MapMan ontology visualized by Cytoscape plug-in BiNGO. The color scale indicates significance of enrichment analysis and the size of nodes indicates the numbers of genes which were mapped. The arrows represent the relationship between parent-child terms. UFRGS, Porto Alegre, RS, Brazil. 2018.

The entire multifactor DEGs that were identified in the stress abiotic pathway (p -value $p < 0.01$) were induced in response to heat stress in IRGA 428 (Figure 14 A, B, C and D). However, these genes did not show this consistent response in IRGA 409. For genes related to light reaction pathway (p -value < 0.01), two different expression patterns were observed. In this pathway, the DEGs identified encoding proteins related to photosystem II. The gene encoding the protein D showed a reduction in the transcript level compared to control condition in IRGA 409 and the gene related to the polypeptide of subunit R did not change the level in response to heat (Figure 14 E & F). However, for IRGA 428 was observed an inverse response, the transcript level did not change in response to heat for the first gene and increased for the second one in response to heat stress compared to control condition.

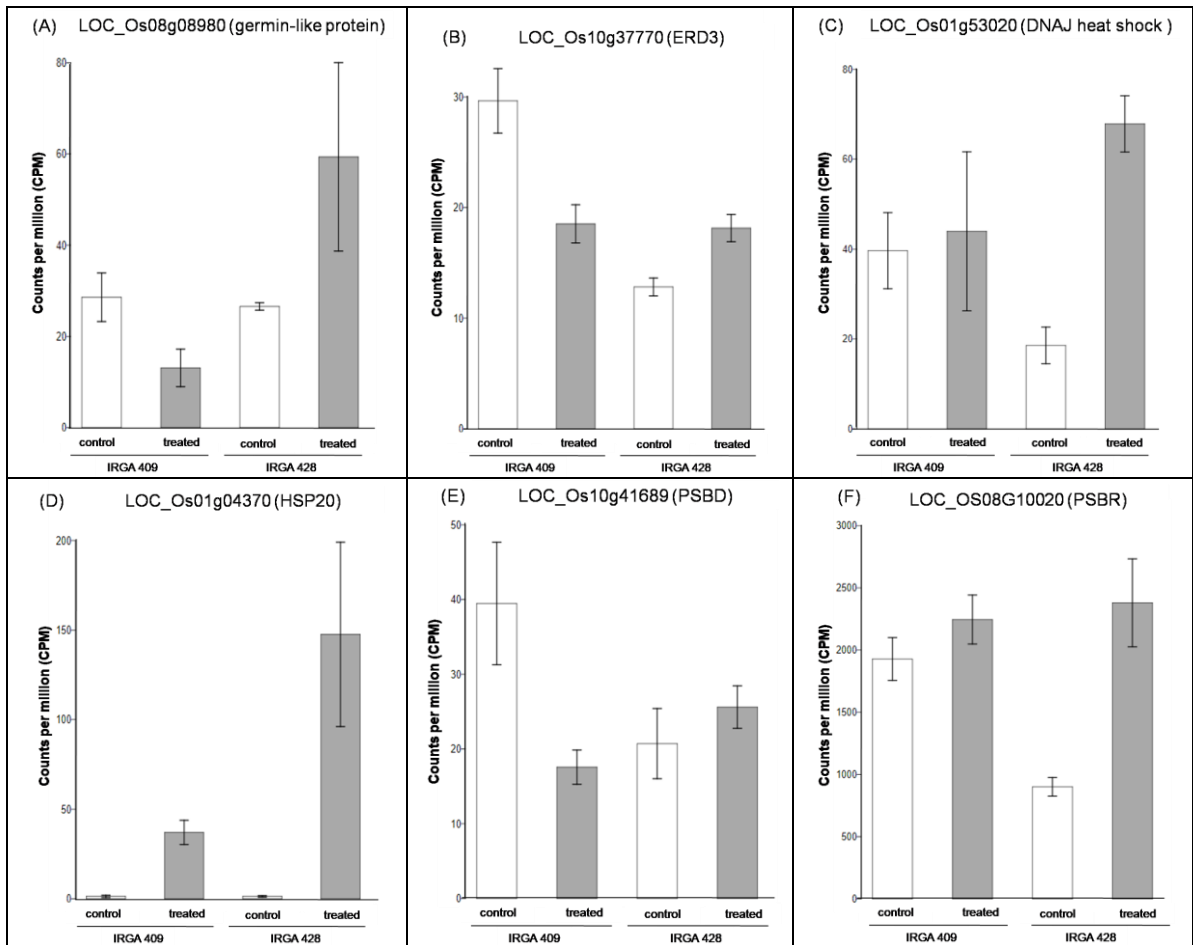


FIGURE 14. Differentially expressed genes involved in abiotic stress (A, B, C and D) and light reaction (E & F) pathways in response to high temperature in the contrast analysis, relative expression value computed from the counts per million (CPM). Bar graph shows each gene and transcript expression value annotated with error bars (\pm SD) that capture both cross-replicate variability and measured uncertainty as estimated by EdgeR statistical model of RNA-seq (adjusted p -value < 0.001). UFRGS, Porto Alegre, RS, Brazil. 2018.

Most of the genes identified in miscellanea pathway (p -value < 0.01) were repressed after heat treatment in IRGA 409 (Figure 15 A, B, C and D). In IRGA 428, however, the expression of those genes was induced in response to heat stress. Two other genes in this pathway (Figure 15 E & F) were highly induced by heat stress in IRGA 409, but did not change in IRGA 428, showing levels after heat treatment similar to the control levels for IRGA 409.

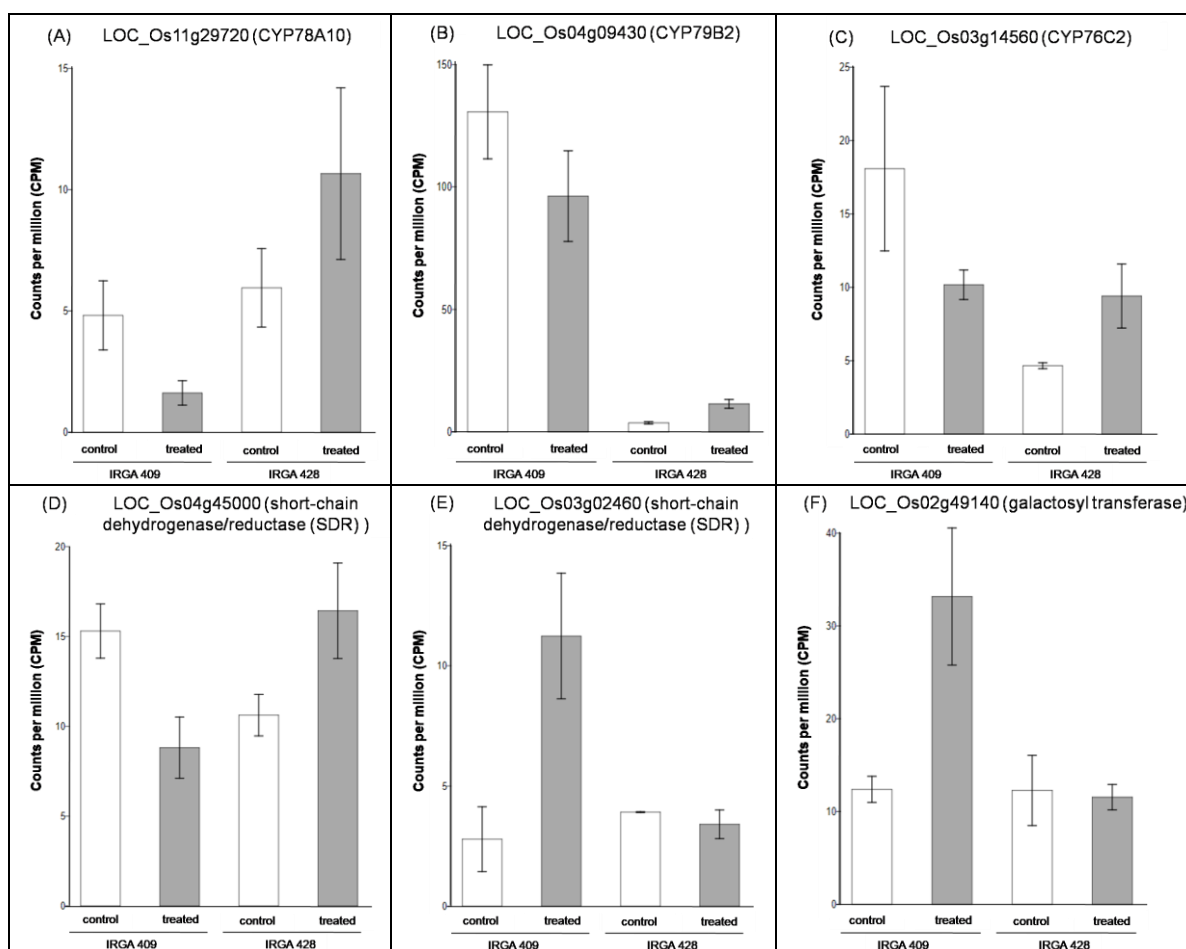


FIGURE 15. Differentially expressed genes involved in miscelanea pathway (A-F) in response to high temperature in the contrast analysis, relative expression value computed from the counts per million (CPM). Bar graph shows each gene and transcript expression value annotated with error bars (\pm SD) that capture both cross-replicate variability and measured uncertainty as estimated by EdgeR statistical model of RNA-seq (adjusted p -value <0.001). UFRGS, Porto Alegre, RS, Brazil. 2018.

DEG related to the raffinose family in the minor CHO metabolism pathway were identified (p -value $p < 0.01$), which presented a reduction in the transcript level in response to heat treatment in IRGA 409, but it was already as high as the heat-induced level in IRGA 428 (Figure 16A). In the hormone metabolism pathway (p -value $p < 0.03$) a key gene in abscisic acid (ABA) biosynthesis was identified. The transcript level of NCED1 which codes for 9-cis-epoxycarotenoid dioxygenase was already as high as the heat-induced level in IRGA 409 and it increased in

response to heat in IRGA 428 (Figure 16B). Similar pattern of transcript level was observed for the gene LOC_Os11g15040, which encodes S-adenosyl-L-methionine: salicylic acid carboxyl methyltransferase (Figure 16C).

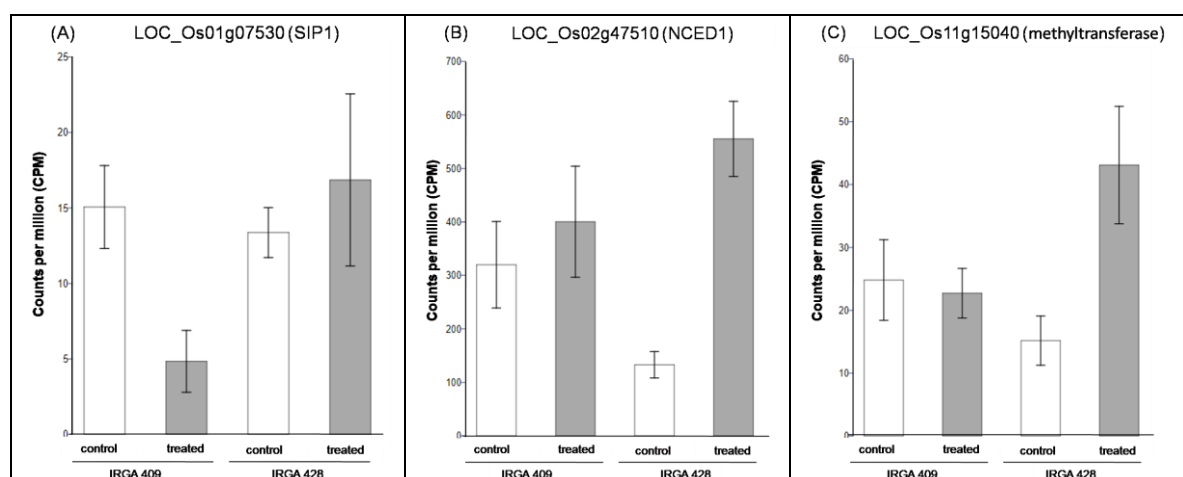


FIGURE 16. Differentially expressed genes involved in minor CHO metabolism (A) and hormone metabolism (B & C) pathways in response to high temperature in the contrast analysis, relative expression value computed from the counts per million (CPM). Bar graph shows each gene and transcript expression value annotated with error bars (\pm SD) that capture both cross-replicate variability and measured uncertainty as estimated by EdgeR statistical model of RNA-seq (adjusted p -value < 0.001). UFRGS, Porto Alegre, RS, Brazil. 2018.

Genes identified in mitochondrial electron transport pathway (p -value $p < 0.03$) showed the same pattern of transcript level (Figure 17 A & B). Their level in heat condition was higher than in control for IRGA 409 and did not change in IRGA 428. Genes were identified related to isoprenoids family in the secondary metabolism pathway (p -value $p < 0.04$), also, showed a similar pattern of expression (Figure 17 C & D). In IRGA 409 the transcript level of those genes did not change between control and heat treatment, suggesting that they may not need to be induced in this cultivar. However, in IRGA 428, an increase in the transcript level of those genes related to isoprenoids family was observed in response to heat compared to control condition.

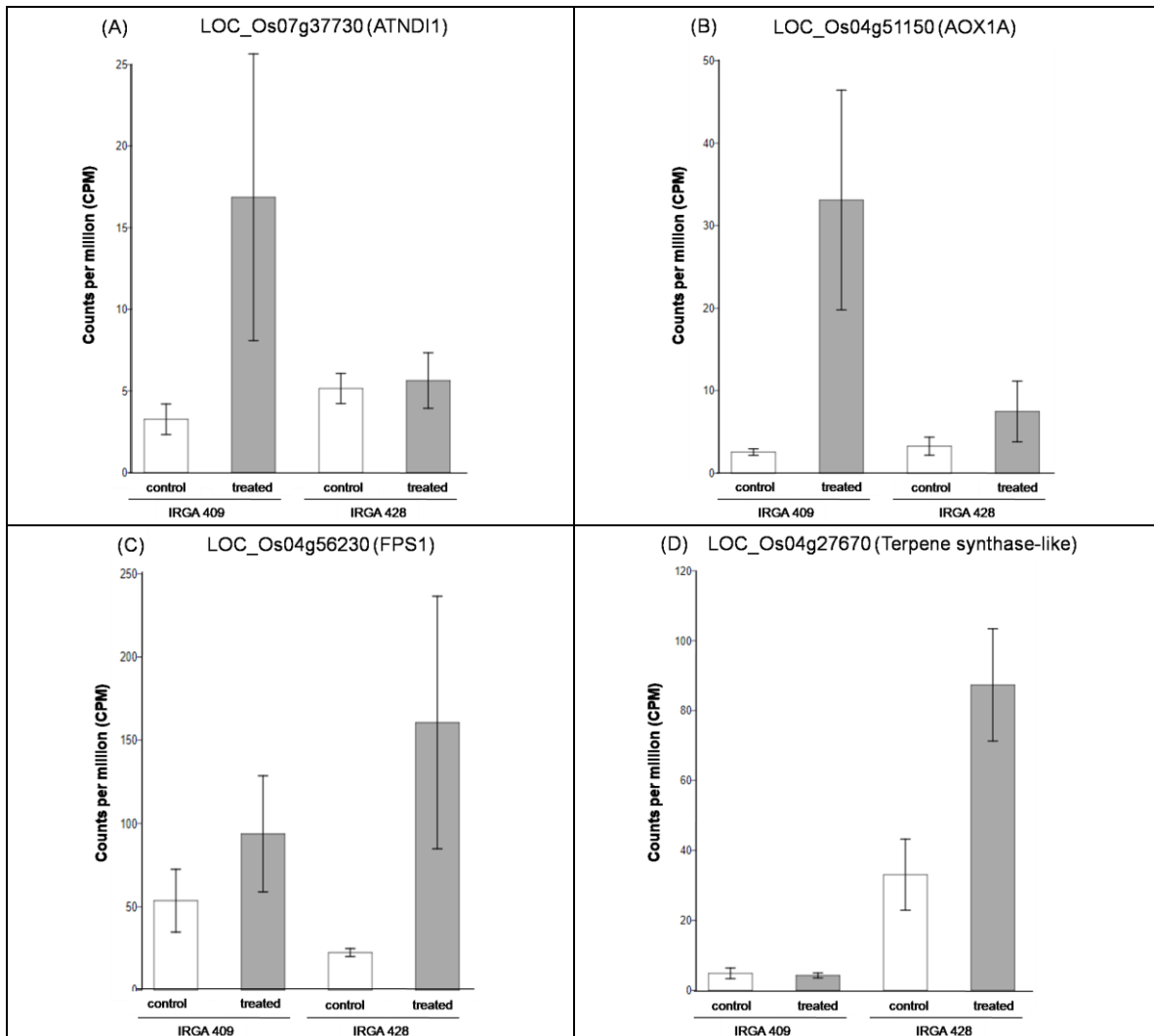


FIGURE 17. Differentially expressed genes involved in mitochondrial electron transport (A & B) and secondary metabolism (C & D) pathways in response to high temperature in the contrast analysis, relative expression value computed from the counts per million (CPM). Bar graph shows each gene and transcript expression value annotated with error bars (\pm SD) that capture both cross-replicate variability and measured uncertainty as estimated by EdgeR statistical model of RNA-seq (adjusted p -value <0.001). UFRGS, Porto Alegre, RS, Brazil. 2018.

Genes involved in the metal transport pathway (p -value $p < 0.03$) showed a singular response for each cultivar (Figure 18 A & B). In IRGA 409, an increase of transcript level was observed in response to heat stress for the gene encodes a vacuolar iron transporter, but the level did not change for the gene encodes a

copper transporter protein. Contrary pattern was observed in IRGA 428, in vacuolar iron transporter gene had a reduction in the transcript level and copper transporter gene an increase in the level compared to control condition. In the transport major intrinsic protein pathway (p -value $p < 0.05$), a gene was identified which encodes a water channel protein (Figure 18C). In the cultivar IRGA 409, there was a reduction in the transcript level, while in IRGA 428 the level did not change compared to control condition.

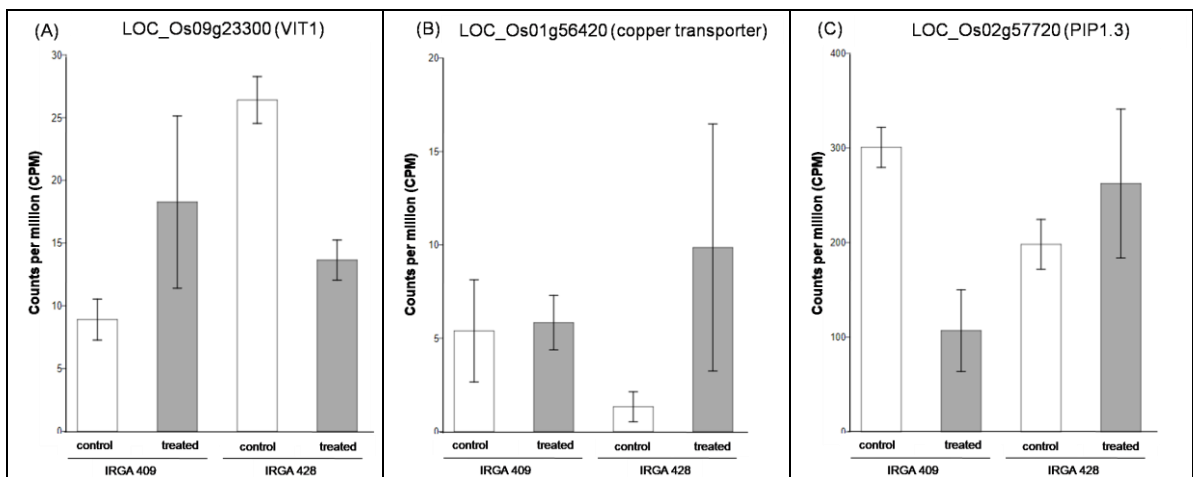


FIGURE 18. Differentially expressed genes involved in metal transport (A & B) and transport major intrinsic protein (C) pathways in response to high temperature in the contrast analysis, relative expression value computed from the counts per million (CPM). Bar graph shows each gene and transcript expression value annotated with error bars (\pm SD) that capture both cross-replicate variability and measured uncertainty as estimated by EdgeR statistical model of RNA-seq (adjusted p -value < 0.001). UFRGS, Porto Alegre, RS, Brazil. 2018.

5 DISCUSSION

5.1 Physiological response to heat stress

This is the first study describing the physiologic and molecular response of Brazilian flooded rice cultivars. In Brazil, the heat damage on flooded rice has recently become a serious problem (IRGA 2014; Walter *et al.*, 2010). Increase in temperature will lead to heat stress, which affects yield of agriculture crops. Although several studies have been performed to understand the effect of heat stress in crops and particularly in rice (Prasad *et al.*, 2006; Jagadish *et al.*, 2009; Sailaja *et al.*, 2015), most of these studies were based on exposing the plants to high temperature for short duration period at either vegetative or reproductive phase and using Asian genotypes.

In general, high temperature is unfavorable for flowering and grain filling in rice because it causes spikelet sterility and shortening the grain-filling phase (Sailaja *et al.*, 2015). In the present study, the duration of high temperature stress showed significant impact on yield through sharp reduction on fertilized spikelet percentage (Figure 1A). Maximum filled grain reduction was observed at seven days of heat stress, above 95 % for all cultivars. On the other hand, minimum reduction in the number of fertilized spikelet was observed at three days of stress. The cultivar IRGA 409 (55 %) presented the highest spikelet fertility compared to IRGA 428 (39 %) and DULAR (22 %) at three days of stress. Based on the

spikelet fertility, these cultivars were considered to have variable susceptibility to duration of heat stress. IRGA 409 is moderately tolerant and IRGA 428 and DULAR are susceptible to a short stress (three days), based on similar classification used in previous heat stress studies (Jagadish *et al.* 2009; Salaija *et al.*, 2015).

In order to understand the important physiological and biochemical phenomena contributing to differential high temperature response, parameters such as photosynthesis, chlorophyll fluorescence and antioxidant content were measured in all cultivars at anthesis phase. In plants, photosynthesis is one of the most susceptible processes to high temperature stress (Yin *et al.*, 2010). Sailaja *et al.* (2015) reported that high temperature during both vegetative and reproductive stage caused a reduction in photosynthetic rate of flag leaf in different rice cultivars. In the present study, photosynthetic parameters such as net photosynthetic rate (P_N) and stomatal conductance (g_s) were analyzed in all cultivars at anthesis stage at control and heat condition. These parameters were significantly affected, suggesting that photosynthesis is highly sensitive to high temperature in flooded rice cultivars. While analyzing the gas exchange by g_s , the effect of heat stress was more pronounced in the cultivar IRGA 428 than in the other two cultivars. Egeh *et al.*, (1992) reported that high g_s contribute to high temperature tolerance due to result in considerable lowering of leaf canopy temperature, which reduces the harmful effect of high temperature. Although photosynthetic parameters were significantly influenced by high temperature in this study, they did not show distinct correlation with spikelet fertility. The cultivar DULAR, which presented the lowest spikelet fertility, showed an increase in the photosynthetic parameters at three days of stress. On the contrary, cultivar IRGA

409, which presented the highest spikelet fertility in the same time point showed reduction in the photosynthetic parameters. Therefore, in the present study, the physiological differences observed between cultivars were not associated to differences in spikelet fertility under high temperature stress.

In stress physiology, chlorophyll fluorescence is another important technique to evaluate the damage on leaf photosynthetic apparatus, in particular photosystem II (PSII) activity (Maxwell & Johnson 2000). In the present study, high temperature stress showed marginal reduction in quantum yield of PSII and electron transport rate (ETR) for all stress duration in the sensitive cultivars (IRGA 428 and DULAR). On the other hand, IRGA 409 showed slight increase in those parameters across stress duration periods, suggesting that it may be due to the gradual adaptation of this cultivar to high temperature condition. According to Luo *et al.*, (2010) reduction in ETR under high temperature stress is due to inactivation of oxygen-evolving complex (OEC) and less utilization of NADPH and ATP under reduced photosynthesis.

Increased antioxidant activity under heat stress is a general response shown by plants (Wahid *et al.*, 2007). Plants continuously produce reactive oxygen species (ROS), such as superoxide radical ($^{\bullet}\text{O}_2^-$), hydrogen peroxide (H_2O_2) and singlet oxygen ($^1\text{O}_2$) as a consequence of normal cellular metabolism and when subjected to environment stress excess ROS is generated which causes oxidative stress. H_2O_2 and $^{\bullet}\text{O}_2^-$ have been implicated as signal molecules that can activate defense responses (Rao *et al.*, 2000). In the present study, increased in H_2O_2 content was observed in susceptible as well as in moderate tolerant cultivars. However, at three days of stress duration, IRGA 409 accumulated less H_2O_2 content than IRGA 428 and DULAR, being less sensitive to oxidative stress. The

result of H_2O_2 content indicates that more ROS were produced and the photosynthetic activity was decreased as a response to heat stress, especially in the cultivar IRGA 428. This result suggests that different cultivars may have evolved different mechanisms to support the heat stress, which indicates the complexity of pathways associated with high temperature response.

Important biochemical and physiological traits contributing to heat tolerance need to be characterized in individual genotypes to facilitate the breeding of climate-resilient rice genotypes. Based on biochemical and physiological performance of the most heat tolerant cultivar (N22) some useful traits were identified by Sailaja *et al.* (2015), which can be used to develop high-temperature tolerant rice cultivars. In that study, the cultivar N22 showed best performance in almost all parameters studied at vegetative and reproductive phases, e.g. less reduction in P_N , increase gas exchange and increase antioxidant enzymes activity, supporting minimum reduction in spikelet fertility. Therefore, it is important to understand the response of plants exposed to high temperature, particularly during reproductive stage. In order to better understand the adaptation plasticity of different genotypes the gene expression analysis can further support biochemical and physiological traits.

5.2 Common heat responsive genes in rice panicle

High temperature is a major abiotic stress limiting rice growth and development, and rice alters gene expression in response to heat stress to cope with the stress. In the present study, transcriptome analysis of rice spikelet was performed in the cultivars IRGA 409 and IRGA 428 at three days of heat stress duration. This time point presented the largest difference in spikelet fertility (Figure

1A). In rice, high temperature at flowering phase reduce yield by causing spikelet sterility (Yoshida *et al.*, 1981). Previous studies have identified sets of heat responsive genes during reproductive development. González-Schain and colleagues found 630 genes whose expression changes significantly in rice spikelets in a short (30 min) heat stress (38 °C) in the heat tolerant cultivar N22 (González-Schain *et al.*, 2015). Comparison of this N22, short-term heat stress data set and our analysis shows a significant overlap in responsive genes (hypergeometric enrichment test, p-value $<6 \times 10^{-4}$ for IRGA 409 and p-value $<2 \times 10^{-12}$) (Figure 19). This core set of genes was common between cultivars and González-Schain's work, indicating that these may be associated with basal response to heat. Some of the genes, such as small heat shock proteins (*sHSP* and *DnaJ*) and heat shock factor (*HSF*), are well-known members of the canonical response to heat stress in plants. However, this list also includes other genes with no previous association to heat responses, such as transcription factors (TF), cell wall modification and sugar partitioning enzymes, transporters and RNA binding proteins. Therefore, as was previously published for heat tolerant varieties, rice spikelets of these two Brazilian varieties perceive and respond to heat stress by adjusting their transcriptome and activating cellular protection, such as chaperone network activity. This core set of common genes between this work and González-Schain's data set are provided in Appendix 13 & 14.

HSPs and HSFs play a central role in the heat response (Baniwal *et al.*, 2004, Mittler *et al.*, 2012). Yet, it has been reported that the transcriptional regulation of these basal heat responses differs based on the cultivar subjected to study, the intensity and duration of heat treatment, and the developmental stage in which the stress is applied. The general response pattern of HSF transcripts is that

their exhibit either an early, rapid response to heat stress that then returns to the pre-stress state or are constitutively up-regulated during the period of heat treatment. In this study, transcripts which belong to *HsfA* and *HsfB* sub-families were up-regulated at three days of heat stress in both cultivars (Figure 10). However, these TFs were slightly induced (lower than 4-fold) compared to the high levels of induction observed in tolerant cultivars (higher than 100-fold for *HsfA2a*) (Zhang *et al.* 2012, González-Schain *et al.*, 2015). The duration of the applied heat treatment was different, our study reflects a long-term response compared to these studies (3d compared to 30 min in González-Schain's work and 2 h in Zhang's work), which may explain the lower level of induction observed a new steady-state may have been reached. *HSFA2a*, *small HSPs* and *OsFKBP62b* are strongly induced in N22 in response to different heat treatments (Endo *et al.* 2009, Zhang *et al.*, 2012, González-Schain *et al.*, 2015). *HSFA2a* was not induced in either cultivar in the present study at three days, while *OsFKBP62b* was induced in both cultivars in response to heat treatment. In Arabidopsis, *ROF1* is a close homolog of *OsFKBP62b*, it is a peptidyl prolyl isomerase that has been described as a modulator of basal thermotolerance by interacting with *HSP90.1* and affecting the accumulation of *HSFA2*-regulated *HSPs* (Meiri & Breiman, 2009). *ROF1* is essential for extending the duration of thermotolerance but not for its induction. The observation that the canonical heat responsive factors are generally induced in response to heat stress in both cultivars suggests that the activation of the cellular protection system in reproductive development and heat response in rice panicle is still preserved in these "Brazilian" cultivars which were not selected for heat tolerance. Furthermore, the conservation of the response of these classic heat response genes between both IRGA 409 and IRGA 428 cultivars suggests

that the observed physiological differences are not due to differences in these classic heat response pathways.

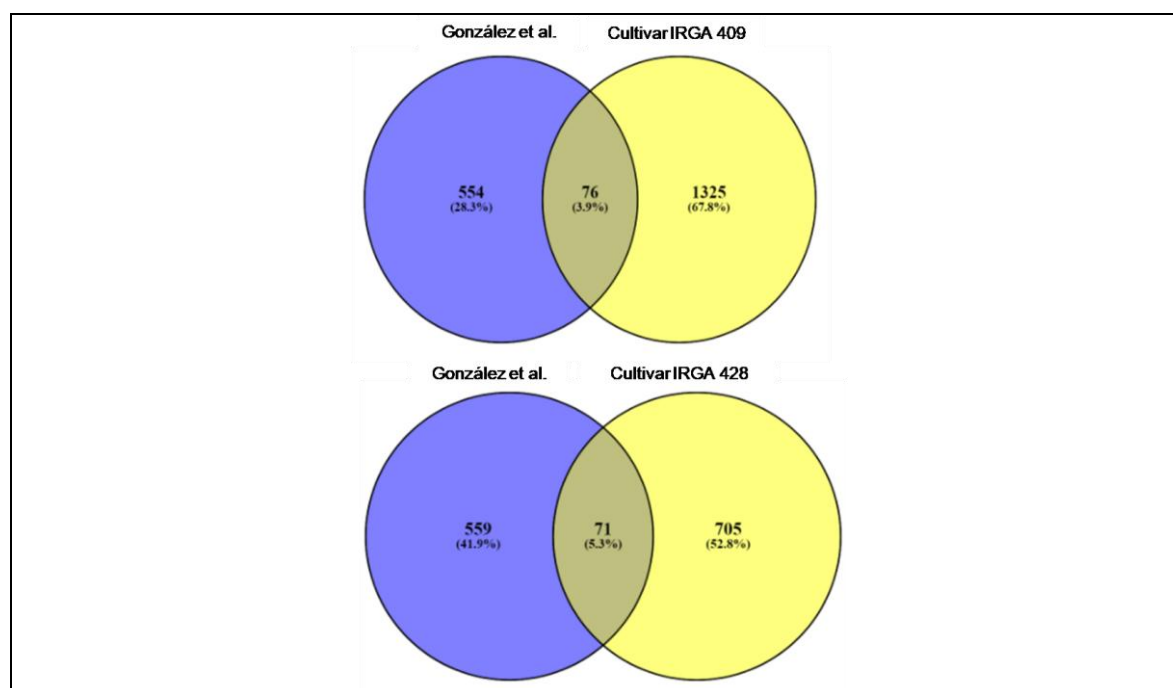


FIGURE 19. Venn diagram showing heat responsive genes identified in one independent rice heat stress data set. List of heat responsive genes from González-Schain *et al.*, (2015) was compared with the list obtained by RNA-seq analysis in the present study. UFRGS, Porto Alegre, RS, Brazil. 2018.

5.3 Induction of light reaction genes in response to heat stress

Among the physiological processes in plants, photosynthesis is one of the most sensitive processes to heat stress, with inhibition occurring at temperatures only slightly higher than optimal for growth (Allakhverdiev *et al.*, 2008). In the present study, under the heat stress the photosynthetic rate of flag leaf decreased in the cultivars IRGA 409 and IRGA 428, but the value of reduction was greater in IRGA 428 than in IRGA 409 (Figure 2A). Consistently, only in IRGA 428 were DEGs associated with light reaction pathway identified. These transcriptional changes were observed in rice panicle at three days of stress (Figure 9B).

Photosynthesis is known to occur in rice panicles, but little has been reported about the photosynthetic characteristics of such panicles. The photosynthesis activity in the spikelets is due to the presence of chlorophyll in the lemmas and paleae (Imaizumi *et al.*, 1997). According to Imaizumi *et al.*, (1990), in the cultivar Nipponbare in optimum growth conditions, rice panicle can present 30 % of the photosynthetic capacity per unit area of a flag leaf. Grain growth would not be limited by the availability of carbohydrates, but by the capacity of grains utilize them. However, source limitation is present in several abiotic stresses, thus the relative contribution of panicle photosynthesis (compared with the flag leaf and other plant parts) may be more important under stress conditions (Tambussi *et al.*, 2007).

In the present study, genes related to light reaction pathway were induced in the panicle of the cultivar IRGA 428, while these genes in cultivar IRGA 409 were already expressed highly in control conditions. The basal level of these genes in IRGA 409 was as high as the heat-induced level in the more sensitive IRGA 428 (Appendix 10). The DEGs are related to photosystem I and II subunits, and light harvesting complex. Photosystem II is one the most thermosensitive component of photosynthetic apparatus (Allakhverdiev *et al.*, 2008). Heat inactivation of PSII is easy to happen due to the dissociation of OEC, which is involved in the photo-oxidation of water during the light reaction of photosynthesis (Li *et al.*, 2017). To cope with heat stress, plants have developed a sophisticated mechanism to repair photosystem damage. Therefore, in IRGA 428 the induction of these genes suggests the activation of a repair mechanism to reverse damage on the photosynthetic apparatus caused by the three days of heat stress. We also observed in IRGA 428 the induction of genes related to redox pathway such as

thioredoxin and thylakoid ascorbate peroxidase (*OSAPX8*) genes, suggesting oxidative stress effect. The difference in basal levels of these photosynthetic components may be a contributing factor to the differences in spikelet fertility between the varieties under heat stress.

Additionally, cultivars IRGA 409 and IRGA 428 presented induction of ferredoxin transcripts (*OSFED2* and *OSFED3*, Appendix 10), which is a component of the photosynthetic electron transport chain and important in noncyclic photosynthetic light reaction by allowing electron cycling in the system for maintaining the energy metabolism under heat stress. The present study indicates that the capacity to maintain active genes related to photosynthesis in the panicle and the maintenance of photosynthesis activity of flag leaf may favor thermotolerance. Combined, these findings indicate that heat tolerance is a process with a high energy cost in which maintaining basal metabolic processes for the plant will result in successful recovery. Further study of the intersection between photosynthetic capacity and heat stress will improve our understanding of the importance of photosynthesis activity in rice panicle in response to heat treatment.

This is the first study to evaluate the heat tolerance of Brazilian rice cultivars, which have not been under specific selection for heat tolerance. Two Brazilian cultivars were characterized for heat stress response at physiological and molecular level. Several important physiological, biochemical and molecular traits were identified, which would be useful in phenotyping and breeding for heat tolerance. This study emphasizes that the characterization of heat stress responses in individual cultivars provides insights into both the basic mechanisms

of heat response and assists with understanding the complex phenomenon of responses to high temperature stress.

6 CONCLUSIONS

The effect of high temperature on the fertilization of rice spikelet varies among cultivars and the duration of the heat stress. The critical role of heat stress in reducing grain number is greater the longer the duration of stress. In the present study, cultivar IRGA 409 is moderate tolerant to heat stress, maintaining the highest spikelet fertility among the cultivars at three days of stress duration.

In panicle tissue, most canonical heat responsive genes, such as HSF family, small HSP family and *OsFKBP62b*, show a similar response in both Brazilian cultivars, despite the fact that these cultivars have not been specifically selected for heat tolerance.

The response of photosynthetic genes to heat stress is a major difference between the cultivars IRGA 409 and IRGA 428. This study indicates that the basal expression of photosynthetic genes in the panicle and the ability to maintain photosynthetic capacity in the flag leaf during stress provides improved spikelet fertility under heat stress. This may provide potential markers that can be used to identify heat tolerant genotypes among the Brazilian cultivars. However, the detailed molecular processes involved in the heat effects on electron transport through photosystems (I and II), and the connection between photosynthesis activity in the leaves and in the rice panicle remain to be further elucidated.

7 REFERENCES

ALLAKHVERDIEV, S.I. et al. Heat stress: an overview of molecular responses in photosynthesis. **Photosynthesis Research**, Dordrecht, v. 98, n. 1-3, p. 541, 2008.

BAKER, J.T.; ALLEN JR., L.H.; BOOTE, B.K. Response of rice to carbon dioxide and temperature. **Agricultural and Forest Meteorology**, Amsterdam, v. 60, n. 3-4, p. 153-166, 1992.

BANIWAL, S.K. et al. Heat stress response in plants: a complex game with chaperones and more than twenty heat stress transcription factors. **Journal of Biosciences**, Bangalore, v. 29, n. 4, p. 471-487, 2004.

BHEEMANAHALLI, R. et al. Is early morning flowering an effective trait to minimize heat stress damage during flowering in rice? **Field Crops Research**, Amsterdam, v. 203, n. Supplement C, p. 238-242, 2017.

BOLGER, A.M.; LOHSE, M.; USADEL, B. Trimmomatic: a flexible trimmer for Illumina sequence data. **Bioinformatics**, Oxford, v. 30, n. 15, p. 2114-2120, 2014.

BUU, C.B. et al. Rice breeding for heat tolerance at initial stage. **Omonrice**, Philippines, v. 19, n. 1, p. 1-10, 2013.

COUNCE, P.A. et al. A uniform, objective, and adaptive system for expressing rice development. **Crop Science**, Madison, v. 40, n. 2, p. 436-443, 2000.

EGEH, A.O.; INGRAM, K.T.; ZAMORA, O.B. High temperature effects on leaf gas exchange of four rice cultivars. **Philippine Journal of Crop Science**, Philippines, v. 17, n. 1, p. 21-26, 1992.

GONZÁLEZ-SCHAIN, N. et al. Genome-wide transcriptome analysis during anthesis reveals new insights into the molecular basis of heat stress responses in tolerant and sensitive rice varieties. **Plant and Cell Physiology**, Kyoto, v. 57, n. 1, p. 57-68, 2015.

GOURDJI, S.M. et al. Global crop exposure to critical high temperatures in the reproductive period: historical trends and future projections. **Environmental Research Letters**, Bristol, v. 8, n. 2, p. 240-41, 2013.

HASANUZZAMAN, M. et al. Physiological, biochemical, and molecular mechanisms of heat stress tolerance in plants. **International Journal of Molecular Sciences**, Basel, v. 14, n. 5, p. 9643-9684, 2013.

HECKATHORN, S.A. et al. In vivo evidence from an *Agrostis stolonifera* selection genotype that chloroplast small heat-shock proteins can protect photosystem II during heat stress. **Functional Plant Biology**, Collingwood, v. 29, n. 8, p. 935-946, 2002.

IMAIZUMI, N.; SAMEJIMA, M.; ISHIHARA, K. Characteristics of photosynthetic carbon metabolism of spikelets in rice. **Photosynthesis research**, Boston, v. 52, n. 2, p. 75-82, 1997.

IMAIZUMI, N. et al. Changes in the rate of photosynthesis during grain filling and the enzymatic activities associated with the photosynthetic carbon metabolism in rice panicles. **Plant and Cell Physiology**, Kyoto, v. 31, n. 6, p. 835-844, 1990.

INSTITUTO RIO GRANDENSE DO ARROZ. IRGA. **Dados de safra**. Porto Alegre, 2018. Disponível em: < <http://www.irga.rs.gov.br/conteudo/6911/safras>>. Acesso em: 28 jan. 2018.

SAFRA 2013/2014. **Revista Lavoura Arrozeira**. Porto Alegre, v.62, n.462, p.10-13, 2014. Disponível em:< <http://www.irga.rs.gov.br/lista/345/publicacoes/>> Accessed in: 25 jan. 2018.

INTERGOVERNMENTAL PANEL ON CLIMATE CHANGE - IPCC. **Climate change 2013: The physical science basis, summary for policymakers**. 2013. Available in:<http://www.climatechange2013.org/images/report/WG1AR5_SPM_FINAL.pdf> Accessed in: 05 feb. 2018.

JAGADISH, K.S.V.; MURTY, M.V.; QUICK, W.P. Rice responses to rising temperatures: challenges, perspectives and future directions. **Plant Cell Environment**, Oxford, v. 38, n. 9, p. 1686-98, 2015.

JAGADISH, K.S.V. et al. A phenotypic marker for quantifying heat stress impact during microsporogenesis in rice (*Oryza sativa* L.). **Functional plant biology**, Victoria, v. 41, n. 1, p. 48-55, 2014.

JAGADISH, K.S.V. et al. Genetic analysis of heat tolerance at anthesis in rice. **Crop Science**, Madison, v. 50, n. 5, p. 1633-1641, 2010.

JAGADISH, K.S.V. et al. Physiological and proteomic approaches to address heat tolerance during anthesis in rice (*Oryza sativa* L.). **Journal of Experimental Botany**, Oxford, v. 61, n. 1, p. 143-156, 2009.

JAGADISH, K.S.V.; CRAUFURD, P.Q.; WHEELER, T.R. High temperature stress and spikelet fertility in rice (*Oryza Sativa* L.). **Journal of Experimental Botany**, Oxford, v. 58, n. 7, p. 1627-1635, 2007.

KAWAHARA, Y. et al. Improvement of the *Oryza sativa Nipponbare* reference genome using next generation sequence and optical map data. **Rice**, New York, v. 6, n. 1, p. 4, 2013.

KIM, J. et al. Relationship between grain filling duration and leaf senescence of temperate rice under high temperature. **Field Crops Research**, Amsterdam, v. 122, n. 3, p. 207-213, 2011.

KRISHNAN, P. et al. High-temperature effects on rice growth, yield, and grain quality. **Advances in Agronomy**, Lausanne, v. 111, p. 87-206, 2011.

LI, L. et al. A phosphoinositide-specific phospholipase C pathway elicits stress-induced Ca^{2+} signals and confers salt tolerance to rice. **New Phytologist**, London, v. 214, n. 3, p. 1172-1187, 2017.

LUO, H.B. et al. Photosynthetic responses to heat treatments at different temperatures and following recovery in grapevine (*Vitis amurensis* L.) leaves. **PLOS ONE**, San Francisco, v. 6, n. 8, p. 23033, 2011.

MAERE, S. et al. Bingo: a Cytoscape Plugin to assess overrepresentation of gene ontology categories in biological networks. **Bioinformatics**, Oxford, v. 21, n. 16, p. 3448-3449, 2005.

MATSUI, T.; OMASA, K.; HORIE, T. The difference in sterility due to high temperatures during the flowering period among japonica-rice varieties. **Plant Production Science**, Kyoto, v. 4, n. 2, p. 90-93, 2001.

MAXWELL, K.; JOHNSON, G.N. Chlorophyll fluorescence: a practical guide. **Journal of Experimental Botany**, Oxford, v. 51, n. 345, p. 659-668, 2000.

MEIRI, D.; BREIMAN, A. Arabidopsis *ROF1* (*FKBP62*) modulates thermotolerance by interacting with *HSP90.1* and affecting the accumulation of *HsfA2*-regulated SHSPs. **The Plant Journal**, Oxford, v. 59, n. 3, p. 387-399, 2009.

MENEZES V.G. et al. **Projeto 10** – Management strategies to increase productivity and sustainability of irrigated Rice growth in the state of Rio Grande do Sul, Brazil: Development and challenges. Cachoeirinha; IRGA, 2013. 100p.

MERCHANT, N. et al. The IPlant collaborative: cyberinfrastructure for enabling data to discovery for the life sciences. **PLOS Biology**, San Francisco, v. 14, n. 1, p. 1-5, 2016.

MITTLER, R.; FINKA, A.; GOLOUBINOFF, P. How do plants feel the heat? **Trends in Biochemical Sciences**, Washington, v. 37, n. 3, p. 118-125, 2012.

NETA-SHARIR, I. et al. Dual role for tomato heat shock protein 21: protecting photosystem II from oxidative stress and promoting color changes during fruit maturation. **The Plant Cell Online**, Rockville, v. 17, n. 6, p. 1829-1838, 2005.

NORMILE, D. Agricultural research: reinventing rice to feed the world. **Sciences**, Washington, v. 321, n. 5887, p. 330-333, 2008.

NOURI, M.Z.; MOUMENI, A.; KOMATSU, S. Abiotic stresses: insight into gene regulation and protein expression in photosynthetic pathways of plants. **International Journal of Molecular Sciences**, Basel, v. 16, n. 9, p. 20392-20416, 2015.

OHAMA, N. et al. Transcriptional regulatory network of plant heat stress response. **Trends in Plant Science**, London, v. 22, n. 1, p. 53-65, 2017.

OUYANG, S. et al. The TIGR rice genome annotation resource: improvements and new features. **Nucleic Acids Research**, Oxford, v. 35, n. 1, D883–D887, 2007.

PRASAD, P.V.V.; BHEEMANAHALLI, R.; KRISHNAJAGADISH, S.V. Field crops and the fear of heat stress - opportunities, challenges and future directions. **Field Crops Research**, Amsterdam, v. 200, p. 114-121, 2017.

PRASAD, P.V.V. et al. Species, ecotype and cultivar differences in spikelet fertility and harvest index of rice in response to high temperature stress. **Field Crops Research**, Amsterdam, v. 95, n. 2-3, p. 398-411, 2006.

RAO, M.V. et al. Jasmonic acid signaling modulates ozone-induced hypersensitive cell death. **The Plant Cell**, Rockville, v. 12, n. 9, p. 1633-1647, 2000.

REZAEI, E.E. et al. Heat stress in cereals: mechanisms and modelling. **European Journal of Agronomy**, Amsterdam, v. 64, p. 98-113, 2015.

SAIDI, Y. et al. Membrane lipid composition affects plant heat sensing and modulates Ca²⁺ dependent heat shock response. **Plant Signaling & Behavior**, Philadelphia, v. 5, n. 12, p. 1530-1533, 2010.

SAILAJA, B. et al. Integrated physiological, biochemical, and molecular analysis identifies important traits and mechanisms associated with differential response of rice genotypes to elevated temperature. **Frontiers in Plant Science**, Lausanne, v. 6, n. 1044, p. 1-13, 2015.

SHI, W. et al. Popular rice cultivars show contrasting responses to heat stress at gametogenesis and anthesis. **Crop Science**, Madison, v. 55, n. 2, p. 589-596, 2015.

SHI, W. et al. High day- and night-time temperatures affect grain growth dynamics in contrasting rice genotypes. **Journal of Experimental Botany**, Oxford, v. 68, n. 18, p. 5233-5245, 2017.

SMITH, A.M.O.; RATCLIFFE, R.G.; SWEETLOVE, L.J. Activation and function of mitochondrial uncoupling protein in plants. **The Journal of Biological Chemistry**, Baltimore, v. 279, n. 50, p. 51944-51952, 2004.

SONG, J.M. et al. Rice Information GateWay (RIGW): a comprehensive bioinformatics platform for *indica* rice genomes. **Molecular Plant**, Oxford, v. 11, n. 3, p. 505-507, 2017.

SOCIEDADE BRASILEIRA DE ARROZ IRRIGADO. SOSBAI. **Arroz irrigado: recomendações técnicas da pesquisa para o Sul do Brasil**. Pelotas: [s.n.], 2016. 200 p.

TAMBUSSI, E.A. et al. The photosynthetic role of ears in C3 cereals: metabolism, water use efficiency and contribution to grain yield. **Critical Reviews in Plant Sciences**, Boca Raton, v. 26, n. 1, p. 1-16, 2007.

TEIXEIRA, E.I. et al. Global hot-spots of heat stress on agricultural crops due to climate change. **Agricultural and Forest Meteorology**, Amsterdam, v. 170, n. 1, p. 206-215, 2013.

THIMM, O. et al. Mapman: a user-driven tool to display genomics data sets onto diagrams of metabolic pathways and other biological processes. **The Plant Journal**, Oxford, v. 37, n. 6, p. 914-939, 2004.

UNITED STATE DEPARTMENT OF AGRICULTURE – USDA. **Rice**. [S.I.], 2017. Available in: <<https://www.ers.usda.gov/topics/crops/rice/>> Accessed in: 10 sept. 2017.

WAHID, A. et al. Heat tolerance in plants: an overview. **Environmental And Experimental Botany**, Elmsford, v. 61, n. 3, p. 199-223, 2007.

WALTER, L. C. et al. Mudança climática e seus efeitos na cultura do arroz. **Ciência Rural**, Santa Maria, v. 40, n. 11, p. 2411-2418, 2010.

WANG, X. et al. Heat-responsive photosynthetic and signaling pathways in plants: insight from proteomics. **International Journal of Molecular Sciences**, Basel, v. 18, n. 10, p. 20-28, 2017.

WANG, Z.; GERSTEIN, M.; SNYDER, M. RNA-Seq: a revolutionary tool for transcriptomics. **Nature Reviews Genetics**, London, v. 10, n. 1, p. 57-63, 2009.

WASSMANN, R. et al. **Regional vulnerability of climate change impacts on Asian rice production and scope for adaptation**. . Lausanne: [s.n.], 2009. cap. 3, p. 91-133. (Advances in Agronomy, v. 102)

YIN, Y. et al. Photosystem II photochemistry, photoinhibition, and the xanthophyll cycle in heat-stressed rice leaves. **Journal of Plant Physiology**, New York, v. 167, n. 12, p. 959-966, 2010.

YOSHIDA, S.; SATAKE, T.; MACKILL, D.S. **High-temperature stress in rice** [study conducted at IRRI, Philippines]. Philippines, 1981. (IRRI Research Paper Series)

ZAFAR, S. A. et al. Mechanisms and molecular approaches for heat tolerance in rice (*Oryza sativa* L.) under climate change scenario. **Science Direct**, Tokyo, v. 16, n. 1, p. 60345-60347, 2017.

ZHANG, J. et al. Extensive sequence divergence between the reference genomes of two elite *indica* rice varieties Zhenshan 97 and Minghui 63. **Proceedings of the National Academy of Sciences**, Washington, v. 113, n. 35, p. 1-14, 2016.

ZHANG, X. et al. Expression profile in rice panicle: insights into heat response mechanism at reproductive stage. **PLOS ONE**, San Francisco, v. 7, n. 11, p. 20-28, 2012.

8 APPENDIX

APPENDIX 1. ANOVA of percentage of spikelet fertility of three flooded rice cultivars.

Sources of variation	Degrees of freedom	Sum of squares	Mean Square	F	Significance
Cultivar (C)	2	400.43	200.22	12.79	<.0001
Duration (D)	2	2271.86	1135.93	72.60	<.0001
Temperature (T)	1	64296.19	64296.19	7.15	0.0002
Int. CxD	4	447.56	111.89	4109.43	<.0001
Int. CxT	2	737.69	368.84	23.57	<.0001
Int. DxT	2	4238.47	2119.23	135.44	<.0001
Int. CxDxT	4	713.78	178.44	11.40	<.0001
Treatment	17	73.78	4300.35	274.85	<.0001
Residue	36	563.25	15.64		
Total	53	73669.25			

*CV% = 7.53

APPENDIX 2. ANOVA of reduction on fertilized spikelets of three flooded rice cultivars.

Sources of variation	Degrees of freedom	Sum of squares	Mean Square	F	Significance
Cultivar (C)	2	1012.44	506.22	19.52	<.0001
Duration (D)	2	9290.01	4645.00	179.15	<.0001
Int. CxD	4	1743.19	435.79	16.80	<.0001
Treatment	8	12045.65	1505.70	58.07	<.0001
Residue	18	466.69	25.92		
Total	26	12512.34			

*CV% = 6.48

APPENDIX 3. ANOVA of photosynthetic rate of flag leaf of three flooded rice cultivars.

Sources of variation	Degrees of freedom	Sum of squares	Mean Square	F	Significance
Cultivar (C)	2	325.09	162.54	56.77	<.0001
Duration (D)	2	51.16	25.58	8.93	0.0004
Temperature (T)	1	397.00	397.00	138.67	0.0172
Int. CxD	4	37.79	9.44	3.29	<.0001
Int. CxT	2	296.89	148.44	51.85	<.0001
Int. DxT	2	92.08	46.04	16.08	0.0002
Int. CxDxT	4	72.97	18.24	6.37	<.0001
Treatment	17	1273.00	74.88	26.15	<.0001
Residue	54	154.59	2.86		
Total	71	1427.60			

*CV% = 8.53

APPENDIX 4. ANOVA of stomatal condutance measured in the flag leaf of three flooded rice cultivars.

Sources of variation	Degrees of freedom	Sum of squares	Mean Square	F	Significance
Cultivar (C)	2	0.962	0.481	75.40	<.0001
Duration (D)	2	0.035	0.018	2.78	0.0706
Temperature (T)	1	0.211	0.211	33.12	0.0193
Int. CxD	4	0.082	0.020	3.21	<.0001
Int. CxT	2	0.335	0.167	26.32	<.0001
Int. DxT	2	0.060	0.030	4.32	<.0125
Int. CxDxT	4	0.255	0.063	10.00	<.0001
Treatment	17	1.943	0.114	17.91	<.0001
Residue	36	0.344	0.006		
Total	53				

*CV% = 14.99

APPENDIX 5. ANOVA of quantum yield of PSII measured in the flag leaf of three flooded rice cultivars.

Sources of variation	Degrees of freedom	Sum of squares	Mean Square	F	Significance
Cultivar (C)	2	0.011	0.0056	38.93	<.0001
Duration (D)	2	0.001	0.0005	3.24	0.0437
Temperature (T)	1	0.002	0.0021	14.71	0.0013
Int. CxD	4	0.003	0.0007	4.86	0.0002
Int. CxT	2	0.007	0.0034	24.13	<.0001
Int. DxT	2	0.001	0.0003	1.79	0.1022
Int. CxDxT	4	0.001	0.0003	2.24	0.0391
Treatment	17	1.943	0.114	10.55	<.0001
Residue	90	0.344	0.006		
Total	107				

*CV% = 1.89

APPENDIX 6. ANOVA of electron transport rate measured in the flag leaf of three flooded rice cultivars.

Sources of variation	Degrees of freedom	Sum of squares	Mean Square	F	Significance
Cultivar (C)	2	388.35	194.17	25.17	<.0001
Duration (D)	2	26.27	13.13	1.70	0.1879
Temperature (T)	1	115.18	115.18	14.93	0.0427
Int. CxD	4	79.49	19.87	2.57	0.0001
Int. CxT	2	428.93	214.46	27.80	<.0001
Int. DxT	2	21.01	10.50	1.36	0.2612
Int. CxDxT	4	88.41	22.10	2.86	0.0276
Treatment	17	1147.67	67.51	8.75	<.0001
Residue	90	694.11	7.71		
Total	107	1841.79			

*CV% = 2.03

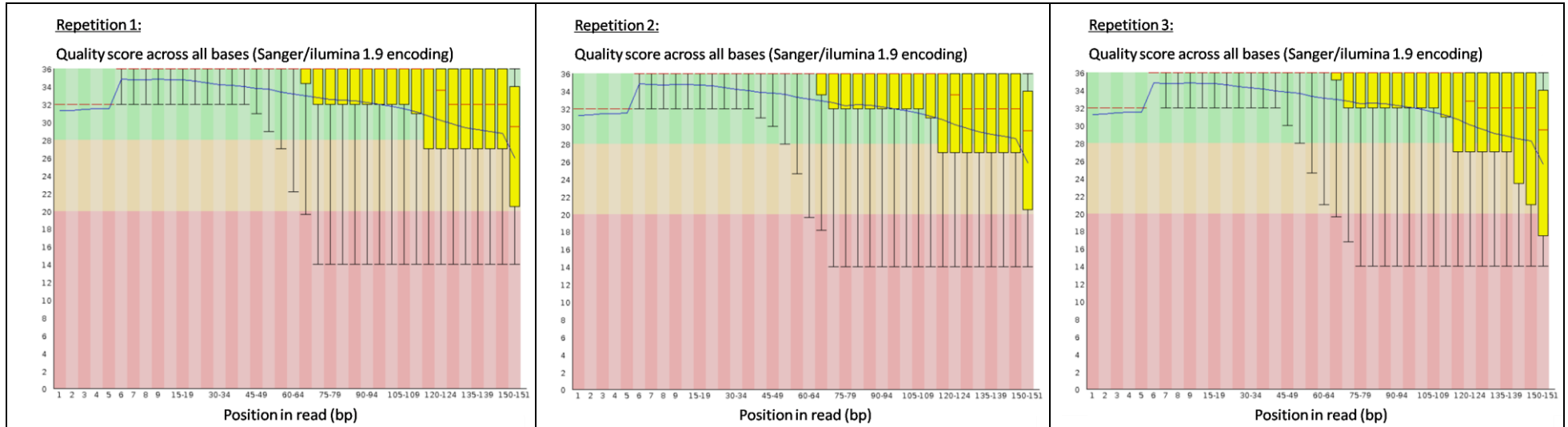
APPENDIX 7. ANOVA of hydrogen peroxide content of three flooded rice cultivars.

Sources of variation	Degrees of freedom	Sum of squares	Mean Square	F	Significance
Cultivar (C)	2	0.482	0.241	26.85	<.0001
Duration (D)	2	1.626	0.813	90.42	<.0001
Int. CxD	4	3.064	0.765	85.18	<.0001
Treatment	8	5.173	0.646	71.91	<.0001
Residue	63	0.566	0.009		
Total	71	5.7394			

*CV% =7.41

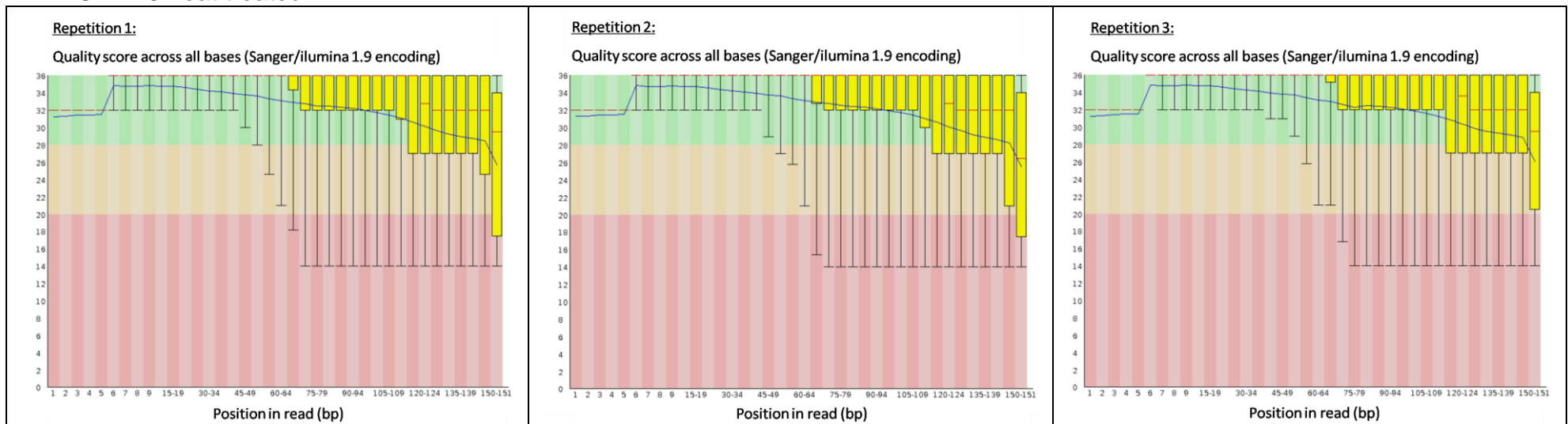
APPENDIX 8. Per base sequence quality of high-throughput mRNA sequencing (RNA-seq) data for IRGA 428 control (A), IRGA 428 heat treated (B), IRGA 409 control (C) and IRGA 409 heat treated (D). The graphics show an overview of the range of quality values across all bases at each position in the FastQ file. For each position a BoxWhisker type plot is drawn as follows: The central red line is the median value. The yellow box represents the inter-quartile range (25-75%). The upper and lower whiskers represent the 10% and 90% points. The blue line represents the mean quality.

A. IRGA 428 control



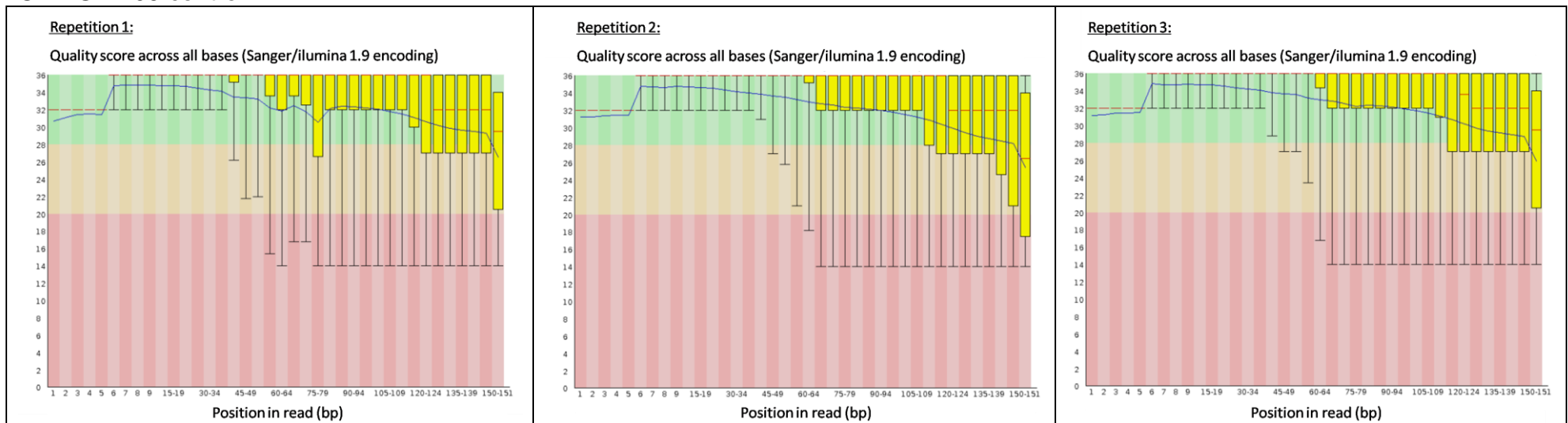
Continuation APPENDIX 8. Per base sequence quality of high-throughput mRNA sequencing (RNA-seq) data for IRGA 428 control (A), IRGA 428 heat treated (B), IRGA 409 control (C) and IRGA 409 heat treated (D). The graphics show an overview of the range of quality values across all bases at each position in the FastQ file. For each position a BoxWhisker type plot is drawn as follows: The central red line is the median value. The yellow box represents the inter-quartile range (25-75%). The upper and lower whiskers represent the 10% and 90% points. The blue line represents the mean quality.

B. IRGA 428 heat treated



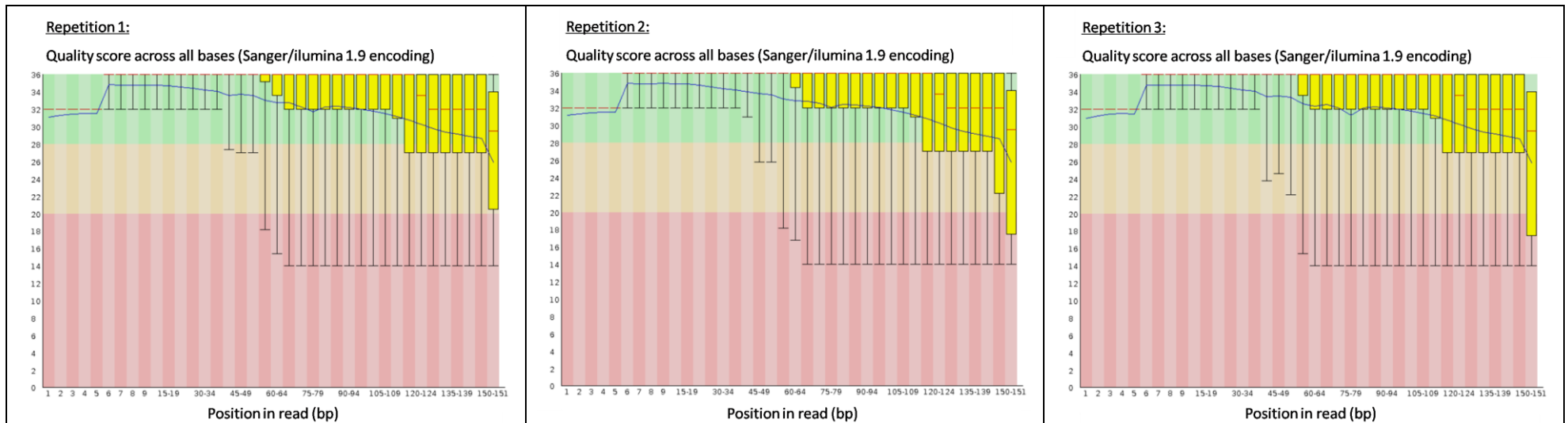
Continuation APPENDIX 8. Per base sequence quality of high-throughput mRNA sequencing (RNA-seq) data for IRGA 428 control (A), IRGA 428 heat treated (B), IRGA 409 control (C) and IRGA 409 heat treated (D). The graphics show an overview of the range of quality values across all bases at each position in the FastQ file. For each position a BoxWhisker type plot is drawn as follows: The central red line is the median value. The yellow box represents the inter-quartile range (25-75%). The upper and lower whiskers represent the 10% and 90% points. The blue line represents the mean quality.

C. IRGA 409 control



Continuation APPENDIX 8. Per base sequence quality of high-throughput mRNA sequencing (RNA-seq) data for IRGA 428 control (A), IRGA 428 heat treated (B), IRGA 409 control (C) and IRGA 409 heat treated (D). The graphics show an overview of the range of quality values across all bases at each position in the FastQ file. For each position a BoxWhisker type plot is drawn as follows: The central red line is the median value. The yellow box represents the inter-quartile range (25-75%). The upper and lower whiskers represent the 10% and 90% points. The blue line represents the mean quality.

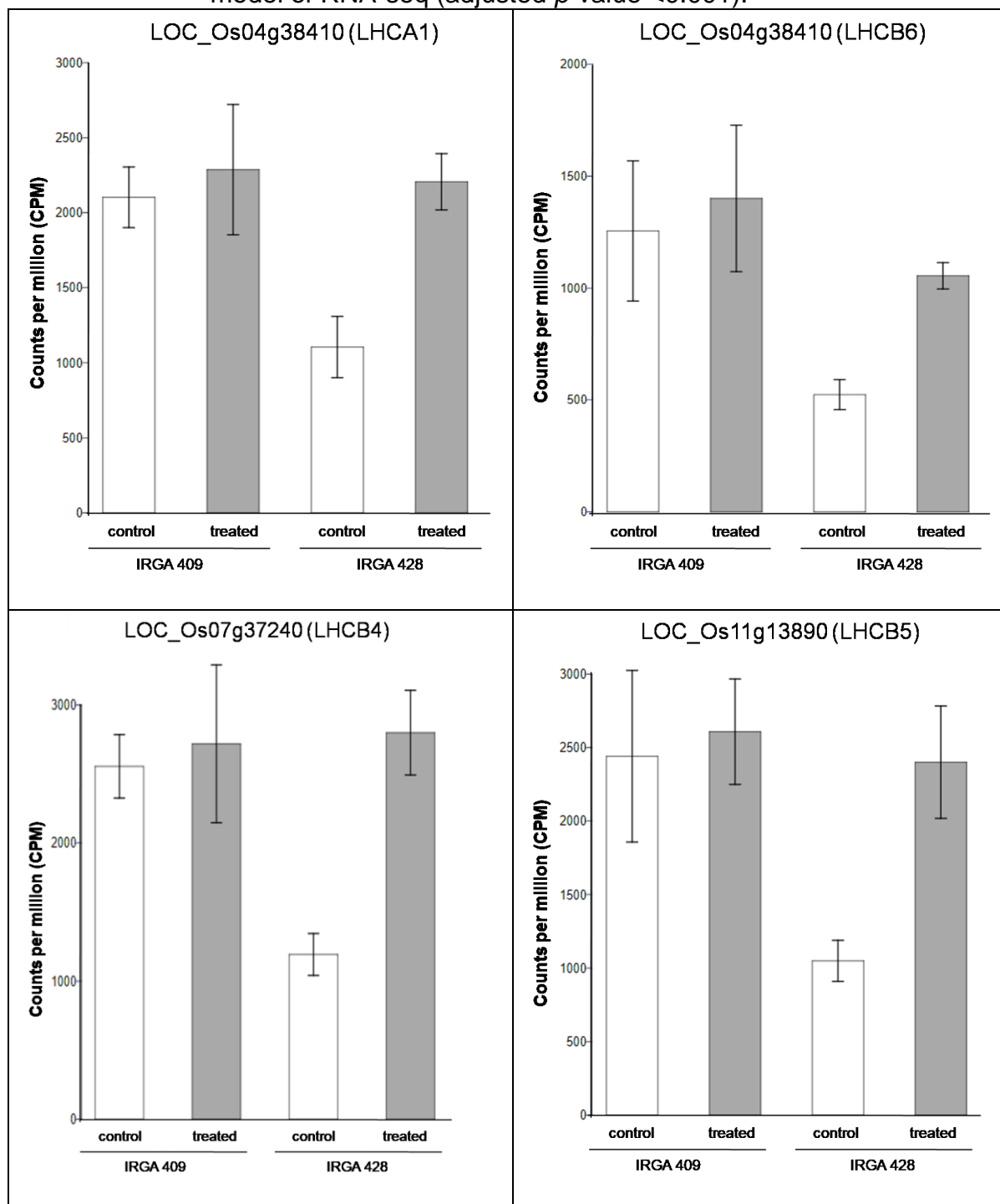
D. IRGA 409 heat treated



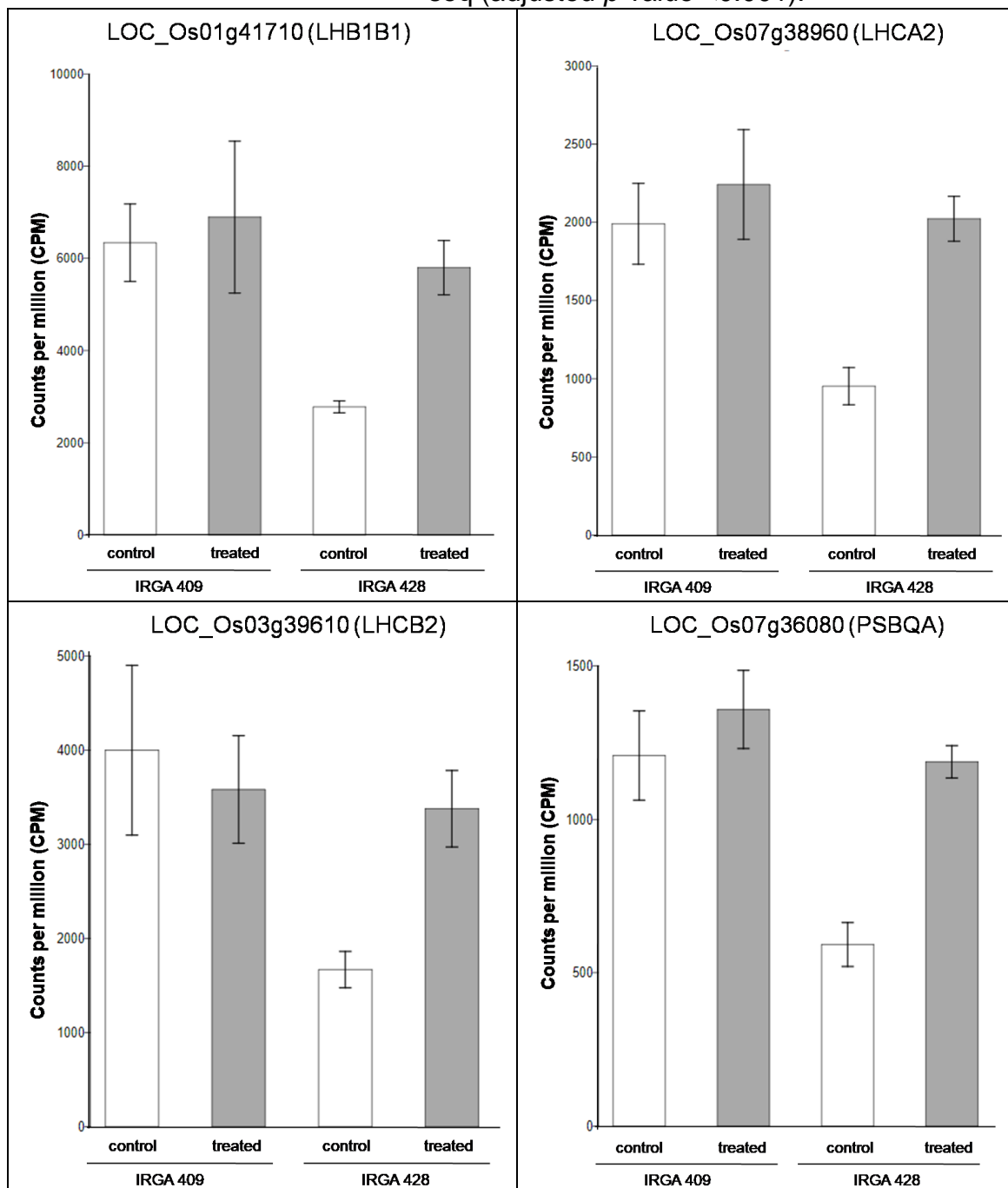
APPENDIX 9. Number of reads, sequence length, sequences flagged as poor quality and % GC obtained for each sample submitted to RNA-sequencing.

Sample	Number of reads	Sequence length	Sequences flagged as poor quality	%GC
1 IRGA 428 – Control – R1	20,992,066	36-145	0	50
2 IRGA 428 – Control – R2	20,628,186	36-145	0	50
3 IRGA 428 – Control – R3	19,656,128	36-145	0	50
4 IRGA 428 – Heat – R1	20,479,453	36-145	0	50
5 IRGA 428 – Heat – R2	22,064,885	36-145	0	50
6 IRGA 428 – Heat – R3	24,536,232	36-145	0	50
7 IRGA 409 – Control – R1	20,651,367	36-145	0	50
8 IRGA 409 – Control – R2	21,435,541	36-145	0	50
9 IRGA 409 – Control – R3	19,525,244	36-145	0	50
10 IRGA 409 – Heat – R1	19,492,857	36-145	0	50
11 IRGA 409 – Heat – R2	24,068,919	36-145	0	50
12 IRGA 409 – Heat – R3	22,736,515	36-145	0	50
TOTAL:	256,267,393			

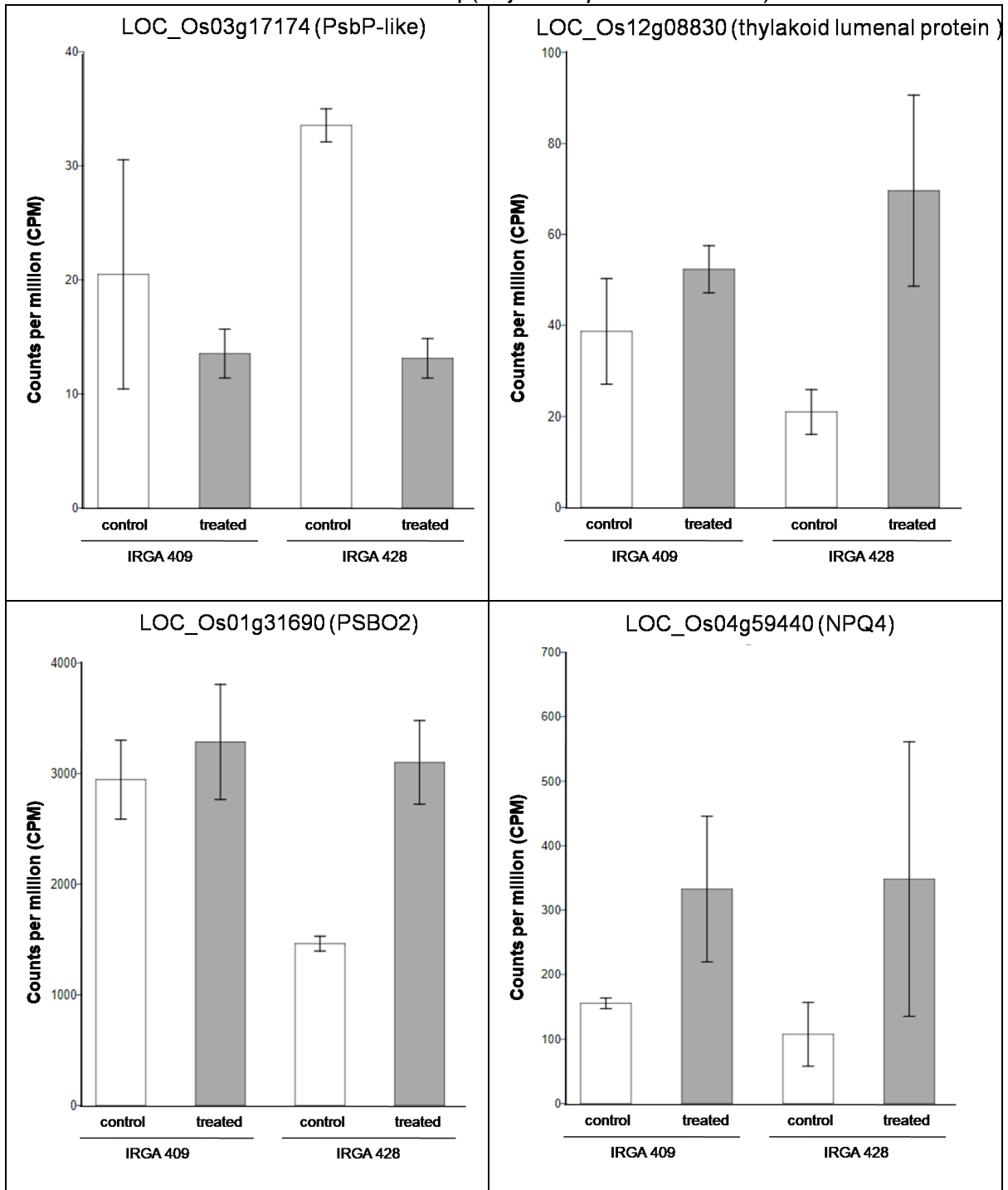
APPENDIX 10. Differentially expressed genes involved in photosynthesis pathway in the cultivar IRGA 428 in response to high temperature, relative expression value computed from the counts per million (CPM). Bar graph shows each gene and transcript expression value annotated with error bars (\pm SD) that capture both cross-replicate variability and measured uncertainty as estimated by EdgeR statistical model of RNA-seq (adjusted p -value <0.001).



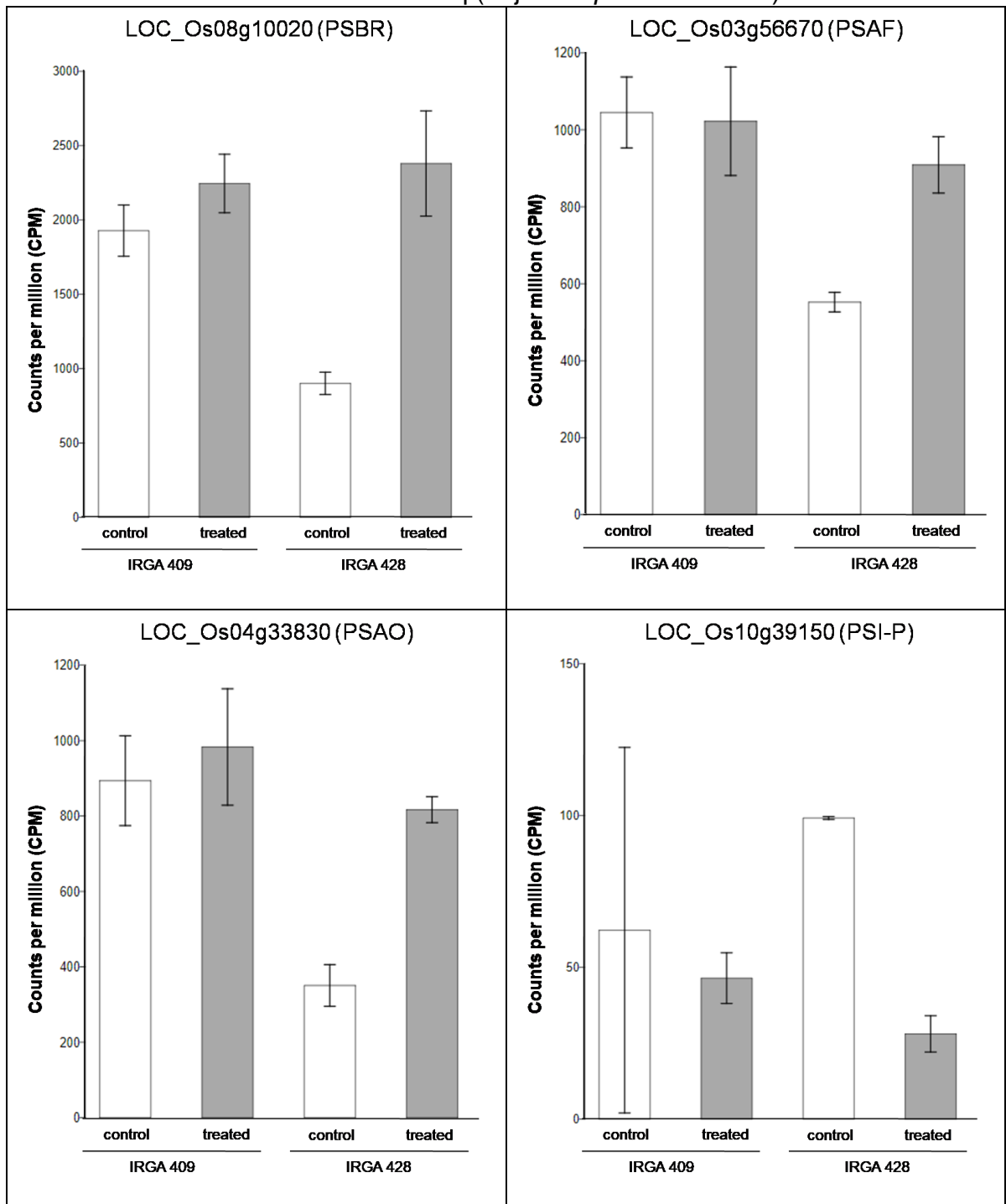
Continuation APPENDIX 10. Differentially expressed genes involved in photosynthesis pathway in the cultivar IRGA 428 in response to high temperature, relative expression value computed from the counts per million (CPM). Bar graph shows each gene and transcript expression value annotated with error bars (\pm SD) that capture both cross-replicate variability and measured uncertainty as estimated by EdgeR statistical model of RNA-seq (adjusted p -value <0.001).



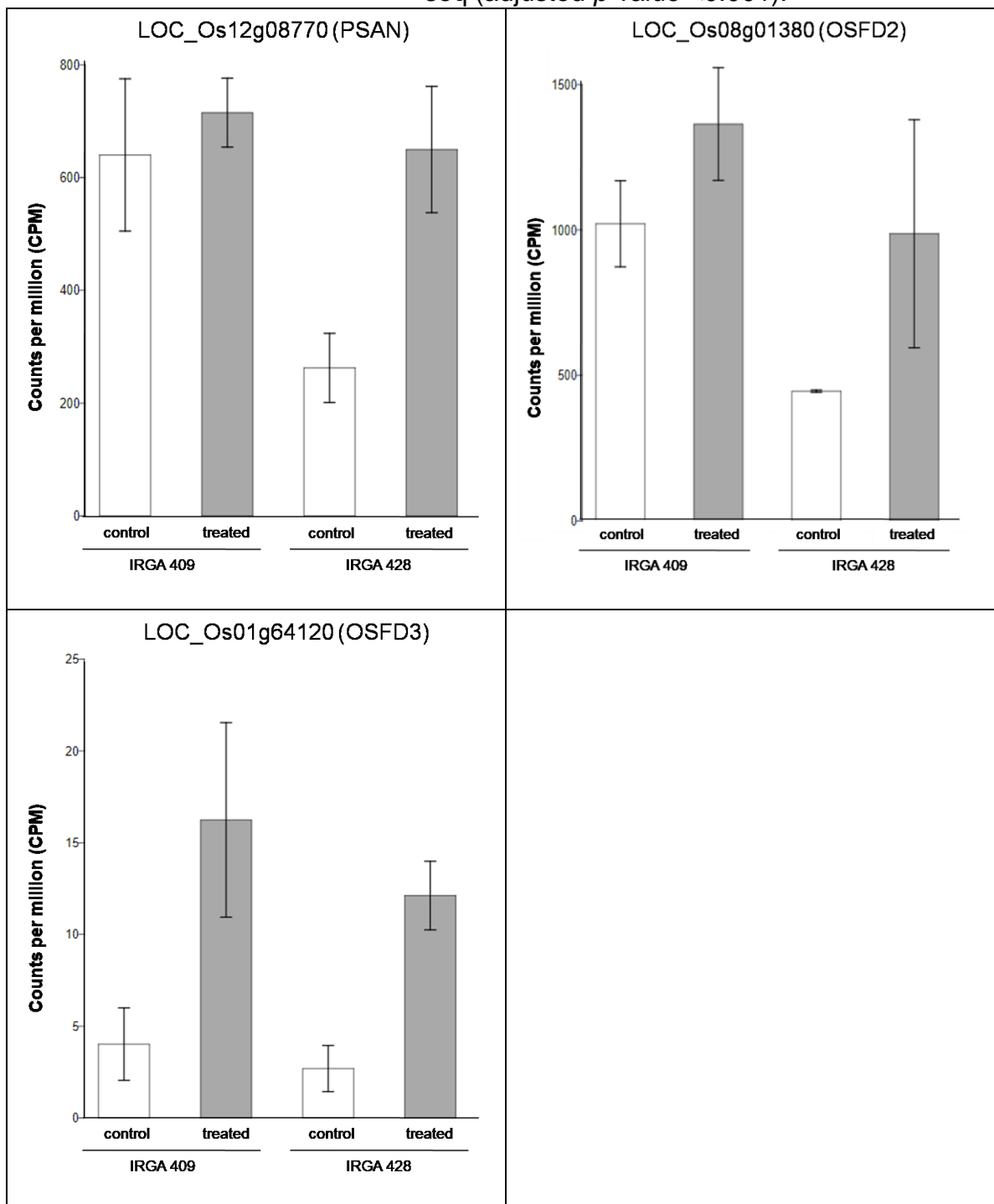
Continuation APPENDIX 10. Differentially expressed genes involved in photosynthesis pathway in the cultivar IRGA 428 in response to high temperature, relative expression value computed from the counts per million (CPM). Bar graph shows each gene and transcript expression value annotated with error bars (\pm SD) that capture both cross-replicate variability and measured uncertainty as estimated by EdgeR statistical model of RNA-seq (adjusted p -value <0.001).



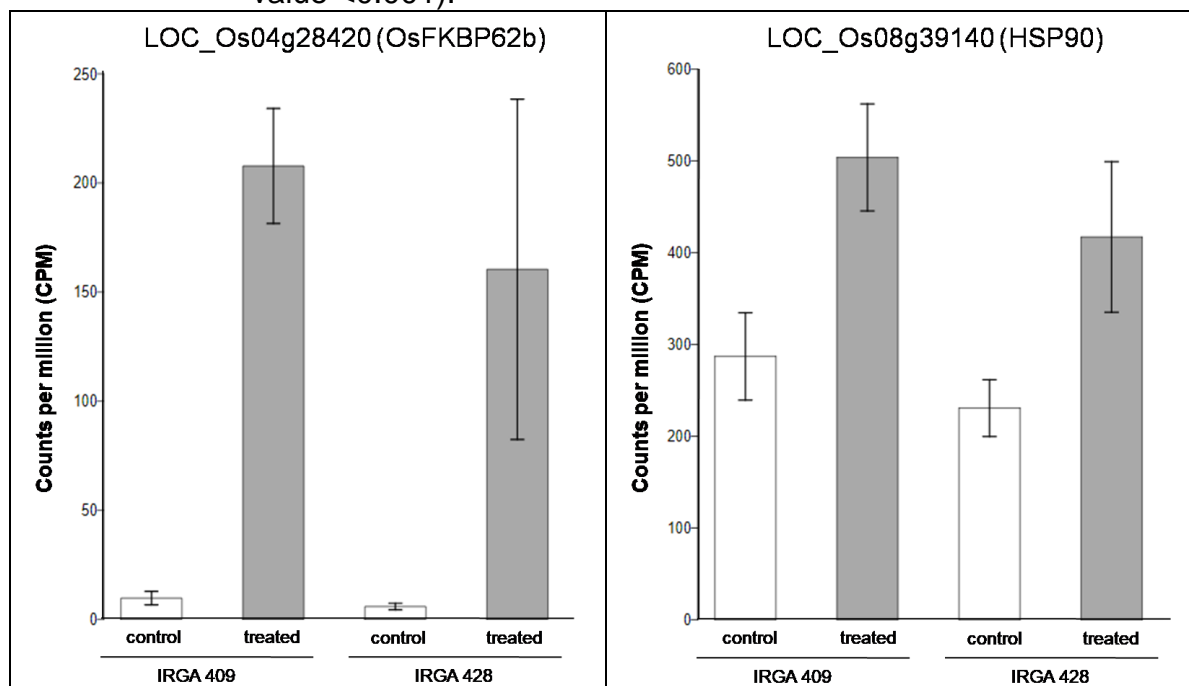
Continuation APPENDIX 10. Differentially expressed genes involved in photosynthesis pathway in the cultivar IRGA 428 in response to high temperature, relative expression value computed from the counts per million (CPM). Bar graph shows each gene and transcript expression value annotated with error bars (\pm SD) that capture both cross-replicate variability and measured uncertainty as estimated by EdgeR statistical model of RNA-seq (adjusted p -value <0.001).



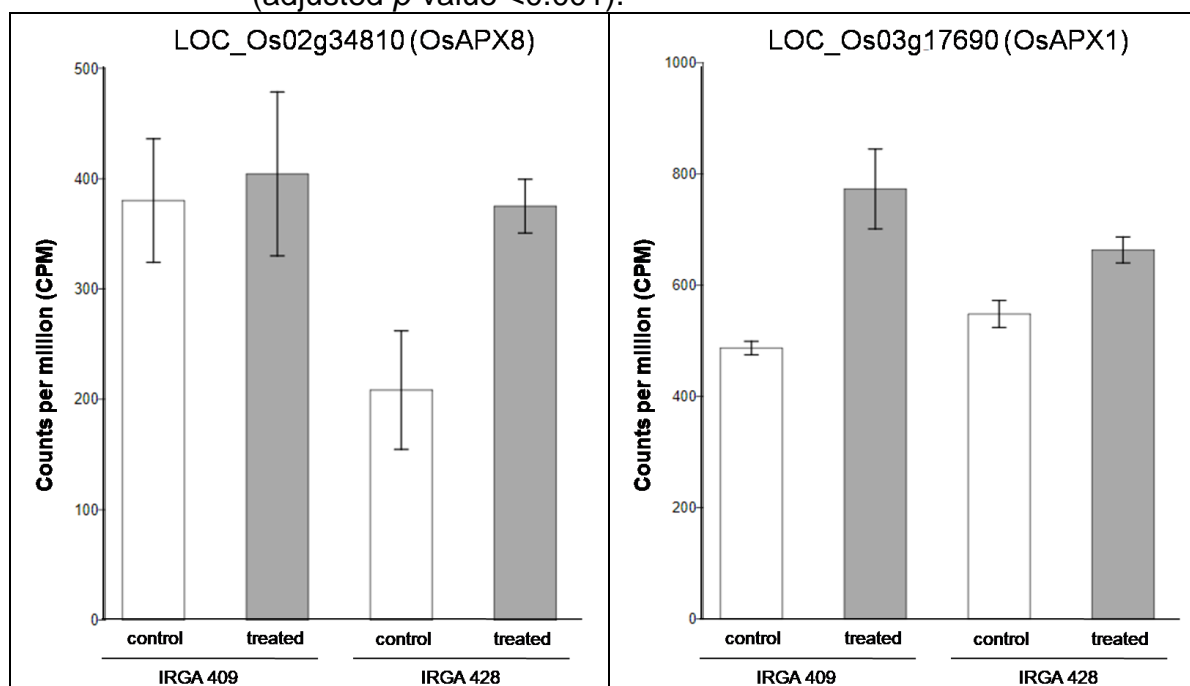
Continuation APPENDIX 10. Differentially expressed genes involved in photosynthesis pathway in the cultivar IRGA 428 in response to high temperature, relative expression value computed from the counts per million (CPM). Bar graph shows each gene and transcript expression value annotated with error bars (\pm SD) that capture both cross-replicate variability and measured uncertainty as estimated by EdgeR statistical model of RNA-seq (adjusted p -value <0.001).



APPENDIX 11. Differentially expressed genes involved in the canonical response to high temperature, relative expression value computed from the counts per million (CPM). Bar graph shows each gene and transcript expression value annotated with error bars (\pm SD) that capture both cross-replicate variability and measured uncertainty as estimated by EdgeR statistical model of RNA-seq (adjusted p -value <0.001).



APPENDIX 12. Differentially expressed genes involved in the redox pathway in response to high temperature, relative expression value computed from the counts per million (CPM). Bar graph shows each gene and transcript expression value annotated with error bars (\pm SD) that capture both cross-replicate variability and measured uncertainty as estimated by EdgeR statistical model of RNA-seq (adjusted p -value <0.001).



APPENDIX 13. Table of gene identification (ID) and description of differentially expressed genes in cultivars IRGA 409 that the overlap were significantly between the in this study and González-Schain et al. (2015).

Gene ID	Description
LOC_Os01g05650	metallothionein, putative
LOC_Os01g07530	uncharacterized glycosyltransferase, putative
LOC_Os01g08860	hsp20/alpha crystallin family protein, putative
LOC_Os01g55270	SGS domain containing protein
LOC_Os01g62290	DnaK family protein, putative
LOC_Os02g04160	transcription elongation factor 1, putative
LOC_Os02g28980	peptidyl-prolyl isomerase, putative
LOC_Os02g40900	RNA recognition motif containing protein, putative
LOC_Os02g52150	heat shock 22 kDa protein, mitochondrial precursor, putative
LOC_Os02g54140	hsp20/alpha crystallin family protein, putative
LOC_Os02g54730	transmembrane amino acid transporter protein, putative
LOC_Os03g02260	DnaK family protein, putative
LOC_Os03g11910	DnaK family protein, putative
LOC_Os03g14180	hsp20/alpha crystallin family protein, putative
LOC_Os03g15960	hsp20/alpha crystallin family protein, putative

Continuation APPENDIX 13. Table of gene identification (ID) and description of differentially expressed genes in cultivars IRGA 409 that the overlap were significantly between the in this study and González-Schain et al. (2015).

Gene ID	Description
LOC_Os03g25050	chaperonin, putative
LOC_Os03g38500	expressed protein
LOC_Os03g51459	expressed protein
LOC_Os03g53910	tetratricopeptide repeat domain containing protein
LOC_Os03g63970	gibberellin 20 oxidase 1, putative
LOC_Os04g28420	peptidyl-prolyl isomerase, putative
LOC_Os04g36750	hsp20/alpha crystallin family protein, putative
LOC_Os04g38570	multidrug resistance protein, putative
LOC_Os04g39489	amino acid transporter, putative
LOC_Os05g23140	retrotransposon protein, putative, LINE subclass
LOC_Os05g39250	phosphatidylethanolamine-binding protein, putative
LOC_Os06g09560	heat shock protein DnaJ, putative
LOC_Os06g14240	hsp20/alpha crystallin family protein, putative
LOC_Os06g22960	aquaporin protein, putative
LOC_Os06g46900	phosphosulfolactate synthase-related protein, putative
LOC_Os06g51100	transmembrane protein, putative
LOC_Os07g43950	RNA recognition motif containing protein, putative
LOC_Os07g48160	alpha-galactosidase precursor, putative
LOC_Os08g01370	expressed protein
LOC_Os08g39140	heat shock protein, putative
LOC_Os09g35790	HSF-type DNA-binding domain containing protein
LOC_Os10g25180	phosphoinositide phosphatase family protein, putative
LOC_Os10g39500	expressed protein
LOC_Os12g05210	expressed protein
LOC_Os01g17214	major facilitator superfamily antiporter, putative
LOC_Os01g45990	potassium channel AKT1, putative
LOC_Os01g60110	E2F-related protein, putative
LOC_Os01g60640	WRKY21
LOC_Os02g11070	3-ketoacyl-CoA synthase, putative
LOC_Os02g55380	AP2 domain containing protein
LOC_Os03g03790	AMP-binding domain containing protein
LOC_Os03g09910	aminotransferase, classes I and II, domain containing protein
LOC_Os03g10640	calcium-transporting ATPase, plasma membrane-type, putative
LOC_Os03g16860	DnaK family protein, putative
LOC_Os03g46440	BTBA4 - Bric-a-Brac, Tramtrack, Broad Complex BTB domain with Ankyrin repeat region
LOC_Os03g58790	ATPase, putative
LOC_Os04g35540	amino acid permease family protein, putative
LOC_Os04g42520	phosphoribosyl transferase, putative
LOC_Os04g47420	transmembrane amino acid transporter protein, putative

Continuation APPENDIX 13. Table of gene identification (ID) and description of differentially expressed genes in cultivars IRGA 409 that the overlap were significantly between the in this study and González-Schain et al. (2015).

Gene ID	Description
LOC_Os05g21180	phosphatidic acid phosphatase-related, putative
LOC_Os05g25770	WRKY45
LOC_Os05g36260	soluble inorganic pyrophosphatase, putative
LOC_Os05g46020	WRKY7
LOC_Os06g03580	zinc RING finger protein, putative
LOC_Os06g46270	no apical meristem protein, putative
LOC_Os07g22400	POLA3 - Putative DNA polymerase alpha complex subunit
LOC_Os07g27780	aminotransferase, putative
LOC_Os07g34070	auxin-induced protein 5NG4, putative
LOC_Os07g37730	NADH-ubiquinone oxidoreductase, mitochondrial precursor, putative
LOC_Os07g42924	dehydrogenase, putative
LOC_Os07g48450	no apical meristem protein, putative
LOC_Os07g48550	no apical meristem protein, putative
LOC_Os08g03350	amino acid transporter, putative
LOC_Os08g32120	expressed protein
LOC_Os09g38610	ZOS9-18 - C2H2 zinc finger protein
LOC_Os10g05790	POEI4 - Pollen Ole e I allergen and extensin family protein precursor
LOC_Os10g37770	dehydration response related protein, putative
LOC_Os10g39140	flavonol synthase/flavanone 3-hydroxylase, putative
LOC_Os10g39680	CHIT14 - Chitinase family protein precursor
LOC_Os12g08760	carboxyvinyl-carboxyphosphonate phosphorylmutase, putative
LOC_Os12g43640	receptor-like protein kinase HAIKU2 precursor, putative

APPENDIX 14. Table of gene identification (ID) and description of differentially expressed genes in cultivars IRGA 428 that the overlap were significantly between the in this study and González-Schain et al. (2015).

Gene ID	Description
LOC_Os03g14180	hsp20/alpha crystallin family protein, putative
LOC_Os04g36750	hsp20/alpha crystallin family protein, putative
LOC_Os06g14240	hsp20/alpha crystallin family protein, putative
LOC_Os04g28420	peptidyl-prolyl isomerase, putative
LOC_Os01g08860	hsp20/alpha crystallin family protein, putative
LOC_Os02g52150	heat shock 22 kDa protein, mitochondrial precursor, putative
LOC_Os03g15960	hsp20/alpha crystallin family protein, putative
LOC_Os06g09560	heat shock protein DnaJ, putative
LOC_Os05g23140	retrotransposon protein, putative, LINE subclass
LOC_Os09g35790	HSF-type DNA-binding domain containing protein
LOC_Os08g01370	expressed protein

Continuation APPENDIX 14. Table of gene identification (ID) and description of differentially expressed genes in cultivars IRGA 428 that the overlap were significantly between the in this study and González-Schain et al. (2015).

Gene ID	Description
LOC_Os01g62290	DnaK family protein, putative
LOC_Os02g54140	hsp20/alpha crystallin family protein, putative
LOC_Os02g40900	RNA recognition motif containing protein, putative
LOC_Os06g46900	phosphosulfolactate synthase-related protein, putative
LOC_Os05g39250	phosphatidylethanolamine-binding protein, putative
LOC_Os07g36190	hydrolase, NUDIX family, domain containing protein
LOC_Os03g53910	tetratricopeptide repeat domain containing protein
LOC_Os03g11910	DnaK family protein, putative
LOC_Os03g07180	embryonic protein DC-8, putative
LOC_Os12g29400	GRAM domain containing protein
LOC_Os05g46480	late embryogenesis abundant protein, group 3, putative
LOC_Os07g43950	RNA recognition motif containing protein, putative
LOC_Os12g05210	expressed protein
LOC_Os02g28980	peptidyl-prolyl isomerase, putative
LOC_Os02g02340	glycerol-3-phosphate acyltransferase, putative
LOC_Os03g05290	aquaporin protein, putative
LOC_Os04g05010	CBS domain containing membrane protein, putative
LOC_Os01g55270	SGS domain containing protein
LOC_Os10g25180	phosphoinositide phosphatase family protein, putative
LOC_Os03g02260	DnaK family protein, putative
LOC_Os10g39500	expressed protein
LOC_Os03g17790	OsRC12-5 - Putative low temperature and salt responsive protein
LOC_Os05g10670	zinc finger CCCH type family protein, putative
LOC_Os01g05650	metallothionein, putative
LOC_Os06g22960	aquaporin protein, putative
LOC_Os03g59430	uncharacterized glycosyltransferase, putative
LOC_Os03g38500	expressed protein
LOC_Os02g53490	cation efflux family protein, putative
LOC_Os03g51920	peptidase, M50 family, putative
LOC_Os08g39140	heat shock protein, putative
LOC_Os05g30140	RNA recognition motif containing protein
LOC_Os08g03430	extracellular ligand-gated ion channel, putative
LOC_Os03g63970	gibberellin 20 oxidase 1, putative
LOC_Os07g08840	thioredoxin, putative
LOC_Os01g52160	heavy metal-associated domain containing protein
LOC_Os04g38570	multidrug resistance protein, putative
LOC_Os12g08760	carboxyvinyl-carboxyphosphonate phosphorylmutase, putative
LOC_Os06g40170	phospholipase D, putative
LOC_Os10g30690	MYB family transcription factor, putative

Continuation APPENDIX 14. Table of gene identification (ID) and description of differentially expressed genes in cultivars IRGA 428 that the overlap were significantly between the in this study and González-Schain et al. (2015).

Gene ID	Description
LOC_Os11g05050	stem-specific protein TSJT1, putative
LOC_Os03g31690	GCN5-related N-acetyltransferase, putative
LOC_Os10g40740	helix-loop-helix DNA-binding domain containing protein
LOC_Os08g32960	endonuclease/exonuclease/phosphatase family domain containing protein
LOC_Os03g16860	DnaK family protein, putative
LOC_Os01g43480	AAA-type ATPase family protein, putative
LOC_Os08g03350	amino acid transporter, putative
LOC_Os10g39680	CHIT14 - Chitinase family protein precursor
LOC_Os07g42924	dehydrogenase, putative
LOC_Os02g51020	expressed protein
LOC_Os10g39140	flavonol synthase/flavanone 3-hydroxylase, putative
LOC_Os07g22400	POLA3 - Putative DNA polymerase alpha complex subunit
LOC_Os05g46020	WRKY7
LOC_Os03g58790	ATPase, putative
LOC_Os09g38610	ZOS9-18 - C2H2 zinc finger protein
LOC_Os10g36390	monocopper oxidase, putative
LOC_Os05g25770	WRKY45
LOC_Os01g60640	WRKY21
LOC_Os07g34070	auxin-induced protein 5NG4, putative
LOC_Os03g03790	AMP-binding domain containing protein
LOC_Os03g09910	aminotransferase, classes I and II, domain containing protein

9 VITA

Silmara da Luz Correi, is daughter of Vorli Antunes Correia and Julia da Aparecida Correia, was born in Porto Alegre/RS on December 24th, 1983. In 2002, completed High School at the Colégio Estadual Dom João Becker in Porto Alegre/RS. In 2004, joined the Agronomy School at the Universidade Federal do Rio Grande do Sul (UFRGS) in Porto Alegre/RS and graduated as Agronomist in 2010. From 2007 to 2010, took a Scholarship for Scientific Initiation (IC) in Soil management. In 2011, joined the Master's degree program in Agronomy, at the UFRGS with a CNPq scholarship. Holds a Master Degree in Crop Science since April 2013. In the same year, joined internship at South Dakota State University, Brookings/USA, in winter wheat breeding program. In 2014, joined the PhD in Plant Science with emphasis on Plant Physiology, at UFRGS, in Porto Alegre/RS, and was a CNPq scholarship student during the period. In the year of 2017, joined the North Carolina State University as a Guest Student with a CAPES scholarship. After 6 months, returned to Brazil for finishing the PhD.